Inaugural-Dissertation zur Erlangung der Doktorwürde
der Tierärztlichen Fakultät der Ludwig-Maximilians-Universität
München

Phenotyping of the Visceral Adipose Tissue Using Dual Energy X-ray Absorptiometry (DXA) and Magnetic Resonance Imaging (MRI) in Pigs

von Anna Christine Weigand

aus Moosburg an der Isar

München 2021

Aus dem Lehr- und Versuchsgut der Tierärztlichen Fakultät

der Ludwig-Maximilians-Universität München

Arbeit angefertigt unter der Leitung von

Prof. Dr. Armin M. Scholz

Gedruckt mit Genehmigung der Tierärztlichen Fakultät
der Ludwig-Maximilians-Universität München

Dekan: Univ.-Prof. Dr. Reinhard K. Straubinger, Ph.D.

Berichterstatter: Prof. Dr. Armin M. Scholz
Korreferent: Univ.-Prof. Dr. Joris Peters

Tag der Promotion: 06. Februar 2021

Wir sind, was wir denken. Alles, was wir sind, entsteht aus unseren Gedanken.

Mit unseren Gedanken formen wir die Welt.

– Buddha (560-480 v. Chr.) –

TABLE OF CONTENTS

LIST OF ABBREVIATIONS

ADG Average daily gain

AT Adipose tissue

BMI Body mass index

BRS German Livestock Association

CT Computed tomography

CV Coefficient of variation

CVD Cardiovascular disease

DXA Dual energy X-ray

EGZH Erzeugergemeinschaft und Züchtervereinigung für Zucht- und Hybridzuchtschweine in Bayern w.V

F Filial generation

FAO Food and Agriculture Organization

FCR Feed conversion rate

L Lumbar vertebra

LfL Bavarian State Research Center for Agriculture

MHF1 Multi-hybrid-F1

MHF2 Multi-hybrid-F2

MHS Malignant hyperthermia syndrome

MRI Magnetic resonance imaging

OECD Organisation for Economic Cooperation and Development

QTL Quantitative trait loci

R^2 Regression coefficient

RMSE Root mean squared error

S Caudal vertebra

SAT Subcutaneous adipose tissue

TAT Total adipose tissue

TE Time to echo

TR Time to repeat

VAT Visceral adipose tissue

LIST OF FIGURES

PUBLICATION – FIGURES

LIST OF TABLES

PUBLICATION – TABLES

I. INTRODUCTION

"In the age of the genotype, phenotype is king" is a statement that – meanwhile – has been used by many different researchers to underline the importance of the phenotype, especially for the "postulated" post-genomic era (Coffey, 2010). The phenotype builds the basis for all genomic analyses, because the accuracy of a genomic evaluation depends on a most precise description of the phenotype. Furthermore, a continuous measurement of the performance test data is essential to be able to adapt genomic predictions if necessary. In addition – besides environmental effects, the estimation of the genetic performance of the individuals (genomic breeding value) is meanwhile mainly based on the genetics of the parental generations. To evaluate the genotype prediction, the performance of the individual itself must be determined, and therefore *in-vivo* methods are being preferably applied due to the potential further use of the individual within the breeding process.

Sambraus (1987) described the pig as a species superior in fertility to all species having approximately an equal size. The pig is capable of producing numerous offsprings and thus generations of piglets in a short period of time (Sambraus, 1987). Besides the great similarity in anatomy and genomic sequence compared to the human organism, the short generation interval makes the pig a suitable animal model. The pig as an omnivore animal has a similar digestive tract anatomy as humans and the fact, that the pig will voluntarily eat to obesity, explains the use of porcine models for researches of effects and diseases which are associated with overweight and obesity in humans (Rohrer et al., 2002). In this field of research, the visceral adipose tissue (VAT) in particular, is a fat depot of interest due to its high metabolic activity. It plays an important role in the pathogenesis of cardiovascular diseases, which represent the most common cause of death worldwide. Phenotyping the visceral adipose tissue in pigs would provide new opportunities for human research. Therefore, a VAT determination as simple and precisely as possible is necessary. With their CoreScan mode, GE Healthcare offers the possibility of measuring VAT by using dual energy X-ray absorptiometry. *In vivo* methods provide the option to conduct consecutively studies on the same animal, and thus allowing investigating the development of fat accumulation during growth and aging. In addition, the animals may find use in other studies leading to a reduction of the number of animals necessary for these purposes.

The aim of this thesis was to evaluate the CoreScan feature in pigs by comparing the results of VAT measured by DXA to those of the MRI examination as a reference method in body composition analyses. Furthermore, by phenotyping the visceral adipose tissue, a basis for genomic analyses has been created, which might have an impact on the future pig breeding work and on human research through the identification of new or better characterized fatness traits. Additionally, sex and genotype related differences of multiple hybrid pig lines of two crossbreeding generations (F1 and F2) were studied for visceral adipose tissue and for the whole body composition by MRI and DXA.

II. REVIEW OF THE LITERATURE

1. Visceral adipose tissue in humans

1.1. Definition and classification

Visceral adipose tissue (VAT) is a specific depot of adipose tissue (AT). In Latin, “viscera” stands for organs in the cavities of the body and visceral means belonging to the organs. Adipose tissue is one of the largest body compartments and is different from fat which is primarily in AT, but also found in other tissues and can be differentiated in essential and storage fat. Essential fat is located for example in the bone marrow, heart, lungs, liver, and kidneys. Adipose tissue is the major storage of fat. AT is composed of 80% fat and 20% non-fat components including protein, minerals, and water (Shen et al., 2003; Wells, 2007). There is still no officially accepted taxonomy of adipose tissue. Shen et al. (2003) and Marcadenti and de Abreu-Silva (2015) tried to find a classification system for AT in order to reduce definition problems for investigators studying AT (Figure 1). First, adipose tissue can be divided into subcutaneous adipose tissue (SAT) and internal adipose tissue. SAT constitutes the layer between the dermis and the aponeuroses and fasciae of the muscles, and can be further divided into a deep and a superficial layer. The superficial layer is located between the skin and a fascial plane in the lower trunk and gluteal-thigh area, and the deep layer between this fascial plane and the muscle fascia. Visceral and non-visceral adipose tissues are the two compartments of internal adipose tissue. Non-visceral adipose tissue includes intramuscular and perimuscular adipose tissue. As described previously, visceral stands for the organs in the cavities of the body: the chest, the abdomen, and the pelvic. The terms for the adipose tissue in the main cavities are intrathoracic, intraabdominal, and intrapelvic. Most studies describe VAT as intraabdominal adipose tissue or the sum of intraabdominal and intrapelvic AT. In the region of the abdomen, the peritoneum provides an anatomic landmark to subdivide the intraabdominal AT further into an intraperitoneal and an extraperitoneal compartment. The intraperitoneal AT includes the omental and mesenteric depots, and extraperitoneal AT includes the depots located perirenal, pararenal, and periaortic (Shen et al., 2003).

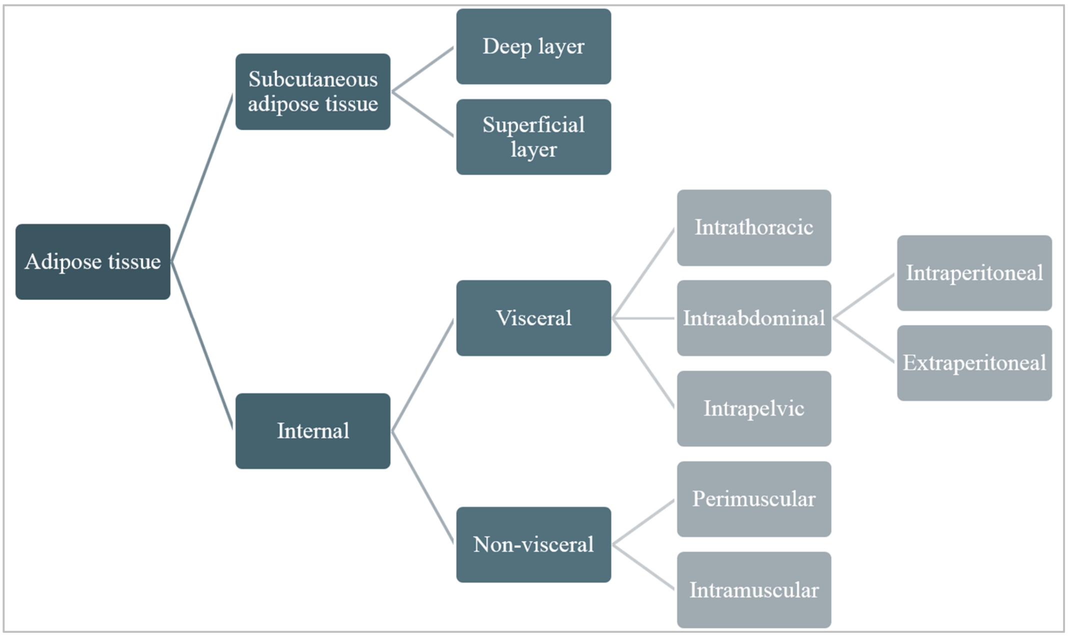

Figure 1. Classification system modified according to Shen et al. (2003)

The major functions of adipose tissue in mammals are acting as 1) energy storage depot in the form of triglycerides, 2) thermal isolator, and 3) mechanical cushion. The regulation of energy storage and mobilization combined with the endocrine functions of AT are essential for the whole body metabolism (Shen et al., 2003; Karastergiou et al., 2012; Marcadenti and de Abreu-Silva, 2015).

1.2. Adipose tissue as an endocrine organ

Adipose tissue has been recently named an “endocrine organ” (Galic et al., 2010). The reason for this classification is the metabolic activity of AT by secreting a multiple number of proteins, called adipokines, which influence several processes in the human body. The major adipokines are leptin and adiponectin. Furthermore, tumor necrosis factor, resistin, and interleukin 6 are released (Shuster et al., 2012).

In proportion to their triglyceride content, the adipocytes produce the polypeptide hormone Leptin and release it into the blood. The hormone is able to cross the blood-brain-barrier and unfolds its effect especially in the hypothalamus. Leptin is involved in the regulation of feeding and energy balance. Activating the lipid oxidation by inducing the expressions of enzymes of the lipid oxidation process leads to a decrease of body weight. A variety of factors regulates the expression of leptin. For example, overfeeding, obesity, insulin, glucocorticoids, and cytokines may increase the expression of leptin, whereas fasting and testosterone reduce it

(Ahima and Flier, 2000). Paradoxically, obese individuals show elevated levels of leptin that usually must lead to a reduction of food intake, and an increase of energy consumption. This finding reinforces the assumption of a leptin resistance (Rosická et al., 2003). Mechanisms of the resistance are a dysregulation of leptin synthesis and/or secretion, abnormalities of brain leptin transport, and abnormalities of leptin receptors and/or post-receptor signaling. Leptin resistance is associated with insulin resistance and abdominal obesity and may have an additional effect to the metabolic syndrome. Markers for the resistance are low soluble receptor concentrations, and a low fraction of specifically bound leptin (Sandhofer et al., 2003). Regarding the functions of leptin, it can be considered as an anti-obesity hormone, but its use is often limited by the increasing resistance towards leptin particularly in obese individuals (Ahima and Flier, 2000; Myers et al., 2010).

The second major adipokine secreted by AT is adiponectin, an insulin sensitizing and anti-inflammatory hormone (Meier and Gressner, 2004; Karastergiou et al., 2012). Adiponectin is associated with type 2 diabetes and can be used as a predictor for cardiovascular risk (Hotta et al., 2000). A negative correlation between circulating adiponectin and obesity has been reported. In addition, the concentrations of adiponectin increase with weight loss (Faraj et al., 2003).

The metabolic activity of SAT and VAT differs, whereby the adipocytes of VAT are more metabolic active. Consequently, the influence of adipose tissue on physiological and pathological processes in the body varies by the specific depots. VAT is more vascular innervated, contains a larger number of inflammatory cells, and a greater percentage of large adipocytes compared to SAT. Due to these reasons, VAT is more pathogenic than SAT and is a greater predictor of mortality (Ibrahim, 2010). A potential hypothesis states that the anatomical location of VAT should have an impact on the pathogenicity. VAT is more sensitive to lipolysis and drains the free fatty acids and other metabolites directly into liver cells via the portal circulation. All these facts explain the association of abdominal obesity with dyslipidemia, hyperinsulinemia, and other metabolic complications (Shen et al., 2003; Marcadenti and de Abreu-Silva, 2015).

1.3. Influence of different factors on VAT

Visceral adipose tissue and the distribution of adipose tissue are influenced by many factors including sex, age, genotype, diet, physical activity, and hormone levels. Sex differences in fat phenotypes are well described. Women tend to store more fat subcutaneously in the gluteo-femoral region, whereas men deposit higher amounts of visceral adipose tissue (Karastergiou et al., 2012). In general, women present about 10% higher body fat than men with the same body mass index (BMI) (Jackson et al., 2002). Shadid et al. (2007) observed in their study a possible reason for the higher amounts of body fat in women. Women showed a direct free fatty acid uptake in SAT of 8% which was twice as high as in men (Shadid et al., 2007). The sex related differences are further due to the influence of sexual steroids. Various studies found that adipose tissue presents sexual steroid receptors for estrogens, androgens, and progesterone (Dieudonne et al., 1998; O'Brien et al., 1998; Pedersen et al., 2001). The expression of these receptors varies by depot and gender. In intraabdominal preadipocytes the number of androgen binding sites is higher than in subcutaneous fat depots, both in males and females (Dieudonne et al., 1998). In males, the density of estrogen receptors in visceral adipose tissue is lower than in subcutaneous depots, and also the binding capacity in SAT is higher compared to VAT (Pedersen et al., 1996; Wells, 2007). Another fact, which underlines the effect of sexual hormones, is that sexual maturity influences total body fat, subcutaneous, and visceral adipose tissue. In late puberty, the gynoid body fat of boys decreases, whereas in girls the amount increases. SAT seems to be relatively stable during puberty. Boys accumulate more VAT than girls in the late puberty (Staiano and Katzmarzyk, 2012).

The age of an individual influences the volume of SAT and VAT. Borkan et al. (1983) examined in their study the body composition in middle-aged and older men. In the old-men-group, lower weight accompanies a decrease of lean tissue mass and an increase of VAT. The subcutaneous depot was higher in middle-aged men (Borkan et al., 1983). Consequently, the proportion of VAT on the total adipose tissue (TAT) increases with age, whereas the proportion of SAT decreases (Shen et al., 2009).

Furthermore, fat deposition underlies genetic differences. Many studies reported higher values of VAT in white men compared to African-American men. SAT was higher in African-American women than in white women (Demerath et al., 2007).

In a group of 80 individuals, Hoffman et al. (2005) found genetic differences in VAT mass when controlling for sex hormones. Those results are only found in men but not in women. African-Americans had an increased VAT mass compared to white men (Hoffman et al., 2005). In a multicultural study of VAT, Lear et al. (2007) compared the relation between abdominal adipose tissue and total body fat among individuals with Aboriginal, Chinese, South Asian, and European origin. A relatively greater amount of abdominal adipose tissue was found in the Chinese and South Asian cohorts, and the difference was especially due to higher VAT. No significant differences were observed between Aboriginals and Europeans (Lear et al., 2007).

1.4. VAT and cardiovascular diseases

Cardiovascular disease (CVD) is still the leading cause of death worldwide, and also in Germany during the last years. In 2016, 17.9 million people worldwide died from CVDs which were 31% of all deaths (World Health Organization, 2017). In Germany, the percentage was even higher, representing 37% of all deaths (Figure 2) (Statistisches Bundesamt, 2020). The complex of CVD can be subdivided. The main groups are coronary heart disease and cerebrovascular disease. Coronary heart disease, described as disease of the blood vessels supplying the heart muscle, is manifested by myocardial infarction and heart failure. Whereas, diseases of the blood vessels supplying the brain – including stroke – are being called cerebrovascular diseases. To counteract the development of a high number of deaths due to CVD, it is important to characterize risk factors and prevent these. Risk factors for CVD are hypertension, dyslipidemia, and metabolic syndrome. These risk factors are affected by several aspects such as tobacco use, unhealthy diets and obesity, physical inactivity, and harmful use of alcohol (World Health Organization, 2017). During the last years, the number of diagnosed obesities in Germany rose constantly. A body mass index of ≥ 30 kg/m² mainly defines obesity, while overweight starts at a BMI of ≥ 25 kg/m². In 1998, the proportion of obesity-diagnosed humans in Germany was 19% for men and 22.5% for women. A recent study of the Robert-Koch-Institute shows an increase of obesity to 23.3% in men and 23.9% in women in the years 2008 to 2011 (Robert Koch-Institut, 2012). The prevalence of overweight or obesity is also growing worldwide, and the number of obesity-diagnosed humans has nearly tripled since 1975. Worldwide, 39% of adults were overweight (BMI ≥ 25 kg/m²) and 13% were obese (BMI ≥ 30 kg/m²) in 2016

(World Health Organization, 2020).

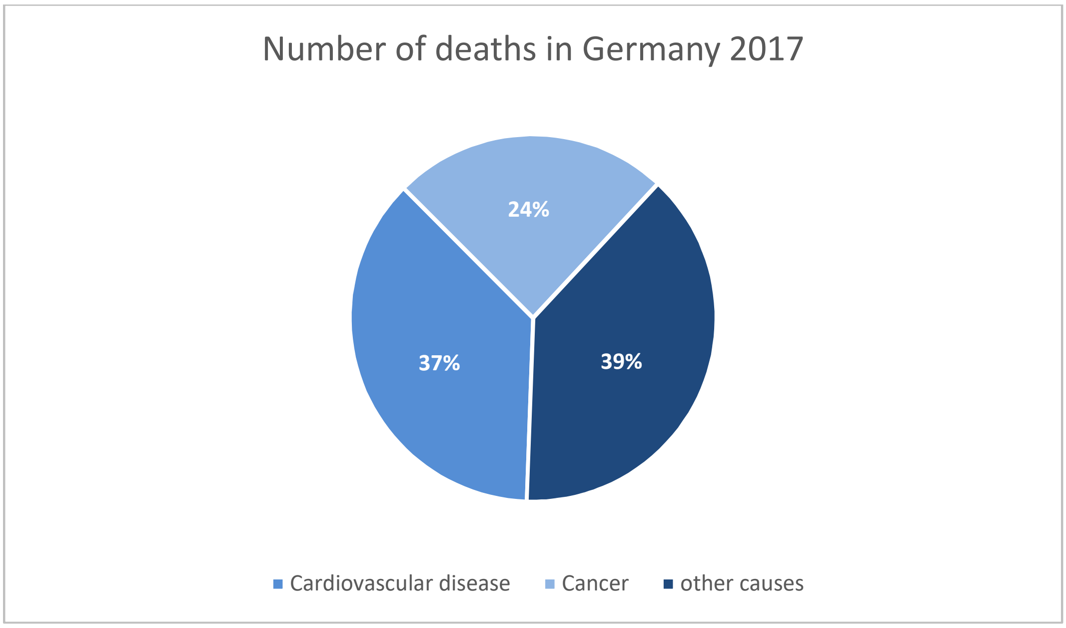

Figure 2. Number of deaths in Germany in 2017 (Statistisches Bundesamt, 2020)

In general, obesity itself influences the risk for CVDs. Many studies, however, found that the strength of impact (on developing CVD) differs depending on the regional distribution of adipose tissue. These findings are confirmed by the fact that the waist circumference as a measure of the adipose tissue in the abdomen including VAT and SAT correlates better with obesity-associated risk factors than does BMI (Zhu et al., 2002). Furthermore, Krotkiewski et al. (1983) described increased metabolic aberrations, such as an increase in triglycerides, fasting insulin, and glucose, associated with the abdominal type of obesity (Krotkiewski et al., 1983). Specific studies examined especially the associations between VAT and cardiovascular risk factors. Although VAT represents only a small body compartment in non-obese adults, it is important for the health risk associated with obesity. An elevated level of VAT is an independent risk factor for type 2 diabetes (Neeland et al., 2012), myocardial infarction (Nicklas et al., 2004), hypertension (Chandra et al., 2014), and all-cause-mortality (Kuk et al., 2006). VAT is also associated with insulin resistance, dyslipidemia, and systemic inflammation (Montague and O'Rahilly, 2000; Fox et al., 2007). Liu et al. (2010) examined in their study nearly 2,500 participants with computed tomography (CT) to measure VAT and SAT. They studied the relationship of those adipose tissue depots with cardiometabolic risk factors. Per 1-sd (standard deviation) increment in VAT or

SAT, they observed elevated levels of fasting plasma glucose and triglyceride, lower levels of high-density lipoprotein-cholesterol, and increased odds ratios for hypertension, diabetes, and metabolic syndrome. The effect size of VAT, however, was larger than that for SAT (Liu et al., 2010). The increased cardiometabolic risk of VAT origins from a higher metabolic activity, a larger number of inflammatory cells, and higher levels of free fatty acids which are drained into the portal vein, as described above (Chapter II.1.2 Adipose tissue as an endocrine organ).

2. Adipose tissue in pigs

2.1. Pig as a model for obesity

"Between animal and human medicine there is no dividing line — nor should there be. The object is different but the experience obtained constitutes the basis of all medicine." is one of the best known citations stated by Rudolph Virchow in the field of comparative medicine in 1858 (Giusti et al., 2019). In the last years, the porcine model has become more relevant for researches especially in the fields of obesity, cardiovascular diseases, diabetes, and organ transplantation. Due to the similar anatomy including the similar size of organs and physiological characteristics involving the cardiovascular, urinary, integumentary, and digestive system, pigs are a suitable model for humans. Further advantages of the use of swine (as model animal for humans) are provided by their omnivore feeding behavior and their willingness to voluntarily consume until reaching obesity. Pigs are therefore prone to many of similar dietary health problems as humans (Rohrer et al., 2002; Swindle et al., 2012). Renner et al. (2016) reviewed comparative aspects of rodents and nonrodent models for mechanistic and translational diabetes research. Main categories were economics, ethics, husbandry, genetics, behavior, reproductive biology, and body dimensions. In summary, when comparing pigs to nonhuman primates, pigs have several advantages like viable reproduction biology with a shorter interval and therefore the ability to produce a larger number of individuals and successive generations in a shorter period. Further, the similar body size delivers adequate amounts of blood and tissue material, which might result in a smaller number of animals needed for research purposes. In the field of genomic research, the methods for genetic modification are also well-established in the porcine model (Renner et al., 2016). Against the background of an increasing proportion of obesity (among humans) worldwide, the interest in research of

obesity-related genes is immense. The size, the complexity, and the chromosomal organization of the porcine genome is similar to humans and comparative genome analyses showed a closer match between pigs and humans compared to mice (Rettenberger et al., 1995; Rohrer et al., 2002). Mutations in the apolipoprotein B allele and the low-density lipoprotein receptor gene result in hypercholesterolemia in pigs. These gene modifications have been likewise described in humans (Innerarity et al., 1990; Aiello et al., 1994; Goldstein, 1995; Hasler-Rapacz et al., 1998). Another example to underline the suitability of the porcine genome in the field of obesity-related research is the candidate gene *ZNF608* associated with the variation of fat mass in pigs (Rothammer et al., 2014). In humans, *ZNF608* has likewise been reported to be associated with the body mass index (Speliotes et al., 2010; Ntalla et al., 2013). Summarizing the advantages and similarities of pigs with humans, the importance of porcine models – especially in the field of obesity related research – becomes obvious.

2.2. Adipose tissue in pigs as livestock

2.2.1. Adipose tissue in meat production

The global meat consumption per capita has risen in the last decades and this trend still continues. The Organisation for Economic Cooperation and Development (OECD) together with the Food and Agriculture Organization (FAO) of the United Nations released an agricultural outlook for the years 2019 to 2028. In this outlook, they still hypothesize an increase of 0.4 kg of global meat consumption per capita compared to the base period 2016-2018. Accordingly, the meat from animals will remain an important source of proteins in the future (OECD/FAO, 2019). The largest pork producers in Europe are Spain with averagely 30.46 million pigs and Germany with 25.96 million pigs (Figure 3). Worldwide, Germany ranked fifth after China, the USA, Brazil, and Spain (Statistisches Bundesamt, 2019; Beckhove, 2019; Statista, 2020).

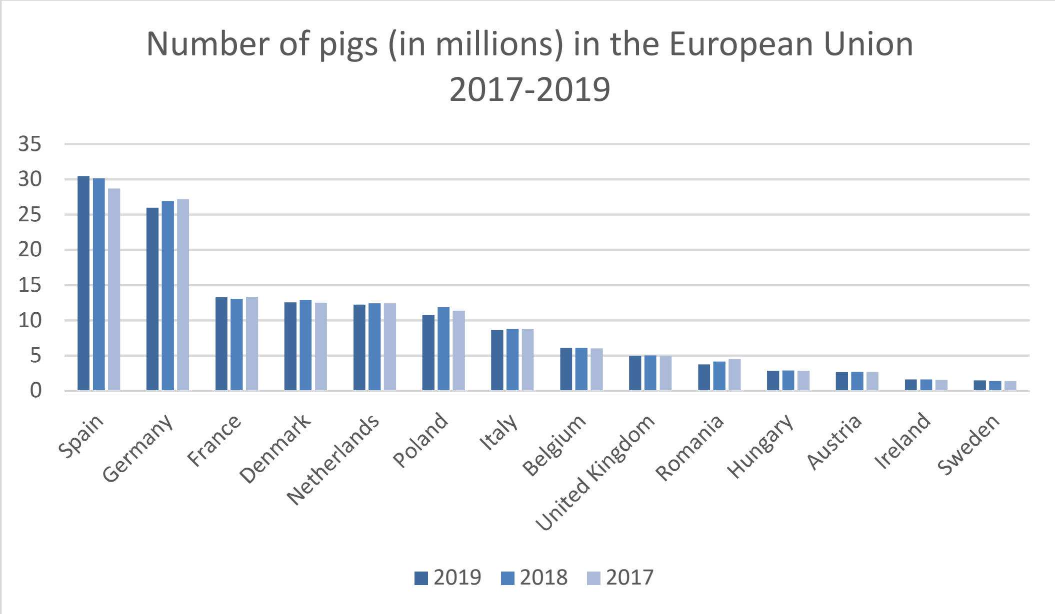

Figure 3. Number of pigs in the European Union 2017-2019 (Statista, 2020)

An average production value of approximately 7 billion euros in the years from 2014 to 2016 indicates the economic importance of the pig industry (Bundesministerium für Ernährung und Landwirtschaft, 2019). For the maintenance of the economic power in the pig industry meeting the demands of the consumers is essential. Therefore, a heavy selection pressure for lean meat in the carcasses with reduced fat resulted (Dunshea and D'souza, 2003). Lean growth, feed intake, and pig survival are the most important traits in pork production (Rothschild et al., 2007). Performance testing in the field or in test stations helps to secure improvements or optimization of these economically important traits for pig breeders in Germany and worldwide. The carcass performance is still very often tested on slaughtered siblings or offsprings of potential breeding pigs (boars /sows) by determining parameters such as lean meat content, backfat thickness, and the meat-to-fat-ratio. Only a very few breeding companies perform a direct test on the potential breeding pigs by using e.g. computed tomography (CT) to measure the amount and percentage of the lean meat. Norsvin, now Topigs-Norsvin, is the pioneer for this commercial performance test strategy (TOPIGS-SNW GmbH, 2019). However, estimating the lean meat percentage based on the thickness of backfat and the longissimus dorsi muscle still classifies the slaughter pigs for payment.

The estimation equation for lean meat content (%) by using an optoelectronic measuring system for the classification is:

$$MF = 60.98501 - 0.85831 * S + 0.16449 * F$$

MF = percentage of estimated lean meat content
S = backfat thickness (including rind), measured 7 cm to the side of the dividing line between the second and third last rib
F = thickness of the longissimus dorsi, using the same position as for S

The classification system includes six different classes for slaughter pigs in the range of 50 to 120 kg.

Table 1. Classification system of pigs in the range of 50 to 120 kg (Schweineschlachtkörper-Handelsklassenverordnung, 2020).

Classes	Percentage of estimated lean meat content
S	≥ 60
E	≥ 55 - < 60
U	≥ 50 - < 55
R	≥ 45 - < 50
O	≥ 40 - < 45
P	< 40

Carcasses of pigs reaching the class “S” yield the highest payments and are therefore desirable for the producers. Against the background of the importance producing high quality meat at “low” costs, it is essential to enforce the growth of lean tissue with a simultaneous reduced growth of backfat. This fact can be seen by the estimation equation in which the backfat thickness influences the percentage of lean meat content to a great extent (Schweineschlachtkörper-Handelsklassenverordnung, 2020). A decrease in total fat content including the inter- and intramuscular fat resulted as a consequence of the development towards a reduced backfat thickness (Vališ et al., 2011). However, a reduction in fat content not only poses merely positive effects. The content of fat, and in particular its composition, influences the processing of specific products and the eating quality. In general, high amounts of polyunsaturated fatty acids are desirable from a human nutritional point of view. But in terms of eating quality, polyunsaturated fatty acids are negatively correlated, whereas monounsaturated or saturated fatty acids are positively associated with flavor and juiciness (Cameron and Enser, 1991). A firmer consistency characterizes polyunsaturated fatty acids, which in turn might negatively influence the quality of raw and dry sausages during processing. In addition, the increased risk of oxidation by fat containing high amounts of polyunsaturated fatty acids influences the quality, too (Leskanich et al., 1993; Pfalzgraf et al., 1995). Biederman et al. (2000) reported that fat layers, which contain high amounts of monounsaturated or saturated fatty acids, are located primarily further away from the surface of the carcass. The content of saturated fatty acids increases in the order of dorsal backfat, ventral backfat, and flare fat, whereas the proportions of mono- and polyunsaturated fatty acids decrease (Biedermann et al., 2000). Furthermore, the increased content of lean meat in the carcass is accompanied by a reduction of the intramuscular fat, which influences meat sensory traits, such as tenderness, juiciness, and flavor (Switonski et al., 2010). In summary, it is important for pig breeding to find a balance between the aim of a high proportion of lean meat and the maintenance of a sufficient content of fat.

2.2.2. Fat accumulation during growth

The development of body composition is determined by different growth intensities of the tissues (Irshad et al., 2013). The development starts with the vital organ systems, followed by the bone system, muscles, and finally fat (Kirchgeßner, 2004). For the development of adipose tissue, Lawrence and Fowler (2002) support the assertion that in the postnatal life of pigs, hyperplasia is the driving force up to an age of approximately 2 months, while hypertrophy is the more important force after an age of approximately 5 months (Lawrence and Fowler, 2002). Against the background of these "developmental" laws, whereby essential tissues are being built first, the strong growth of lean meat content at the beginning, and the increasing fat content at the end of fattening can be explained (Switonski et al., 2010; Bayerische Landesanstalt für Landwirtschaft, 2011). Pigs are normally slaughtered at body weights between 110 and 120 kg, because rearing pigs to heavier slaughter weights results in a lower percentage of lean meat in the carcass (Xue et al., 1997). Fat accumulation speeds up with advancing development. Therefore, the carcass composition is partly determined by the duration of organism growth (Knecht and Duziński, 2016). Consequently, rearing pigs to heavier slaughter weights, leads to an increase of the cost of pork production due to higher costs of keeping the animals longer paired with larger amounts of feed and a proportionally lower payment for the carcass (Switonski et al., 2010). Growth analysis shows a rapid accumulation of subcutaneous adipose tissue after three months, and leads to the fact, that SAT represents the largest fat depot in the body (Davies and Pryor, 1977; Hishikawa et al., 2005). SAT is deposited before the visceral adipose tissue, but Kolstadt (2000) reported an increasing proportion of VAT with increasing live weights (Kolstad, 2000). In accordance, Fischer et al. (2006) found an increase of the abdominal fat in the carcass of heavier pigs. They examined the carcass of Piétrain-Landrace crossbreds at a final weight of 110, 135, and 160 kg. A 9 point scale was used to evaluate the abdomen towards its fatness. The value "1" stands for "heavily fatty" and "9" represents "very lean". In castrated males, the abdominal values changed from 5.0 at a weight of 110 kg to 3.2 at a weight of 160 kg. In females, the values are 7.6 (110 kg) and 4.1 (160 kg) (Fischer et al., 2006). In general, Mohrmann et al. (2006) found the highest accumulation of fat in a weight range between 90 and 120 kg, whereas Giles et al. (2009) reported a range of 80 to 100 kg (Mohrmann et al., 2006; Giles et al., 2009). It can be summarized that the percentage of fat rises as a pig becomes older and heavier (Bracher-Jakob, 2000; Littmann et al., 2006; Bernau, 2011). Besides age and weight, fat accumulation is influenced by other factors (Dunshea and D'souza, 2003), such as ambient temperature (Close and Mount, 1978; Kouba et al., 2001; Trezona et al., 2002), feed intake (Annison and Australia, Standing Committee on Agriculture - Pig Subcommittee, 1987; Gilbert et al., 2007), sex (Chapter II.2.2.3 Sex related differences of adipose tissue in pigs), genetic origin (Chapter II.3 Genetic origin), and selection.

2.2.3. Sex related differences of adipose tissue in pigs

The sex of animals influences the rate of growth, the development, and the tissue composition. Differences between gilts, barrows, and boars can be explained by the anabolic effect of sexual hormones: androgens, especially testosterone, and estrogens. These hormones are produced in the testis of boars. Therefore, boars have the "double dose" of anabolic steroids (Bracher-Jakob, 2000). In gilts, only estrogen of the ovaries is present. As result of castration, these sex hormones are lacking in barrows. Androgens stimulate muscle growth by an increasing protein synthesis, which may lead to a relative and absolute decrease in fat deposition (Irshad et al., 2013). If the dose of androgens is low, energy is transferred to fat at a higher rate (Jaturasitha et al., 2006). Furthermore, androgens have an anti-anabolic effect and therefore protect the muscle against an excessive degradation (Claus and Weiler, 1994). Estrogens effectively promote the deposition of fat, but the effect towards protein synthesis is controversial. Irshad et al. (2013) rates the effect of estrogen as minor, whereas Claus et al. (1994) explains an indirect effect of estrogens on protein synthesis by a stimulation of the release of growth hormones and insulin-like growth factor 1 (Claus and Weiler, 1994; Irshad et al., 2013). In addition, androgens and estrogens lead to a decreased feed intake. Claus et al. (1994) compared the ad libitum feed intake during a three-day control period in barrows to the intake after an injection of steroids. Testosterone in a dose of 0.1 mg/kg leads to a feed intake reduction by 4.4%, and a higher dose of 1 mg/kg even to a change of -21.4%. The same effect can be seen by an injection of estradiol with a dose of 0.1 mg/kg and 1 mg/kg, which leads to a feed intake reduction by 5.3% and 20.2%, respectively (Claus and Weiler, 1994). Newell and Bowland (1972) confirmed the influence of sex towards feed intake in their study. In the growth period up to 50 kg live weight, boars consumed the least and barrows the greatest amount of feed. The feed consumption of gilts was intermediate, but the difference to boars and barrows was not significant. For the entire duration of the project, boars consumed on average 2.17 kg feed per day, gilts 2.38 kg, and barrows 2.48 kg, respectively. The differences in feed intake by sex were not significant for the overall experiment. Nevertheless, the trend established in the growing period, whereby boars consumed the least and barrows the greatest amount of feed, still exists for the overall experiment (Newell and Bowland, 1972). Müller et al. (2010) described a consumption of 2.23 kg per day for boars, 2.27 kg for gilts, and 2.69 kg for barrows (Müller et al., 2010). Furthermore, there is a big debate about the influence of sex towards weight gain. Newell and Bowland (1972) described in the same study, focusing on feed intake, no significant effect of sex on the growth rate, yielding in the average 720 g/day. During the finishing period, boars gained significantly more weight than barrows and gilts (Newell and Bowland, 1972). Jaturasitha et al. (2006) also found no significant effect of "gender" concerning growth rates. Regarding average daily gains (ADG), boars are in first position with 0.68 kg/day, followed by barrows (0.67 kg/day), and gilts (0.64 kg/day) (Jaturasitha et al., 2006). In a Swedish study, Landrace and Yorkshire boars reached slaughter weights of 90, 110, and 130 kg always earlier than barrows and gilts. The peak ADG reach boars at a live weight ten kilograms heavier than barrows. Barrows reached maximum ADG between 70 and 90 kg (Hansson et al., 1975). Bracher-Jakob (2000) and Müller et al. (2010) obtained approximately equal ADG in boars and barrows up to an age of 100 days. After this period, boars show a significantly higher weight gain (Bracher-Jakob, 2000; Müller et al., 2010). In this context, also the feed conversion ratio (FCR), which is influenced by sex, is often examined. In the same study by Müller et al. (2010), the boars need with 2.19 kg/kg the lowest amount of feed for one kilogram weight gain. Gilts reach intermediate values with a FCR of 2.37 kg feed/kg weight gain, while barrows have the highest FCR with 2.66 kg feed/kg weight gain (Müller et al., 2010). In contrast, Jaturasitha et al. (2006) found no significant effect of "gender" concerning the FCR for the overall experiment (body weight range: 30-110 kg). The FCR records, however, are smallest for boars (3.11 kg feed/kg gain) and unexpectedly highest for gilts (3.44 kg feed/kg gain); with barrows being intermediate (3.19 kg feed/kg gain). In the body weight range between 30 and 60 kg, the differences between the sexes were significant showing the same order (Jaturasitha et al., 2006). Newell and Bowland (1972) reported a significant effect of gender on FCR, where barrows reach the highest ratio with 3.40 kg feed/kg gain, followed by gilts (3.31 kg feed/kg gain), and boars (3.01 kg feed/kg gain) (Newell and Bowland, 1972). In a literature review of Xue et al. (1997), concerning the performance, carcass, and meat quality of boars and barrows, the described feed conversion ratios were always higher in barrows with a range between 2.55 and 3.76 kg feed/kg gain compared with boars (2.44-3.47 kg feed/kg gain) (Xue et al., 1997). In the context of growth rates, the ADG, and FCR are records of interest, but of greater importance is which kind of tissues the pig will develop during the fattening period. There, the gain of lean meat tissue is targeted – with a simultaneously low rate of fat deposition. In general, carcasses of boars consist of a higher lean meat content paired with less fat compared to barrows and gilts. Most studies in this field evaluate the conventional carcass traits such as backfat thickness and longissimus muscle area (loin eye area). For barrows, reports state values between 1.4 and 4.4 cm for backfat thickness, and 21.7 to 47.2 cm² for loin eye area. Boars show a lower backfat thickness (1.2-3.5 cm), and larger loin eye areas (24.8-48.5 cm²); while gilts are intermediate (Christian et al., 1980; Xue et al., 1997; Jaturasitha et al., 2006). The same order results for the content of lean meat and fat. Bauer and Judas (2014) obtained the highest lean mean content combined with the lowest fat content for boars (lean meat: 61%, fat: 19%), followed by gilts (lean meat: 59%, fat: 22%), and barrows (lean meat: 57%, fat: 25%) (Bauer Aneka and Judas M., 2014). Xue et al. (1997) reviewed for boars a lean meat percentage in the range of 55.9 to 64.4% with a fat percentage of 18.6 to 34.2%. Barrows showed a higher percentage of fat (27.3-

41.4%) paired with a lower percentage of lean meat (49.7-57.8%) (Xue et al., 1997). In contrast to these results, Jaturashita et al. (2006) described in their study a higher lean meat percentage in gilts (66.6%) compared to boars (63.9%) and barrows (61.8%). The fat content is in accordance with the studies before, where barrows reached the highest percentage with 20.0%, followed by gilts (16.0%) and boars (15.4%) (Jaturasitha et al., 2006). Mitchell et al. (1998) analyzed carcasses of boars and gilts by using dual energy X-ray absorptiometry and found higher percentages of fat for gilts than for boars (33.9% vs. 27.8%). Additionally, the lean meat percentage was lower in gilts (64.5%) compared to boars (70.7%) (Mitchell et al., 1998a). In a study of Pappenberger (2014), examining the body composition in MRI and DXA scans, gilts showed a higher lean meat content (82.6%) and a lower fat percentage (15.0%) than barrows (lean meat: 79.7%, fat: 18%) at an age of approximately 150 days. Further, the lean meat content in the loin (80% vs. 83.8%) and in the ham region (88.9% vs. 90.4%) was lower in barrows compared to gilts. Consequently, barrows showed a higher fat percentage in the loin (20.0% vs. 16.2%) and in the ham (11.1% vs. 9.6%) than gilts (Pappenberger, 2014). Although, bellies from boars contained a higher percentage of lean meat compared to barrows and gilts. Müller et al. (2010) described 60.4% lean meat content in the bellies of boars, 59.2% for gilts and only 55.7% for barrows (Müller et al., 2010). In accordance, Duziński et al. (2015) and Correa et al. (2008) found a higher accumulation of fat in the belly of barrows than of gilts (Correa et al., 2008; Duziński et al., 2015). In a study of Peinado et al. (2008) the same sex related differences of adipose tissue emerged by comparing carcass traits of intact females with castrated females, and castrated males. The lack of anabolic steroid in both animals explains the similarity of all carcass traits for castrated males and castrated females. Carcasses of the castrated individuals were heavier and the backfat as well as the gluteus medius fat thickness were greater. Castrated males got 24.4 mm, castrated females 24.6 mm, and intact females 21.6 mm backfat. Furthermore, the content of muscular fat of the loin was higher in castrated females and castrated males, but no difference was found between the two sexes (Peinado et al., 2008). In summary, sex influences the rate of fat and protein deposition and results in a more muscular and less fat carcass of males compared to females and castrated males.

3. Genetic origin

The pig is one of the oldest domesticated animals and has its origin in the wild boar (Ribani et al., 2019). The domestication of the wild boar started about 9,000 years ago in the Near East. Towards the end of the High Middle Ages, interest in improving pig performance arose in Germany, but coordinated breeding did not begin until after the establishment of a studbook or respectively a herd book in the 1880s together with the founding of the Chamber of Agriculture. In Germany, the most common pig breeds are German Landrace, Large White, and Piétrain. The different demands of breeders, fatteners, and meat processors lead to various breeding objectives for the breeds. A number of 73 herd book holdings in Bavaria are organized within the producer organization “Erzeugergemeinschaft und Züchtervereinigung für Zucht- und Hybridzuchtschweine in Bayern w.V. (EGZH)” securing a standardized breeding scheme. In 2016, the genomic estimation of breeding values was introduced for EGZH pig breeders in Bavaria (Bayerisches Staatsministerium für Ernährung, Landwirtschaft und Forsten, 2018). In general, the determination of breeding values as early as possible is desirable and will lead to a shorter generation interval with a faster achievement of the breeding objectives (Schaeffer, 2018). Furthermore, the classifications for pig breeds are sire or dam breeds, and within these the requirements towards specific traits vary. In Germany, German Landrace and Large White are classified as dam breeds with a stronger focus on fertility related traits, whereas Piétrain belongs to the sire breeds with a major focus on carcass quality traits. Within the breed Duroc, a sire and a dam breed line exist in Germany. However, this classification system is not standardized worldwide. For example, a sire breed line out of the Large White dam bred was selected in Switzerland in the year 2002 (Willam and Simianer, 2017). Actually, every breed could theoretically serve either as dam or as sire breed – always depending on the breeding objectives and the selection program. Figure 4 illustrates the EGZH breeding objectives with their proportional weights within the overall breeding value for the breeds: Piétrain – as a classical sire breed, and for German Landrace and Large White – as dam breeds. The main breeding objectives for sire breeds are fattening and carcass performance, which show up as very efficient feed conversion, as well as outstanding lean meat contents including large loin eye areas and small (back) fat areas (or depths). High fertility and good mothering skills are of major interest in dam breeds. The following chapters describe the four breeds used in this study and the crossbreeding scheme is illustrated in Figure 6 (Chapter VIII Supplementary Material).

Highlighting the differences in the breeding objectives and characteristics will help to explain the influences of genetic origins towards fat accumulation.

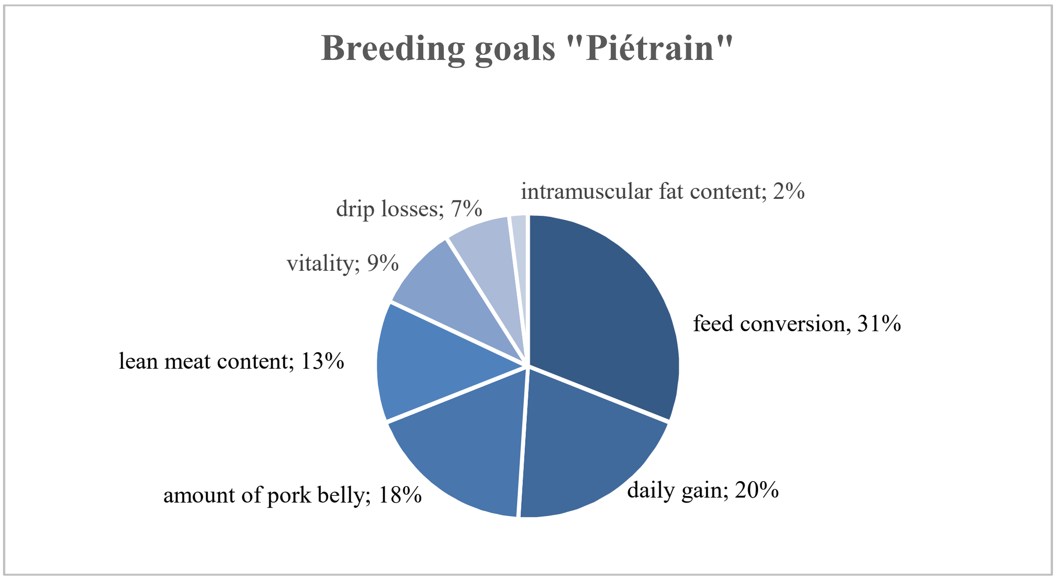

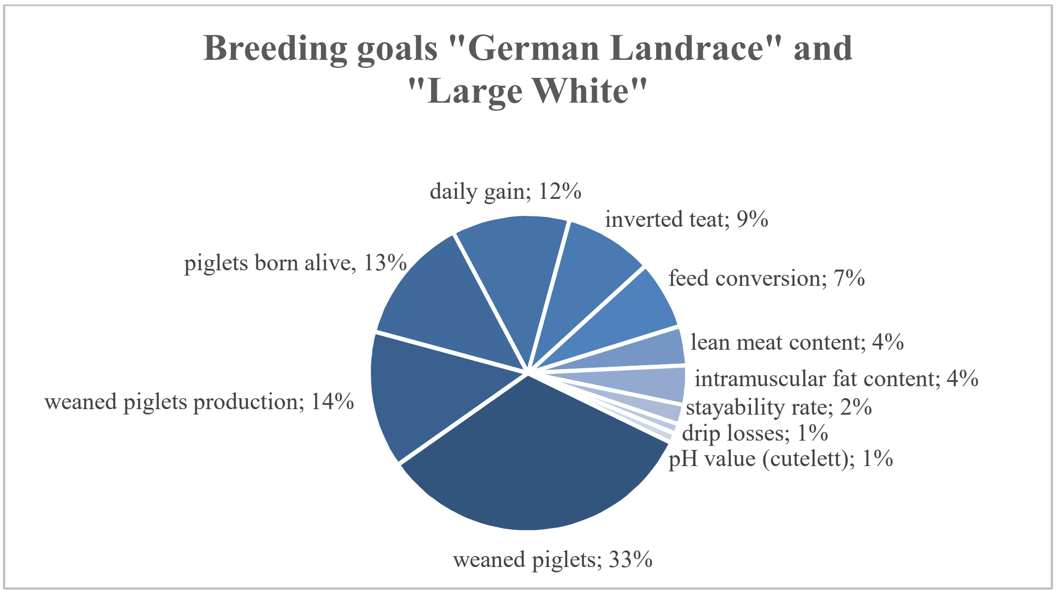

Figure 4. Breeding goals of sire (Piétrain) and dam (German Landrace and German Large White) breeds modified according to "Erzeugergemeinschaft und Züchtervereinigung für Zucht- und Hybridzuchtschweine in Bayern w.V" (EGZH) (2015)

3.1. German Landrace

German Landrace is the most common dam breed in Germany. In 2018, 6,028 sows and 153 boars were registered (Weiß, 2011; Gesellschaft zur Erhaltung alter und gefährdeter Haustierrassen e. V., 2020a). The crossing of different local breeds by including "Yorkshire" boars led to the Landrace breed at the end of the 19th century (German Genetic, 2020). In the 1950s, the demands of the society changed towards leaner pigs and therefore, especially pigs with Danish "genetic" were crossed into the local Landrace lines. As result of this "refinement" crossing, our typical "German Landrace" emerged as a long meat pig (porker). German Landrace is large-sized with a white skin, white bristles, and dropping ears (Bellof and Granz, 2018). Furthermore, a high fertility, which shows up as excellent rearing performance combined with a high milk yield, is characteristic for this breed. Besides the important traits in the context of fertility, high daily gains with a favorable feed conversion resulting in an optimal meat performance with a high percentage of valuable parts are attained (Sambraus, 1987). The German Landrace is consequently a stress stable and fertile universal pig (Vogt, 2016). Breeding goals are being consistently adapted to reach the demands of the consumers, the breeders, and the fatteners. Presently, animal welfare and ethnicity play a major role besides the performance. The Bavarian State Research Center for Agriculture (LfL), for example, specified the breeding objectives in 2010 towards better fertility, what resulted in an initial fall of the lean meat content. After changing the breeding strategy again in 2015, it took another 5 years to return to the level of 2010. Since 2016, in addition to the number of weaned piglets, the weight of the piglets and the number of stillborn piglets have been recorded in order to achieve homogeneous litters and a good rearing performance, which are reflected in the breeding goals for 2020 (Bayerische Landesanstalt für Landwirtschaft, 2020). Current breeding objectives are: more than 14 piglets born alive, more than 900 g daily gains, a lean meat content of over 56% in barrows, and less than 2.7 kg feed per kg gain (Hybridschweinezuchtverband Nord/Ost e.V., 2020). The breeding report of 2019 by the LfL describes for German Landrace daily gains of 959 g for boars and 1,000 g for barrows, a lean meat content of 57.6% for boars and 53.7% for barrows, as well as a meat-to-fat-ratio of 0.41 for boars and 0.51 for barrows (Bayerische Landesanstalt für Landwirtschaft, 2020). Table 2 summarizes the achieved performance testing results regarding growth and carcass traits for all examined breeds in Germany.

The trend in fertility and weaning performance in Germany shows an increasing number of piglets born alive, a higher number of piglets weaned per sow and year, but also an increase of piglet losses. The means of the last decade are 13.6 piglets born alive, 27.3 piglets weaned per sow and year, and 14.7% piglet losses. In 2018, German Landrace sows gave birth to averagely 15.2 piglets alive and raised 29.9 piglets per sow and year until weaning. The piglet losses increased by 0.5% to 15.2% in 2018 compared to the average of the last ten years (Bundesverband Rind und Schwein e.V., 2019).

Table 2. Performance test results for growth, feed efficiency, and carcass quality of four German pig breeds - 2018 (Bundesverband Rind und Schwein e.V., 2019)

		Piétrain	German Landrace	Large White	Duroc
	boar	202	611	67	
Number of animals	sow	720	47	2	54
	barrow		1,463	455	
	boar	882	941	927	
Daily gains (g)	sow	833	885	900	920
	barrow		996	951	
	boar		2.3	2.4	
Feed conversion (kg feed/kg gain)	sow		2.6	2.6	2.5
	barrow		2.6	2.6	
	boar		46	45	
Loin eye area (cm²)	sow	71	50		52
	barrow		46	47	
	boar		0.4	0.3	
Lean-fat-ratio	sow	0.1	0.3		0.3
	barrow		0.5	0.5	
	boar		18.6	19.7	
Backfat thickness (mm)	sow	14.1	20.7		21
	barrow		23.9	25.1	
	boar		58.1	58.3	
Lean meat content (%)	sow	67.6	58.2		62.3
	barrow		54.4	54.4	

3.2. Large White

The Large White originated from the “Marschschwein” and the English Yorkshire by displacement breeding in the second half of the 19th century. In 1904, Germany recognized the “Large White” as an official breed. Since the breeding goals for Large White already aimed at meat performance, the changed consumer requirements in the post-war period did not lead to drastic changes of the type. In 2018, 4,149 female and 99 male Large White pigs formed the population in Germany (Gesellschaft zur Erhaltung alter und gefährdeter Haustierrassen e. V., 2020b). The exterior of the Large White resembles the German Landrace: large-framed, white skin, and white bristles; but is further characterized by a medium length, a broader head, and prick ears. Prematurity, a “good” feed conversion, a stable constitution, as well as a high fertility and a “good” meat performance are specific characteristics of this breed (Sambraus, 1987; Falkenberg and Hammer, 2007). In addition, the Large White is only slightly susceptible to stress and is sometimes even considered to be 100% homozygous stress stable (Bellof and Granz, 2018; Gesellschaft zur Erhaltung alter und gefährdeter Haustierrassen e. V., 2020b). As mentioned before (Chapter II.3 Genetic origin), the Large White is classified as a dam breed in Germany, whereas a dam and a sire line exist in Switzerland since 2002. Both lines differ accordingly in their breeding goals. The breeding association "Hybridschweinezuchtverband Nord/Ost e.V." describes the following breeding objectives for the Large White: more than 13 piglets born alive, less than 2.6 kg feed per kg body weight gain, more than 900 g daily gain and a lean muscle content of more than 56% in barrows (Hybridschweinezuchtverband Nord/Ost e.V., 2020). In the review of Leenhouwers and Merks (2013), different performance objectives in various European countries (including inter alia Denmark, Sweden, Italy and Spain) were collected in the years 2006 to 2010. For the Large White, they report 11.5 piglets born alive, 9.4 weaned piglets per litter, and 2.2 litters per year (Leenhouwers and Merks, 2013). Using the database of the Hybridschweinezuchtverband Nord/Ost e.V. of the years 1997 to 2010, Freyer and Mayer (2012) described 10.5 piglets born alive in the first litter and 11.3 in further litters (Freyer and Mayer, 2012). In the field of carcass performance, the Large White achieved similar results as the German Landrace, but the significantly lower number of examined animals is inevitable to consider. Table 2 contains the corresponding records. Barrows reached a lean meat content of 54.4%, with a meat-to-fat-ratio of 0.5 and a backfat thickness of 25.1 mm. The daily gains were 927 g for boars, 900 g for sows, and 951 g for barrows.

3.3. Piétrain

The name of this breed can be traced back to a small village called "Piétrain" in Belgium, where a single breeder kept these pigs in the years after the First World War. Already around 1930, higher revenues were achieved with Piétrain pigs, but the breed was not officially recognized until 1951. Its genetic origin is still partially unknown, but it is hypothesized that the breed originated from the French breed Bayeux. In the end of the 1950s, the first pigs were imported to Germany. Nowadays, it is the most often used sire breed (in Germany and other parts of the world) due to its high lean meat content (Sambraus, 1987; Kräusslich and Brem, 1997; Bellof and Granz, 2018). Piétrain pigs are medium framed with a deep and wide body, white to grey colored with black or brown spots, and short prick ears. Characteristics of this breed are a low percentage of fat and a high lean meat content, especially in the shoulder and ham, which is responsible for calling these pigs “Four-Ham-Pig”. However, the high susceptibility to stress and the poor meat quality, were negative characteristics of this breed (Sambraus, 1987; Bellof and Granz, 2018). Since stress influences the meat quality, breeders put strong efforts towards the reduction of the stress susceptibility rate. Genotyping by PCR helped to detect the (homozygous and heterozygous) stress susceptible pigs by identifying the malignant hyperthermia syndrome (MHS) genotype to determine whether a mutation of the ryanodine receptor gene 1 exists, which is responsible for the susceptibility to stress (Littmann et al., 2006; Bellof and Granz, 2018). Even though, homozygous stress stable Piétrain lines are already available, MHS testing is still mandatory for this breed (Littmann et al., 2006; Bellof and Granz, 2018). The breeding objectives of the Hybridschweinezuchtverband Nord/Ost e.V. are daily gains of 800 g, less than 2.4 kg feed per kg body weight gain, and more than 63% lean meat content in barrows (Hybridschweinezuchtverband Nord/Ost e.V., 2020). In 2018, only boars and sows were examined by the German Livestock Association (BRS), they reached daily gains of 882 g for boars and 833 g for sows. With a lean meat content of 67.6%, a backfat thickness of only 14.1 mm, and a meat-to-fat-ratio of 0.1 (values in sows), the Piétrain pigs meet the consumer requirements of lean pork (Table 2) (Bundesverband Rind und Schwein e.V., 2019). Piétrain pigs in Bavaria reached daily gains of 831 g, a feed conversion rate of 2.24 kg feed per kg body weight gain, and a lean meat content of 68% (Bayerisches Staatsministerium für Ernährung, Landwirtschaft und Forsten, 2018). In the field of fertility, Piétrain sows farrow on average 2.36 times a year with 10.3 piglets born alive and a total number of 11.3 piglets per litter (Hybridschweinezuchtverband Nord/Ost e.V., 2013). In summary, the Piétrain pig is suitable to be used as “the” sire breed for the production of fattening hybrids, due to the most preferred conformation (in Germany) and medium daily gains (Bellof and Granz, 2018).

3.4. Duroc

This breed originated in the East of the United States, as well as in Corn Belt. It is assumed that they developed out of the Jersey Red of New Jersey and the "Duroc" of New York (Breeds of Livestock - Department of Animal Science, 2020). Since 1885, a breed standard exists for Duroc. This breed is widely dispersed throughout Europe and North America. In Germany, this breed is present since 1980, but only a few pure breeding sites for Duroc exist. This and other European countries use Duroc especially for crossbreeding programs due to their high robustness and their high intramuscular fat content, which leads to a good meat quality. All pigs are stress stable (Sambraus, 1987; Bellof and Granz, 2018). Weißmann et al. (2010) have shown in their study, that already a proportion of 25% Duroc genes significantly promotes meat quality under organic fattening conditions (Weißmann et al., 2010). Pigs of this breed are large-framed, light red to red-brown colored, have a clear curved (convex) back, and dropping ears (Sambraus, 1987; Kräusslich and Brem, 1997). Durocs are characterized by excellent growth rates (Bellof and Granz, 2018). The Hybridschweinezuchtverband Nord/Ost e.V. defines more than 900 g daily gain, less than 2.8 kg feed per kg body weight gain, a lean meat content of more than 57% in barrows, and more than 11 piglets born alive per litter as breeding goals for Duroc (Hybridschweinezuchtverband Nord/Ost e.V., 2020). In 2018, the examined Duroc sows in Germany achieved daily gains of 920 g with a feed conversion rate of 2.5 kg feed per kg gain, a lean meat content of 62.3%, a backfat thickness of 21 mm, and a meat-to-fat-ratio of 0.3 (Bundesverband Rind und Schwein e.V., 2019). Glodek et al. (2004) compared in their study the effect of different sire breeds on growth, carcass composition, and meat and fat quality. They found a higher daily gain (+ 33 g), but a smaller loin eye area resulting in a smaller lean meat content in crossbreds originating from Duroc terminal boars compared to crossbreds originating from Hampshire or Piétrain terminal boars (Glodek et al., 2004). Some Duroc sow lines are characterized by having good maternal attributes and a high milk yield (Bellof and Granz, 2018). Furthermore, they reached on average 2.3 litters per year, with totally 11.5 piglets born per litter, and 10.6 piglets born alive (Hybridschweinezuchtverband Nord/Ost e.V., 2013). Duroc pigs may be used as terminal sire line or as dam line to positively affect growth, stress stability, and meat quality. However, small losses in the meat content must be expected (Kurt and Klont, 2010; Bellof and Granz, 2018). Pedersen et al. (2019) examined the differences in paternal fertility and mortality during the suckling period of crossbred progeny from Piétrain and Duroc terminal sire lines. The total number of piglets born were higher when Piétrain boars (total number: 18.7) were used as the terminal sire line than when Duroc boars (total number: 18.2) were used. However, the mean litter sizes were 14.5 and 14.9 in Piétrain and Duroc litters, respectively, at 21 days after birth. Consequently, the mortality of Piétrain piglets was significantly higher than for Duroc piglets. The mortality rate including still born piglets was 19.1% in the Duroc litters and 23.6% in the Piétrain litters (Pedersen et al., 2019).

4. Medical imaging methods

4.1. Magnetic resonance imaging

Magnetic resonance imaging (MRI) is a non-invasive medical imaging method to display the inside of the body using magnetic fields and high frequency pulses. Since the 1980s MRI is an important component of clinical diagnostics and is constantly being improved. Besides computed tomography, MRI is the most common method of medical imaging in human medicine. The MRI is remarkable for its accurate, multiplane, and three-dimensional imaging without the need for harmful X-rays. Furthermore, a good soft tissue differentiation characterized the MRI and it is therefore suitable for examination of the abdomen. However, due to long acquisition times and the need of a motionless positioning, sedation may be carried out in humans and it is indispensable in animals. Experts are essential for sedation, for the investigation, and the evaluation of the cross-sectional images. In addition, the investment cost, as well as the running cost of a MRI system are high (Mihaljevic et al., 2009).

4.1.1. Technical functionality of MRI

In contrast to many other imaging techniques, the MRI does not rely on harmful ionizing radiation but rather uses magnetic fields and radio frequency radiation. The object to be examined is placed in an external magnetic field with a strength of typically about 0.5-1.5 (3.0) T. The part that needs to be examined is irradiated with radio waves, and finally the data are obtained by detecting radio waves emitted by the hydrogen atoms in the object.

The underlying physical principle of MRI is the nuclear magnetic resonance, where spinning magnetic moments of atomic nuclei are brought into resonance. In particular, hydrogen nuclei, which are protons, are considered in MRI being the most abundant nuclei in biological tissue. An important characteristic of protons is their spin, which has two states - up and down - while the proton itself is randomly oriented in space. The magnetic moment is proportional to the proton charge and points in the direction of the spin. Given a large number of protons, their random orientation leads to zero net magnetization. When the object is placed in an external magnetic field, the protons either align parallel or antiparallel to the magnetic field vector. Since the parallel orientation is energetically favorable, more protons align in parallel direction (Schild, 1997). This leads to a net magnetization in the direction of the external magnetic field vector (longitudinal magnetization). However, the proton magnetic moments do not align exactly along the field vector but rather precess around it. The precession frequency (Larmor frequency) is unique for every type of atom that has a net spin. Considering only a single proton, the precession leads to a non-zero transversal magnetization. Taking into account all hydrogen nuclei in the examined object, the net transversal magnetization is zero since their precession is out of phase.

In the next step, gradient coils expose the examined tissue to electromagnetic radiation with a frequency matching the precession frequency of the hydrogen nuclei. The resulting resonance initiates two processes elevating the system to a higher energy state:

- Due to the introduction of energy into the system, parallel-aligned spins flip in antiparallel orientation until the number of parallel and antiparallel spins is equal. This leads to a zero net magnetization in longitudinal direction.
- The precession of the protons is brought into coherence leading to a non-zero transverse magnetization.

By turning off the radiation, the system returns to its previous lower energy state through relaxation. Relaxation can be divided into two types. The first one is the longitudinal or spin-lattice relaxation describing the antiparallel spins flipping back to parallel, which increases the longitudinal magnetization. The second type is the transversal or spin-spin relaxation describing the precession of the proton magnetic momenta going out of phase, which decreases the transversal magnetization. The relaxation times are defined as longitudinal (T1) and transversal relaxation time (T2) (Schild, 1997; Mihaljevic et al., 2009). T1 is the time it takes for the increasing longitudinal magnetization to reach 63% of its maximum and T2 is the time it takes for the decreasing transversal magnetization to go down to 37% of its maximum.

T1 and T2 are specific for different types of tissue. Therefore, T1 and T2 time help to distinguish among body tissues. Water characteristically has a very long T1 and T2, whereas larger molecules, such as fat, have a short T1 and T2. The different relaxation times in combination with using several high frequency pulses help to distinguish different tissues (Schild, 1997). Depending on the pulse sequences, T1- or T2- weighted images can show and emphasize different tissue characteristics. Table 3 summarizes how the tissues are displayed in the correspondingly weighted image (Mihaljevic et al., 2009; Weishaupt et al., 2014).

Table 3. Resonance intensity of tissues in T1- and T2-weighted images

	Hyperintens	Hypointens
T1-weighted	Fat, high-fat tissue (white brain matter)	Water (liquor, edema, inflammation) Bones (in general hard to display due to the minimal water content) Muscle Ligaments, tendons Air (no signal)
T2-weighted	Water (liquor, edema, inflammation) Fat (less hyperintens as in T1)	Bones Ligaments, tendons Muscle Air (no signal)

The MRI device measures longitudinal and transversal magnetization. A proper localization of the signal is necessary to obtain an image. Therefore, orthogonal gradient fields in x, y, and z direction are applied where the z-axis points along the main magnetic field leading to a varying magnetic field across the examined object. Since the Larmor frequency of the hydrogen nuclei is proportional to the magnetic field, a superposition of the gradient fields upon the main magnetic field divides the object space into volume elements (voxels) with slightly varying Larmor frequencies. In a final step, the data is subject to an inverse Fourier-Transformation, in order to obtain a greyscale image for every z-slice.

4.1.2. Artifacts in the MR image

The magnetic resonance tomography is prone to artifacts, and the knowledge and especially the recognition of these artifacts are important for a correct evaluation of MR images. The main group of artifacts is patient related and leads to blurred images. Long examination times often lead to motion and flow artifacts. Patient movement, intestinal peristalsis, or the heartbeat, and breathing cause motion artifacts. Whereas, circulating blood in large vessels leads to flow artifacts. For examinations of the abdomen, this group of artifacts plays an important role and must be considered in the evaluation. The next group are signal processing dependent artifacts including chemical shift, phase wrap-around, and partial volume artifacts. The resonance frequency of protons varies according to the chemical surrounding and can lead to a mislocalization of the signal. Water and fat interfaces amplify this artifact, which shows up as dark line around the interfaces. Phase wrap-around is an effect, which projects structures laying outside the image section into it and occurs, when the dimension of the object exceeds the defined field of view. It can be recognized as a folding over of anatomic parts into the area of interest (Mihaljevic et al., 2009). The occurrence of structures with different signal intensities (for example muscle and fat) within a voxel causes partial volume artifacts. The signal intensities are being averaged and show up as an average grey value of all tissues within one voxel (Mihaljevic et al., 2009; Weishaupt et al., 2014).

4.1.3. MRI in pigs

During the last years, many studies evaluated the potential of MRI to evaluate the body composition. In general, the MRI serves as a reference method for body composition analyses in pigs and their carcasses. This non-invasive imaging technology has the ability to determine the exact (direct) volume of tissues, but often estimation equations are being used by analyzing only a defined body region or area. In addition, it is possible to examine the growth dynamics of pigs (or other animals) over a certain period by performing repeated measurements. In the field of livestock breeding, MRI allows a direct study of the potential breeding pig, and testing the offspring combined with slaughtering them could become less important.

Bernau (2011) analyzed the body composition in male and female pigs with a weight of 80 kg and 100 kg and tried to estimate the body composition of the 100 kg pigs based on the values of the pigs with a weight of 80 kg. This study examined the lumbar, the femoral, and the gluteal region of 95 sows and 22 boars with different genetic origins (including crossbreds) by using an open low-field MRI system. In the lumbar region, the volume of the longissimus dorsi muscle, as well as its above located fat volume, showed a high relationship between the two measurements at 80 and at 100 kg body weight (R^2 for the volume of the longissimus dorsi muscle = 0.86, RMSE = 82 cm^3 / R^2 for the fat volume above the longissimus dorsi muscle = 0.91, RMSE = 41 cm^3). The relationship of these values was even higher for boars only (both $R^2 = 0.97$). In the femoral and gluteal region, the regression coefficient for muscle ($R^2 = 0.79$, RMSE = 292 cm^3) and fat ($R^2 = 0.44$, RMSE = 137 cm^3) volume was lower than in the lumbar region. Overall, the results of this study show the ability of MRI to estimate the body composition in pigs with 100 kg based on values at a weight of 80 kg. Therefore, an earlier performance test would provide the opportunity to slightly shorten the generation interval by evaluating the potential breeding animals at younger ages with smaller body weights and to sort out inappropriate animals earlier (Bernau, 2011). Genomic selection, however, makes this approach of an earlier performance test obsolete.

The study of Fowler et al. (1992) quantified the adipose tissue in lean and obese pigs *in vivo* and compared the MRI data with dissection and chemical analyses. The killed and frozen pig was sliced at the location of the MRI sections, in order to analyze the adipose tissue and lipid content of every slice. Fowler et al. (1992) conclude a high accuracy of MRI to quantify adipose tissue *in vivo* due to the high relationships between MRI and dissection or chemical analyses results. MRI underestimated the percent of abdominal adipose tissue and overestimated the percent of cervical adipose tissue by less than 6% (Fowler et al., 1992).

In addition, Monziols et al. (2006) determined the ability of MRI to quantify muscle, subcutaneous and intramuscular fat in carcasses and cuts of pigs. The results of total fat content and subcutaneous fat showed high relationships for all cuts between MRI and dissection ($R^2 > 0.92$). In addition, the regression coefficients for lean meat content between the MRI and the dissection in single cuts and in the whole body were high with values of $R^2 = 0.95$ to 0.99. In conclusion, Monziols et al. (2006) rates the ability of using MRI examination as very high and hypothesized that MRI could replace the classical dissection (Monziols et al., 2006).

Mitchell et al. (2001) tried to find a specific region to best predict the body composition by studying 111 pigs with MRI. By using the fat volume from the 10-cm section of longissimus muscle and the fat-muscle ratio from the 15-cm section of the ham leads to the best prediction of the percentage of total body fat. Whereas a combination of the fat volume from the 10-cm section, the fat-muscle ratio from the 15-cm section of the ham, and the lean volume percentage from the 15-cm section of the ham provided the best prediction of total body lean percentage. Furthermore, the MRI volume of the backfat exceeded slightly (approximately 2%) the dissected back fat weight, whereas the MRI volumes of several muscles were smaller than the dissected muscle weights (Mitchell et al., 2001).

In addition, Baulain et al. (2010) showed that MRI can be applied to estimate the carcass composition in various pig breeds instead of using a full dissection. The carcass and primal cuts of 202 pigs in four different weight classes with an interval of 10 kg from 75 to 115 kg were scanned with MRI. As reference served the lean meat percentage estimated according to the performance test guidelines in Germany using the "Bonner formula". By determination of five virtual cuts on basis of the MRI images, Baulain et al. (2010) tried to find the best region to predict the total carcass composition. The ham region showed the greatest errors for all breeds, whereas scanning only the shoulder region was sufficient to estimate the muscle content of the entire carcass in Piétrain sire lines. In general, the regression coefficients between MRI and performance test results ("Bonner Formula") were always higher than $R^2 = 0.95$ (Baulain et al., 2010).

Bernau et al. (2015) investigated the potential of non-invasive imaging methods (MRI and DXA) to update the used regression equation ("Bonner formula") for stationary tested boars. For the lean meat percentage, a high relationship was observed between the MRI data (thoracic region and ham region), and the dissection results ($R^2 = 0.88$, RMSE = 0.90%). Therefore, the new formula (MRI) could be based on these variables. By comparing the reference lean meat percentage from the dissection with the results of the formulas, the new formula (MRI) ($R^2 = 0.71$, RMSE = 1.35%) achieves nearly the same accuracy as the "Bonner formula" ($R^2 = 0.74$, RMSE = 1.29). If MRI and DXA data are combined (1. DXA shoulder lean tissue, 2. DXA ham lean tissue, 3. Total back fat volume above the *Musculus longissimus thoracis et lumborum*) to create a new formula, the accuracy compared to the dissection results was as accurate as the "Bonner formula, but relies on only three instead of seven variables (Bernau et al., 2015a).

Besides the analysis of body composition, MRI is also used for other purposes in pigs, like e.g. the study of cartilage tissue in growing pigs of different genetic origins (Winkler, 2017). Dölle (2019) studied the effect of different housing systems on the prevalence of osteochondrosis as the main cause of the leg weakness syndrome (Dölle, 2019).

Bernau et al. (2015b) used the MRI technology for safety testing of veterinary vaccines by examining the injection site at frequent intervals. MRI allows a 3D quantification of the extent of local reactions *in vivo* and is therefore suitable as a non-invasive method in the field of safety testing. Furthermore, Bernau et al. (2015b) conclude that the use of MRI may reduce the number of animals for safety testing (Bernau et al., 2015b). Likewise, MRI can be used in suckling pigs in terms of safety testing (Bernau et al., 2018a).

In addition, MRI was used to evaluate the possibility of predicting boar taint in live pigs non-invasively. Bernau et al. (2018b) found out that larger testis volumes and a higher amount of body fat (especially belly fat) are associated with a higher level of androstenone. Consequently, the development of an on-farm testis measurement would help farmers to predict tainted boars and allow earlier slaughtering to prevent tainted meat in single animals (Bernau et al., 2018b).

4.1.4. Use of MRI for VAT examination in humans

MRI is considered as gold standard of VAT determination and is together with CT the *in-vivo* method of choice for directly quantifying the distribution of adipose tissue in humans (Thomas and Bell, 2003; Lee and Gallagher, 2008; Shuster et al., 2012; Staiano and Katzmarzyk, 2012). MRI is characterized by a high accuracy, no radiation exposure and shows a good reproducibility with a coefficient of variation (CV) for repeated VAT measurements of approximately 9% to 18% as Shen et al. (2003) summarized in their review. The higher coefficient of variation for MRI compared to CT (CV approximately 2%) may be explained by the longer acquisition time, the variation of pixel intensities due to magnetic field heterogeneity, and the influence of sequence and motion related artifacts (Chapter II.4.1.2 Artifacts in the MR image) (Shen et al., 2003). The proton relaxation time of fat with a short T1 and a long T2, allows a good identification of fat by using T1-weighted sequences. Fat shows bright signal intensity in these sequences and strongly contrasts surrounding tissues (with lower signal intensities). In the area of the abdomen, especially the partial volume artifact must be considered, and also fat in the bowel may falsify the results (Abate et al., 1994; Scholz et al., 2015). Furthermore, many studies vary in their methodology of MRI examination. Often, only a single-slice method is used, due to a shorter examination and evaluation time, and lower costs. However, single slices are less accurate and can only determine an area and not the volume of VAT as do multiple-slice or whole-body imaging protocols. For single-slice protocols, the L4-L5 (lumbar vertebra) intervertebral space is most often used and in the study of Thomas and Bell (2003) a higher correlation between the whole-body MRI and the image in this region was found compared to an image in the L2-L3 level. Thomas and Bell (2003) scanned 59 premenopausal healthy women with a mean BMI of 28.4 kg/cm² and a range of 13.8 to 86.3 l total body adipose tissue content. They used a single-slice and a whole-body method with a T1-weighted spin-echo sequence (Time to repeat (TR) = 36 ms, Time to echo (TE) = 14 ms). The correlation for intraabdominal fat was stronger for the L4-L5 image ($R^2 = 0.76$) than for the L2-L3 image ($R^2 = 0.56$) when compared to the whole-body-method. In addition, by separating the individuals in two groups, according to their BMI (lean and overweight/obese individuals), the correlation was altered. In the lean group (mean BMI = 22.5 kg/cm²), the L2-L3 image showed a higher relationship with the whole-body measurement and a regression coefficient of 0.88. For overweight/obese individuals (mean BMI = 33.3 kg/cm²), the association significantly decreased for the L2-L3 image ($R^2 = 0.33$). The results of the L4-L5 regions did not change largely by subdividing the individuals according to their BMI. Furthermore, Thomas and Bell (2003) tried to evaluate the ability of single-slice and whole-body methods to detect longitudinal changes in visceral fat content by studying 17 non-obese healthy premenopausal women before and after a period of 6 months of aerobic exercise. In conclusion, single-slice MRI is suitable for assessing changes in intra-abdominal fat content in a large sample. For an accurate determination of the individual intraabdominal fat content and for an inter-subject comparison, however, a multi-slice imaging is needed (Thomas and Bell, 2003). In contrast to the results of Thomas and Bell (2003), where the L4-L5 single slice achieved the closest correlations for the whole cohort, Demerath et al. (2007) obtained the best results for a single slice at 6 cm above the L4-L5 intervertebral space. They concluded that a single slice at about the level of L3 (in 85% of subjects the slice at 6 cm above L4-L5 crossed the L3 vertebra) can accurately estimate the total VAT in individuals with different genetic origins (black, white), and different sexes (female, male). Overall, Demerath et al. (2007) examined 820 individuals with an age range of 18 to 88 years by MRI (TR 322 ms, TE 12 ms) (Demerath et al., 2007). Another important fact to consider when comparing the ability of single-slice and multi-slice methods is the assumption of an identical distribution of VAT within the abdominal cavity by using the single-slice method (Thomas and Bell, 2003). Therefore, changes of fat distribution may not be detected in single-slice protocols (Staiano and Katzmarzyk, 2012). In summary, multi-slice imaging protocols are the preferred option for volume calculation (Thomas and Bell, 2003; Shuster et al., 2012).

To quantify fat in MRI, firstly, the identification and segmentation of fat depots is necessary. To reduce the time and the potential bias of the data concerning a manual analysis, using mainly semi-automated or automated approaches for quantification can be helpful. Kullberg et al. (2007) described a fully automated segmentation of VAT from abdominal MRI with a high accuracy (mean value and standard deviation of the automated analysis and the reference results: 2.0%±14%) and reproducibility ((measurement1-measurement2)/measurement1= 0.24%±7.1%) (Kullberg et al., 2007). Segmentation of abdominal MR images is difficult for several reasons, such as the lack of a homogenous signal intensity profile, the complex shapes, motion artifacts, and a low signal-to-noise-ratio. Image analyses in the abdominal cavity are challenging with the absence of regular boundaries between VAT and other tissues/organs (Bhanu Prakash et al., 2014).

In general, a standardized MRI protocol for VAT determination in humans containing a defined region, uniform settings, and a clear procedure for image evaluation is still not established. A direct comparison of various studies dealing with the determination of VAT by using MRI is therefore difficult.

4.2. Dual energy X-ray absorptiometry

The dual energy X-ray absorptiometry was originally developed to determine the bone mineral density for osteoporosis diagnostics (Prevrhal, 2006). Nowadays, DXA is considered a non-invasive method for body composition analyses and is used as a reference method for body composition analyses (Pandey et al., 2011; Bazzocchi et al., 2016; Shepherd et al., 2017).

4.2.1. Technical functionality of DXA

The principle of DXA is the different absorption of high and low energy X-ray photons by different elements in the body. Tissue components can be identified due to a characteristic mass attenuation coefficient and a specific ratio value between the low and high energy X-ray attenuation for every tissue (Pietrobelli et al., 1996; Scholz et al., 2015). An X-ray source generates an X-ray photon beam, which is "divided" by a K-edge filter into a high and a low energy X-ray photon beam with, for example, energies of approximately 39 keV for the low energy X-ray beam and of 71 keV for the high energy X-ray beam (data from the GE Lunar *i*DXA scanner). The K-edge filter consists of rare earth elements such as Cerium or Samarium and is one of the possibilities to generate X-rays of two different energy levels. The X-rays then pass through the body where they are attenuated to different degrees depending on the thickness of the material and its density. The attenuation increases with rising atomic numbers (Scholz, 2002; Prevrhal, 2006; GE Healthcare, 2017c). Consequently, X-rays are more attenuated by lean tissue (containing protein and water) compared to fat tissue whereas bones have the highest attenuation coefficients (Laskey, 1996; Bazzocchi et al., 2016). In the GE Lunar *i*DXA scanners, a solid state crystal (Cadmium Telluride) semiconductor is used to detect the transmitted radiation. The output is proportional to the X-ray energy (GE Healthcare, 2017c). Generally, DXA is based on a three compartment model for tissue composition, which is shown in Figure 5 and distinguishes between lean soft tissue, fat tissue, and bone mineral (Pietrobelli et al., 1996; Scholz, 2002).

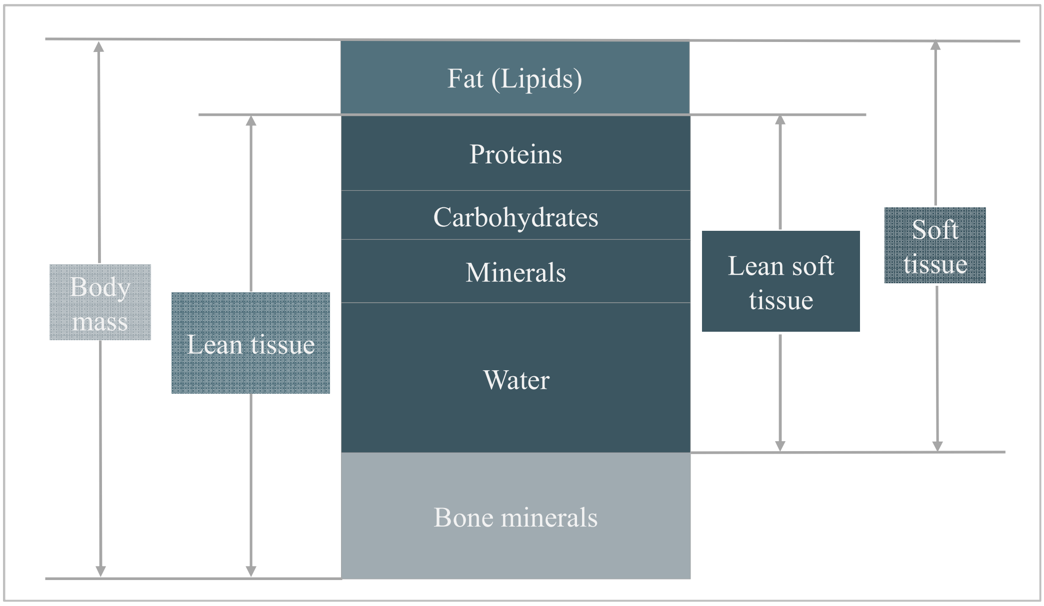

Figure 5. Three compartment model for tissue composition by DXA modified according to Scholz (2002)

For image processing, using a histogram analysis in combination with special algorithms helps to differentiate pixels containing bone mineral and pixels with only soft tissue. Tissue specific mass attenuation coefficients for fat and soft lean tissue help to distinguish between both tissues. Within Pixels containing bone mineral, the calculation of the soft tissue composition is based on the adjacent bone mineral free soft tissue composition (Pietrobelli et al., 1996; Scholz, 2002). DXA provides the following parameters for the whole body or for specific body regions:

- Total tissue mass (g)
- Bone mineral density (g/cm²)
- Bone mineral content (g)
- Amount and percentage of fat tissue (g, %)
- Lean soft tissue mass (g)

4.2.2. The CoreScan feature and the use for detecting VAT in humans

CoreScan by GE Healthcare is a software to quantify VAT using *i*DXA technology and is available since 2012 (GE Healthcare, 2011). Hologic created similar software called InnerCore to determine VAT. Since the CoreScan feature was used in the own study, only this software mode will be discussed here. VAT accumulates especially in the android region, the region below the rib cage to the iliac crest. The *i*DXA system defines the android region for every patient individually based on the length of its trunk using skeletal landmarks as a guide. The size of the android region is set at 20% of the distance between the top of the iliac crest and the base of the skull and starting at the iliac crest. *i*DXA measures the whole fat in the android region, and by a geometric calculation, the subcutaneous adipose tissue is detected and subtracted of the total adipose tissue to obtain VAT (GE Healthcare, 2017b). The algorithm works with the detection of two parameters, the width of the SAT layer on lateral aspects of the body, and the anterior-posterior thickness of the abdomen. The width of the SAT layer is represented by the fat between the skin line and the outer abdominal wall on both sides of the image. By using the DXA attenuation image, the anterior-posterior thickness of the abdomen can be attained (GE Healthcare, 2017a). Consequently, the amount of VAT can only be estimated and not measured directly.

To evaluate the CoreScan software, several studies examine the precision within repeated measurements and the ability of detecting VAT compared to gold standard methods, such as MRI and CT.

Rothney et al. (2013) evaluated the CoreScan feature by scanning a phantom and a clinical population of 32 obese women (average BMI = 35.1 kg/m²). The phantom consists of simulated lean tissue and adipose tissue and was repeatedly measured five times to test the intrascanner precision. Further, to detect the interscanner precision, the phantom was scanned on 10 different *i*DXA systems. All obese women were examined two times by only one *i*DXA system with repositioning between scans. The combination of intrascanner precision of the phantom and interscanner precision yielded a deviation of 47.6 g relative to 1 kg VAT mass, which means a coefficient of variation of 4.76%. The clinical study obtained a precision of 56.8 g at an average VAT mass of 1,110.4 g, which corresponds to a CV of 5.1%. The authors concluded, due to the low precision errors for the phantom and in obese women, that CoreScan might be a useful addition for studies of changes in VAT (Rothney et al., 2013).

Carver et al. (2014) evaluated the CoreScan software in obese patients by determining the precision in repeated measurements. A number of 55 male and female patients with a mean BMI of 49 kg/m² were scanned twice resulting in a precision error of 8.77%. Compared to Rothney et al. (2013), the CV is 3.6% higher. Carver et al. (2014) try to explain this increased CV by the significantly higher BMI of the examined patients in their study (Carver et al., 2014).

Mellis et al. (2014) confirm with their study the assumption of increasing precision errors with increasing BMI. They conducted two consecutive total body scans with repositioning for 45 adults in a wide range of BMI (16.7-42.4 kg/m²). For the precision analyses, two subgroups based on the BMI were formed (normal-weight, overweight/obese) to be able to examine the effect of BMI on precision. The precision error was lower in the normal BMI group with 20.9 g compared to 43.7 g in the overweight/obese group, but the CV decreased between the two groups from 17% to 5.4%. The inverse relationship of the CV with the mean value explains the decrease of the CV even though the precision error increases. The mean value for the normal BMI group was 123 g with a RMSE of 20.9 g. In the overweight/obese BMI group, the RMSE was small with 43.7 g compared to the significantly higher mean value of 814 g. Therefore, the authors recommend that the CV should not be used when the mean values of the population differs. In conclusion, the CoreScan software provides reasonable precision for VAT of individuals with a wide range of BMI (Mellis et al., 2014).

Meredith-Jones et al. (2018) examined the precision of DXA CoreScan software by conducting two consecutive DXA scans with repositioning of a large sample (233 participants) with various body constitutions. The results show an increasing precision error (root mean squares error) and decreasing %CV with increasing BMI. The normal weight groups obtained a precision error of 35.2 g with 44.8% for the CV, and the obese group of 65.0 g with a CV of 6.4%. After adjusting for age and sex, the precision of VAT was significantly lower in the obese group compared to normal (non-obese) participants. The %CV was higher compared to the studies of Mellis et al. (2014) and Rothney et al. (2013). One explanation might be the use of different scanners. Rothney et al. (2013) and Mellis et al. (2014) used the *i*DXA technology, whereas Meredith-Jones et al. (2018) scanned with Prodigy systems. The authors concluded that increasing BMI have a significant effect on the precision error with greater errors in overweight and obese participants (Meredith-Jones et al., 2018).

Overall, the precision error can have several reasons. Soft tissue in the abdominal cavity is not attached to fixed body parts. It can therefore slightly move within the body between the scans. In addition, the amount of VAT determined depends on the amount (thickness) of SAT (what is explained by the algorithm CoreScan is based on), while the proportion of VAT to SAT is not constant (Ergun et al., 2013;

Knapp et al., 2015).

The next section contains comparative studies between CoreScan and CT, and especially between CoreScan and MRI.

Kaul et al. (2012) examined the VAT of 124 adult men and women in a wide range of ages (18-90 years) and BMI (18.5-40 kg/cm²) by GE Healthcare Lunar *i*DXA with the CoreScan feature and CT as the reference method. A total body scan was conducted using standard imaging and positioning protocols combined with automatically defined body regions. The examination of the CT was performed by scanning the abdomen starting at the top of S1 (caudal vertebra) towards the head with a 5-mm slice thickness. Image segmentation took place by using a semi-automatic method. CT and DXA show a high agreement of the VAT volumes with a regression coefficient of 0.96 for females and 0.95 for males resulting in a combined regression coefficient of 0.96. Furthermore, a Bland-Altman analysis helped to characterize the differences between DXA and CT VAT records over the whole range of VAT volumes. The bias for all participants was +56.7 cm³ with 95% limits of agreement between -355 and +468 cm³. In conclusion, the DXA CoreScan has the ability to quantify VAT with a high precision in various genders and a wide range of BMI (Kaul et al., 2012).

In addition, Mohammad et al. (2017) validated DXA estimates of VAT in a Middle Eastern population of 237 Kuwaiti men and women in comparison to MRI measurements as reference. This study uses identical anatomic regions for MRI and DXA to be able to compare the observations of both methods directly. The authors found an overestimation of VAT by DXA of about 7% in men and women with a mean bias of 79.7 cm² in men and 46.8 cm² in women. Furthermore, the Bland-Altman analysis showed an increasing imprecision with increasing levels of VAT. Interestingly, the abdominal fat measured by DXA was lower than by MRI and consequently DXA underestimated this depot (Mohammad et al., 2017). According to the equation of CoreScan, where VAT is resulting by subtracting SAT from the total abdominal fat, the content of SAT must also be underestimated, if an underestimation of abdominal fat is assumed to achieve an overestimation of VAT. SAT, however, was not examined in the study (Mohammad et al., 2017).

Reinhardt et al. (2017) used the same anatomically defined abdominal region for MRI and DXA examination to compare VAT estimates of *i*DXA with MRI. They examined a total of 40 participants by using a total body DXA scan and a multi-slice MRI method to quantify the amount of VAT. The regression coefficients were high for males ($R^2 = 0.96$), females ($R^2 = 0.96$), and combined ($R^2 = 0.95$). The Bland-Altman bias for both examined genders was +104.1 cm^2 (95% limits of agreement: -681.9 - +890.0 cm^3). Additionally, they found, that *i*DXA compared to MRI, underestimated VAT at lower VAT levels and overestimated VAT at higher VAT levels. Overall, they concluded that *i*DXA could be used as an accurate alternative to MRI (Reinhardt et al., 2017).

One aim of the study by McCauley et al. (2020) was the comparison of DXA VAT with MRI VAT to generate a prediction equation for DXA applications. The examined participants had a spinal cord injury. A total body DXA scan and multiaxial imaging by MR were performed. DXA VAT predicted 92% of the variance in MRI VAT. The regression equation showed that one volumetric unit of VAT in DXA results in an increase of 0.931 cm^3 of VAT in MRI. Furthermore, the Bland-Altman analysis achieved a bias of 58.45 cm^3 with limits of agreement of -441.8 to 558.7 cm^3 (McCauley et al., 2020).

In conclusion, the CoreScan feature by GE Healthcare has the ability to quantify the volume of VAT precisely compared to gold standard methods. It offers therefore a fast, simple, and low-cost option to determine VAT in humans.

4.2.3. DXA in pigs

Several studies describe the use of DXA in pigs. In this chapter, the focus is set on the ability of DXA to determine the body composition, especially the fat content of pigs.

Mitchell et al. (1996) evaluated the ability of DXA measuring the body composition in 48 pigs by comparing the DXA results with chemical analysis. The total body fat of both methods was highly correlated ($R^2 = 0.99$). In addition, the DXA estimates for lean tissue mass showed a high relationship to chemical analysis results. In general, DXA overestimated the fat content in pigs with higher fat proportions and underestimated the fat content in leaner pigs (Mitchell et al., 1996). A further study of Mitchell et al. (1998) confirmed the above relationship by studying small pigs in a weight range of 5 to 27 kg. The correlation between DXA and chemical analysis, though, was still high for the fat percentage ($R^2 = 0.86$) and for the amount of fat ($R^2 = 0.96$) (Mitchell et al., 1998b).

Scholz and Förster (2006) analyzed two body weight groups of pigs by DXA and compared these results with dissection according to the EU reference method. In the lighter group (30-50 kg), the relationships between the lean meat content ($R^2 = 0.93$) and the fat content ($R^2 = 0.78$) of the reference parts and the DXA values were high. The regression coefficient for fat content was highest in the heavier group (70-90 kg) with $R^2 = 0.89$, whereas the regression coefficient for the lean meat content declined ($R^2=0.82$) in comparison to the light weight group. The authors attribute the discrepancies between DXA and dissection results mainly to the differences between both methods. The fat measured by DXA consists only of lipids, whereas dissection fat often contains also parts of the skin. Scholz and Förster (2006) showed additionally that DXA is – especially in the higher body weight range – a suitable method for growth studies (Scholz and Förster, 2006).

Soladoye et al. (2016) examined the accuracy of DXA in assessing carcass composition from different pig populations. Carcass halves and four primal cuts (shoulder, ham, loin, belly) of 648 female and male pig from different genetic lines of two slaughter weights (120, 140 kg) were scanned by DXA and analyzed for fat and lean content. DXA estimates were used to predict the dissection results for the carcass halves and their primal cuts. Overall, the fat content (%) can be accurately predicted by DXA even when classified based on diet, gender and slaughter weight ($R^2 > 0.94$). For the determination of the belly composition, they conducted a chemical analysis. The regression coefficient for lean and fat content between the values of the chemical analysis and DXA was high with 0.94. The authors hypothesized, that the DXA technology – due to its accuracy in assessing the carcass composition – may replace the traditional dissection methods presently used in experimental settings (Soladoye et al., 2016).

Furthermore, the attempt to predict the body composition was the focus of various other studies. Mitchell et al. (2002) tried to predict the whole body composition of pigs based on a cross-sectional region analysis by DXA. Totally, 212 pigs were scanned and the fat and lean percentage was analyzed in the total body and in 14 cross-sections. In addition, they compared the DXA results to the chemical analyses of the whole body. The closest agreement between the fat percentage of the total body and the fat percentage of individual slices was found for S4 (slice number 4) in the region of the shoulder ($R^2 = 0.97$). Additionally, the maximum fat percentage with 24.7% was found in the slice number 1 starting at the first rib and the least in the slice number 3 starting at the last rib with 16.4%. Overall, the authors conclude that the total body composition of pigs can be predicted by performing single cross-sectional scans with a reasonable high accuracy (Mitchell et al., 2002).

The aim of the study by Marcoux et al. (2005) was to evaluate the accuracy of predicting the carcass composition in different genetic pig lines by DXA. Total weight, fat and lean mass, and bone mineral content was measured in 95 carcass halves of gilts by DXA and dissection. The equations based on the DXA analysis provide suitable estimates of the fat mass in carcass halves and in the primal cuts ($R^2 > 0.70$). DXA, however, underestimated the fat mass, whereas an overestimation of the lean mass was observed. Furthermore, no correction of the prediction equation is needed among the different genetic lines (Marcoux et al., 2005).

Bernau (2011) analyzed the body composition by MRI and DXA in pigs with a weight of 80 kg and 100 kg and studied the ability to predict the body composition of pigs with 100 kg based on the measurements with 80 kg (Chapter II.4.1.3 MRI in pigs). The regression coefficient of the fat percentage and also of the lean meat content (%) in the whole body between the 80 kg and 100 kg pigs was high with 0.87 (Bernau, 2011).

Overall, DXA achieved acceptable results compared with chemical analysis or dissection. DXA is therefore an appropriate method for the determination of body composition in pigs. In addition, phenotyping of specific parameters by using DXA can serve as a basis for genome analyses (Rothammer et al., 2014).

III. Publication

animals MDPI

Article

Phenotyping of the Visceral Adipose Tissue Using Dual Energy X-Ray Absorptiometry (DXA) and Magnetic Resonance Imaging (MRI) in Pigs

Anna C. Weigand [1,*], Helen Schweizer [1], Deise Aline Knob [2] and Armin M. Scholz [1]

1 Livestock Center Oberschleissheim, Veterinary Faculty of the Ludwig-Maximilians-University Munich, 85764 Oberschleissheim, Germany; Helen.Schweizer@lvg.vetmed.uni-muenchen.de (H.S.); Armin.Scholz@lvg.vetmed.uni-muenchen.de (A.M.S.)

2 Centro de Ciências Agroveterinárias, Universidade do Estado de Santa Catarina, Lages CEP 88.520-000, Brazil; deisealinek@gmail.com

* Correspondence: Anna.Weigand@lvg.vetmed.uni-muenchen.de

Received: 13 May 2020; Accepted: 06 July 2020; Published: 09 July 2020

Simple Summary: Fat depots in the abdomen and around the organs, which are called visceral adipose tissue, play an important role in the field of obesity-associated diseases in humans and for pork production as well. Magnetic resonance imaging—as reference method—and a special X-ray technique called dual energy X-ray absorptiometry were used to measure the visceral adipose tissue in 120 pigs in order to analyze the accuracy of a special X-ray software algorithm (the "CoreScan" mode), and to study sex or crossbreed-related effects. The "CoreScan" mode overestimates the amount of visceral adipose tissue in comparison with magnetic resonance imaging, while castrated males tend to accumulate more visceral adipose tissue than females, and the first crossbred generation deposits more fat than the second generation.

Abstract: The objective of this study was to phenotype visceral adipose tissue (VAT) in pigs. In this context, the ability to detect VAT by using the DXA CoreScan mode within the enCORE software, version 17 (GE Healthcare) was evaluated in comparison with MRI measurements (Siemens Magnetom C!) of the same body region. A number of 120 crossbred pigs of the F1 and F2 generation, with the parental breeds Large White, Landrace, Piétrain, and Duroc, were examined at an age of 150 days. A whole-body scan in two different modes ("thick", "standard") was carried out by a GE Lunar iDXA scanner. Very strong relationships (R^2 = 0.95, RMSE = 175cm^3) were found for VAT between the two DXA modes. The comparison of VAT measured by MRI and DXA shows high linear relationships ("thick": R^2 = 0.76, RMSE = 399.25cm^3/"standard": R^2 = 0.71, RMSE = 443.42cm^3), but is biased, according to the Bland–Altman analysis. A variance analysis of VAT shows significant differences for both DXA modes and for MRI between male and female pigs, as well as between F1 and F2. In conclusion, DXA "CoreScan" has the ability to estimate VAT in pigs with a close relationship to MRI but needs bias correction.

Keywords: dual energy X-ray; MRI; CoreScan; visceral adipose tissue; pig

1. Introduction

Cardiovascular disease (CVD) is the most common cause of death in Germany and the entire world in the last few years. In 2016, 17.9 million people worldwide died from CVDs, which constituted 31% of all deaths. In Germany, the percentage was even higher [1,2]. The most important cardiovascular diseases are coronary heart disease (CHD), manifested by myocardial infarction and heart failure, and cerebrovascular disease, including stroke [1,3–6]. Cardiometabolic risk factors, such as hypertension, dyslipidemia, and metabolic syndrome, are associated with visceral adipose tissue (VAT) [7,8].

Against the backdrop of high mortality, resulting from CVD, the need for precise measurement methods of VAT is immense. With their CoreScan mode, GE Healthcare offers the possibility of determining visceral adipose tissue by using dual energy X-ray absorptiometry (DXA). This study examined the ability of CoreScan to precisely quantify the content of visceral adipose tissue in pigs compared to the results of magnet resonance imaging (MRI).

The pig plays an increasing role as a model in human research due to the similarity in anatomic and physiologic characteristics involving the cardiovascular, urinary, integumentary, and digestive systems [9–11]. Furthermore, the interest in investigating obesity-related genes in pigs is explained by the fact that the porcine genome is even more similar to humans than the genome of mice [12].

In addition, new insights into the fat depot metabolism are important for the commercial rearing of pigs. The production of high-quality meat at low costs is still one of the primary objectives. The combination of exact phenotypic data with genome data will provide further knowledge of the regulation of body composition [13–15].

The aim of this study was to phenotype the visceral adipose tissue in pigs using MRI, and to evaluate the ability of the DXA CoreScan mode to be a fast, simple, and low-cost option to quantify the volume of visceral adipose tissue, compared to an MRI reference examination.

2. Materials and Methods

2.1. Animals

A number of 120 crossbred pigs of the first and second filial generation (F1, F2), with the parental breeds Large White, Landrace, Piétrain, and Duroc, were examined. The number of pigs of the F1 crossbreed, called Multi-hybrid-F1 (MHF1) and the F2 crossbreed, Multi-hybrid-F2 (MHF2), and also the number of females and castrated males, was supposed to be balanced, as shown in Table 1. All pigs were born and raised at the Livestock Center Oberschleissheim and were treated like the other pigs in the facility. Males were castrated on the third day of life. After a suckling period of four weeks the piglets were weaned and moved to a nursery deck, where they stayed in groups of 15–20 animals. With a weight above 25 kg, the pigs were housed in an outdoor-climate barn with various climatic and flooring areas in groups of 30–34 animals. The feeding area is enlarged and consists of concrete-slatted flooring; the rest is deeply bedded with straw and contains a hooded area with a special (warmer) microclimate during the winter season. The feed is individually allocated via an automatic feeder (Double-Fitmix, Mannebeck). All pigs received the same food throughout the experiment.

This study was conducted at the Livestock Center Oberschleissheim of the Veterinary Faculty of the Ludwig-Maximilians-Universität in Munich with the approval of the District Government of Upper Bavaria (No. 55.2-1-54-2532.0-81-2016).

Table 1. Animal sample.

	Number	Age (days)		Weight (kg)	
		Mean	Standard Deviation	Mean	Standard Deviation
Castrated males	63	147.4	3.5	93.9	7.6
Females	57	146.9	3.1	89.0	8.4
MHF1	58	147.8	3.5	93.0	8.1
MHF2	62	146.5	3.1	90.3	8.5

2.2. Test Procedure

The pigs were studied at an average age of 147 days and an average weight of 91.6 kg, as shown in Table 1. Animals were selected by their genetic origin and randomly within the litters. For the scan by MRI and DXA, sedation was needed to achieve profound results by reducing the movement of the individual. One day before the scan, the animals were moved to a barn nearby the MRI unit and housed in groups with concrete flooring and straw bedding. To reduce the risk of an anesthetic accident, the feed was deprived of the experimental pigs for 16 h. Water was available ad libitum. At the day of scan, the health status of each animal was checked, and the weight was measured with a mechanic livestock scale for the exact dosage of the anesthetic. Azaperon (2 mg/kg bw, Stresnil®, Elanco) and ketamine (10–15 mg/kg bw, Ursotamin®, Serumwerk Bernburg) were used for the anesthesia by intramuscular injection. A catheter was inserted into the vena auricularis to be able to administer additional ketamine, if necessary. The monitoring of anesthesia was carried out via a scoresheet by recording different parameters, such as heart rate, respiratory frequency, and capillary filling time.

2.2.1. Magnetic Resonance Imaging

An open low-field MRI system (Siemens Magnetom C!) with a magnetic field strength of 0.35 Tesla was used for the scans. A fully automated quality control was executed by the Siemens Magnetom C! system at each restart of the device [16]. The animals were placed in a prone position with their forelimbs flexed and hind limbs extended to enable the examination of both body halves at the same time. Anatomic landmarks were used for the positioning in order to acquire reproducible and comparable images for the same body region. In the area of the abdomen, the origin of the last rib and in the section of the pelvis, the top of the iliac crest were taken as a guide, as shown in Figure 1A,B.

Figure 1. MRI examination of the abdomen. (**A**) Position of the pig for the examination of the abdomen by a Siemens Magnetom C! system. (**B**) Localizer of the "ViscFat-Sequence" with defined area encompassing visceral adipose tissue. Each line represents an axial sectional image of the abdomen starting at the origin of the last rib to the top of the iliac crest.

Two T1-weighted spin echo sequences in axial acquisition per animal were applied to detect the visceral adipose tissue. The first sequence, called “ViscFat sequence”, covered most of the abdomen, as shown in Figure 1, and the second sequence, “Ham sequence” included the remaining part of the abdomen and the region of the pelvis. In larger animals the first sequence was not sufficient to cover the whole region of interest; therefore, selected slices of the “Ham sequence” were additionally used for the evaluation. The protocols of MRI settings are shown in Table 2.

Table 2. MRI protocol of both T1-weighted sequences—“ViscFat” and “Ham” sequences.

	ViscFat Sequence	Ham Sequence
pixel size (mm x mm)	1.9 × 1.6	1.9 × 1.6
examination time (min)	12.22	10.27
signal-to-noise ratio	1.00	1.00
repetition time (TR) (ms)	441	370
echo time (TE) (ms)	18	18
slice number	30	20
slice thickness (mm)	6	6
Acquisition	axial	axial
distance factor (%)	20	20
matrix size	211 × 250	211 × 250
field of view (FoV) (mm)	400	400

2.2.2. Dual Energy X-Ray Absorptiometry

After the MRI scan, the body composition of the pigs was measured by DXA, as shown in Figure 2. Generally, the measurement of DXA bone mineral and soft tissue amounts (divided into fat and lean) is based on the X-ray attenuation coefficient (R value). The R value (not shown in the *i*DXA system) is derived pixel wise from the quotient of X-ray photons of the high and low X-ray energy level, having passed the object. Low R values define soft tissue and high R values bone mineral. Within soft tissue, fat tissue is characterized by the lowest R values [15,17]. The GE Lunar *i*DXA scanner provides a special mode for the whole body scan, based on the body constitution. For this study, the two different modes—“thick” and “standard”—were used to obtain information about the amount and percentage of fat and lean tissue mass, bone mineral content, and bone mineral density. The whole body scan in “thick” mode takes 13.45 min with an absorbed dose of 6 µGy, and in “standard”mode this was 7.45 min with a dose of 3 µGy. In addition, GE Healthcare, with the CoreScan mode within the enCORE software version 17, offers the ability to determine the mass (g) and volume (cm^3) of the visceral adipose tissue in adults. The *i*DXA system measures the whole fat in the android region. The subcutaneous adipose tissue is detected by a hidden geometric calculation and subtracted from the total adipose tissue to obtain VAT [18]. The algorithm works with the detection of two parameters. The two parameters are: (1) the width of the SAT layer on lateral aspects of the body, which is represented by the fat between the skin line and the outer abdominal wall on both sides of the image; (2) the anterior–posterior thickness of the abdomen, which can be attained using the DXA tissue attenuation image [19]. The algorithms for the determination of VAT are described in detail in the US and world patents: US9179884 (https://patents.google.com/patent/US9179884);US9254101(https://patents.google.com/patent/US9254101);WO2012092533Al(https://patents.google.com/patent/WO2012092533A1/en), from GENERAL ELECTRIC COMPANY, Schenectady, NY (US). Before the examination, a quality control of the *i*DXA system was executed, according to the standard procedures, once a day [20]. The pig was bedded in a prone position with forelimbs and hind limbs extended to simulate the suggested position for whole body DXA scans in humans. Foam cushions were used to create a gap between the abdominal wall and the forelimbs to prevent overlays. The hind limbs were tied together.

Figure 2. DXA examination.

2.3. Data Analysis

2.3.1. MRI Evaluation

For the evaluation of the magnetic resonance images, the “synedra” View Personal software (Version 16.0.0.3, synedra information technologies GmbH, Innsbruck, Austria) and the Able 3D-Doctor® software (Release 4.0; Able Software Corp., Lexington, MA, USA) were used. The region containing VAT was defined as the area between the origin of the last rib and the top of the iliac crest. The number of slices of the “ViscFat” and “Ham” sequences, which cover the region of interest (ROI), was determined with the help of “synedra”, as shown in Figure 1B. For the evaluation of the VAT volume, the regions of VAT were defined manually for every single slice, including the fat depots beneath the abdominal wall, around the kidneys, and in the abdominal cavity, as shown in Figure 3. As the peritoneum is often difficult to discern with the use of MRI, in this study, VAT was defined as the intra-abdominal adipose tissue; no distinction between intra- and extraperitoneal adipose tissue was assigned. Consequently, the Able 3D-Doctor® software provides an option to calculate the volume of the defined areas (VAT) by using the data (slice number, slice thickness, and slice distance), saved in the Dicom format.

2.3.2. DXA Evaluation

To get a meaningful comparison of visceral adipose tissue volume between MRI and CoreScan results, the examined body region must be identical. Therefore, the android region was determined individually to encompass the whole region of interest, as shown in Figure 4. The ROI was defined in the “thick” mode, copied for the “standard” mode, and adapted, if necessary, to cover the ROI of the MRI examination. For the study, weight (kg), bone mineral density (g/cm^2), bone mineral content (g), the amount (g) and percentage of fat tissue and lean tissue mass in the android region, and the mass (g) and volume (cm^3) of the visceral adipose tissue were measured.

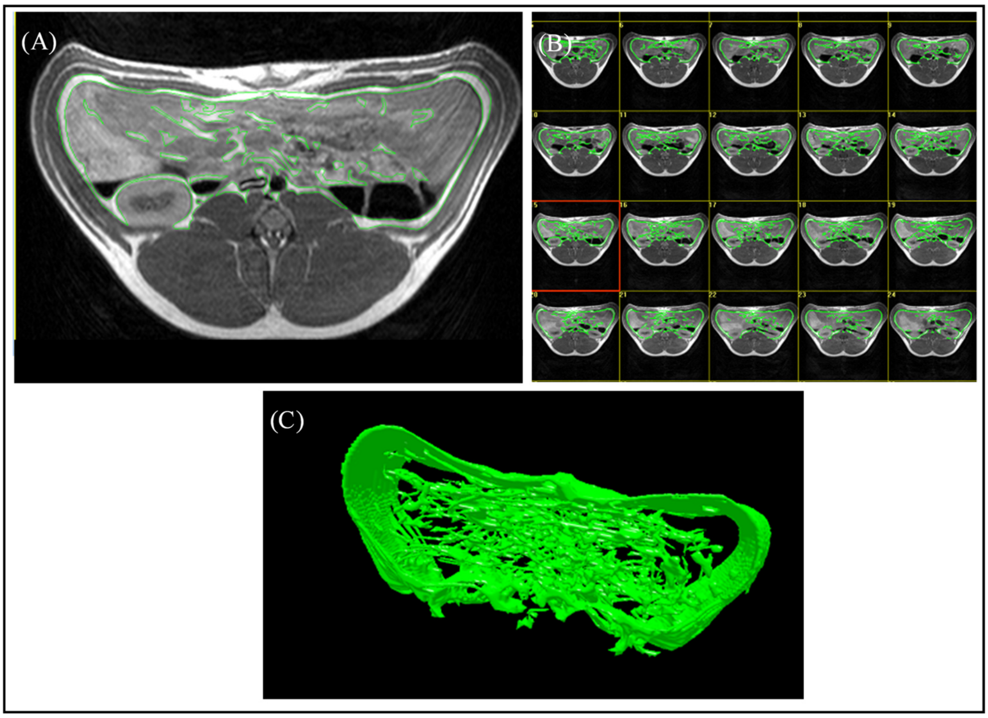

Figure 3. Evaluation of MR images using the Able 3D-Doctor® software. (**A**) T1-weighted axial MR image with green boundaries, including the visceral adipose tissue. (**B**) Analysis of all slices in the defined body region. (**C**) Reconstruction of a 3D-model from the selected boundaries of VAT.

2.3.3. Statistical Analysis

A variance analysis was performed by using a mixed model procedure and restricted maximum likelihood (REML) estimation with the software SAS 9.3 (SAS Institute Inc., Cary, North Carolina, USA). The significance level was set to $p < 0.05$. Genetic origin and the sex of the animals were defined as fixed effects and the date of scan as a random effect. In addition, a linear regression analysis was performed. The coefficient of determination (R^2) in combination with the standard error of estimation (identical with RMSE = root mean squares error) serves as a measure of the quality of the fit of the regression equation between dependent and independent variables. Furthermore, a Bland–Altman analysis [21] was performed to characterize differences between DXA and MRI VAT measurements over the observed range of VAT volumes.

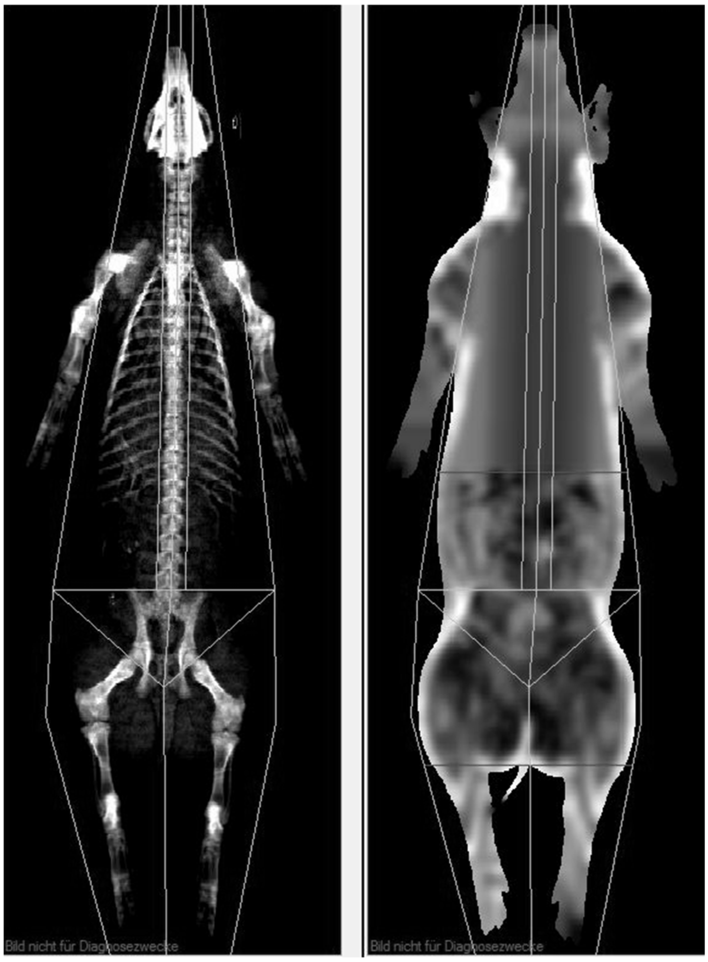

Figure 4. DXA evaluation with enCore software. The uppermost horizontal line (soft tissue image on the right side) defines the level of the origin of the last rib, and the next horizontal line on the top of the iliac crest represents the end of the examined region of VAT.

3. Results

3.1. Internal DXA Measurement Results

To evaluate the CoreScan feature, internal DXA measurement results were compared within each mode and between the two modes, "thick" and "standard". Within the modes, the regression coefficient between mass (g) and volume (cm^3) of VAT is expectedly 1.0 and the model equation provides the density estimate of 0.9435 g/cm^3 for VAT, as shown in Figure 5 (e.g., for thick mode). A very strong relationship (R^2 = 0.95, RMSE = 175 cm^3) was found between the volumes of VAT for the two DXA modes. CoreScan obtained higher values for the "standard" compared to the "thick" mode, as shown in Table 3 and Figure 6. Similar relationships can be seen for the amount (g) and the percentage of whole-body fat tissue. Within the android region, the fat mass was expectedly higher than the amount of VAT, because the android region additionally includes the subcutaneous adipose tissue (SAT) (R^2 = 0.98, RMSE = 114 cm^3), as shown in Figure 7.

Model Equation						
VAT_g_d_core	=	-	0.0255	+	0.9435	Vat_vol_d_core

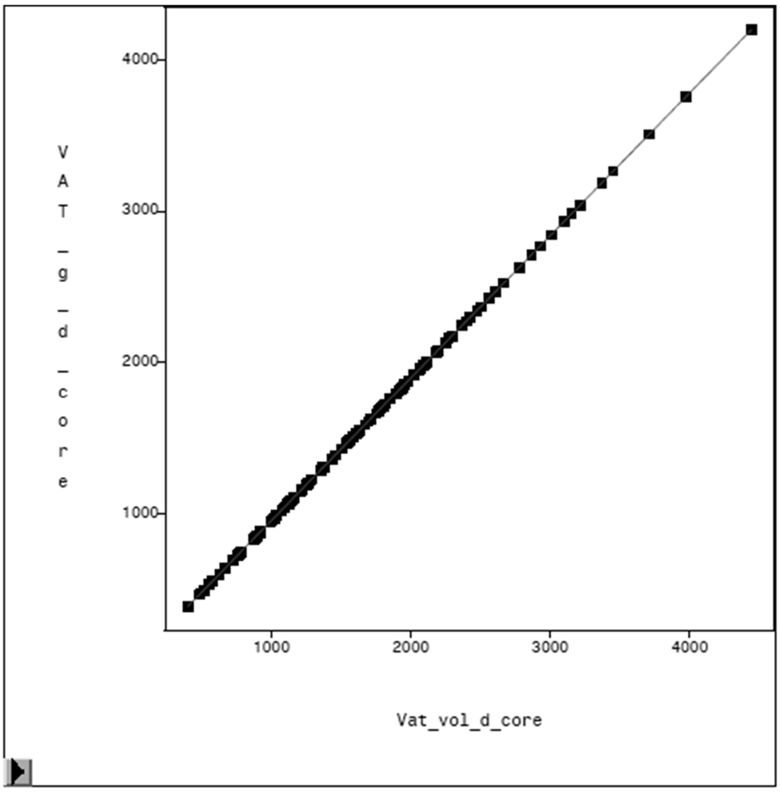

Summary of Fit			
Mean of Response	1591.2797	R-Square	1.0000
Root MSE	0.9822	Adj R-Sq	1.0000

Figure 5. Relationship between VAT mass (VAT_g_d_core, in g) and VAT volume (VAT_vol_d_core, in cm^3) in "thick" mode, measured by DXA. The model equation shows a density of 0.9435 g/cm^3 for VAT.

Table 3. Arithmetic means and standard deviations of VAT volume measured by DXA for "thick" and "standard" modes, and by MRI.

	VAT Volume (cm^3)		
	DXA "Thick"	DXA "Standard"	MRI
Arithmetic mean	1686.69	2173.08	1108.33
Standard deviation	805.08	815.17	283.76

Model Equation					
Vat_vol_d_core	=	-	396.352	+	0.9637 VAT_vol_s_core

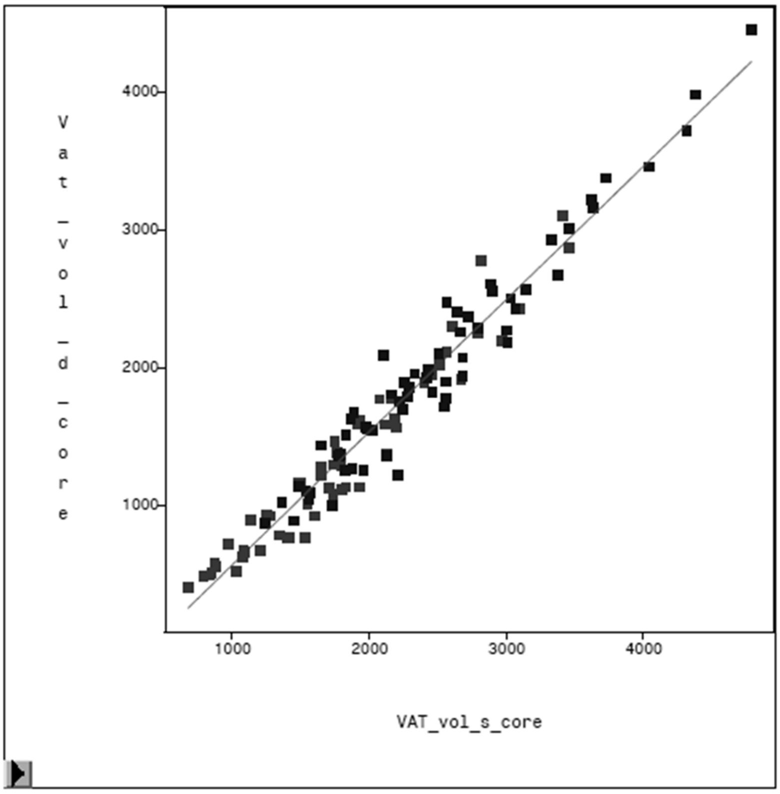

Summary of Fit			
Mean of Response	1697.9138	R-Square	0.9534
Root MSE	175.1723	Adj R-Sq	0.9530

Figure 6. Relationship between VAT volume in "thick" mode (VAT_vol_d_core, in cm^3) and VAT volume in "standard" mode (VAT_vol_s_core, in cm^3) measured by DXA. "Standard" mode yields higher values of VAT volume, as the model equation represents.

Model Equation				
F_g_d_andro	=	609.011	+	0.9932 VAT_g_d_core

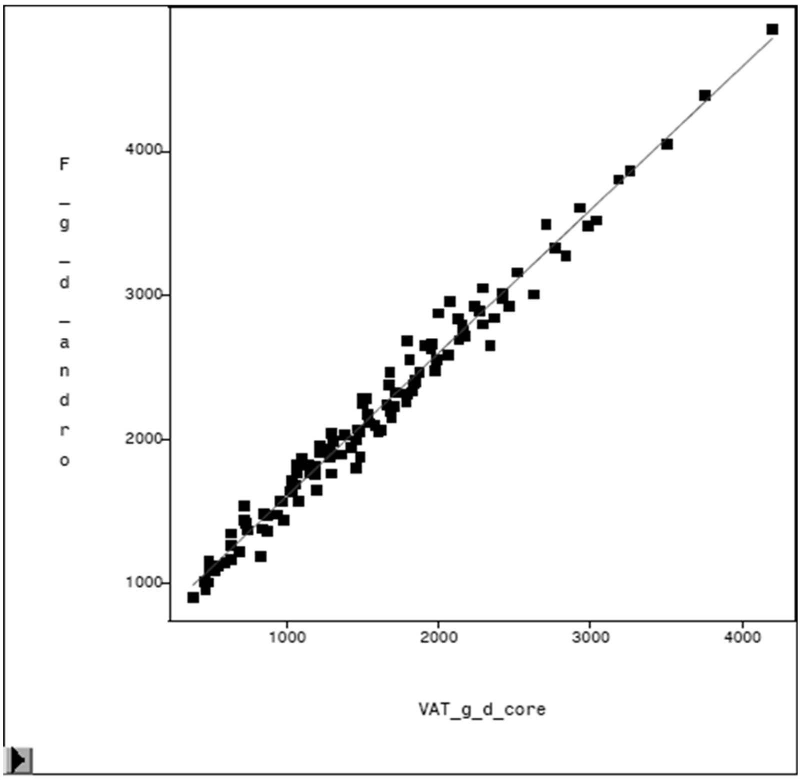

Summary of Fit			
Mean of Response	2189.5424	R-Square	0.9780
Root MSE	114.1081	Adj R-Sq	0.9778

Figure 7. Relationship between fat mass in the android region (F_g_d_andro, in g) and VAT mass (VAT_g_d_core, in g) in "thick" mode, measured by DXA. Regression analysis shows the difference in total fat mass in the android region and VAT. The difference represents the mass of subcutaneous adipose tissue in the average, around 609 g.

3.2. Comparison of MRI and DXA Results

MRI was used as reference method to evaluate the potential of the CoreScan feature in pigs. In Table 3, the arithmetic mean values of VAT volume, measured by DXA in both modes and by MRI are shown. A close linear relationship can be observed by comparing these VAT volumes ("thick": $R^2 = 0.76$; "standard": $R^2 = 0.71$), as shown in Figure 8 and Table 4. In the Bland–Altman analysis, a negative association was observed between the mean and the difference of both methods, as shown in Figure 9. The average volume calculated by CoreScan ("thick" and "standard"), however, is about 1.5- to 2-times greater than the average volume of the MRI scans, as shown in Table 3 and Figure 10 (only DXA "thick" mode). Therefore, DXA (here only "thick" mode) with the CoreScan feature tends to overestimate the VAT volume compared with MRI, providing a mean difference of −579.1 cm^3 (95% confidence interval between −684.7 cm^3 and −473.5 cm^3, $p < 0.001$). The deviation between DXA and MRI measurement results increases with increasing levels of VAT and is shown in Figure 10. The difference in both methods rises with a slope of 1.5 (1.489) cm^3 per cubic centimeter more VAT, measured by MRI.

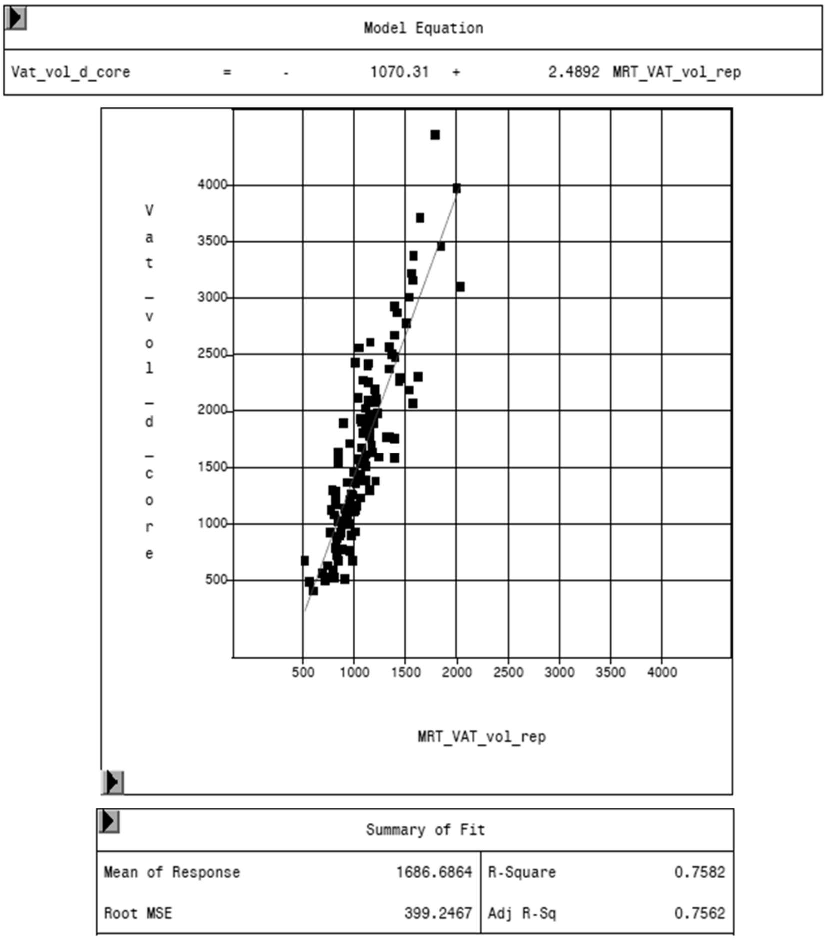

Figure 8. Relationship between volume of VAT measured by MRI (MRT_VAT_vol_rep, in cm³) and DXA "thick" mode (VAT_vol_d_core, in cm³).

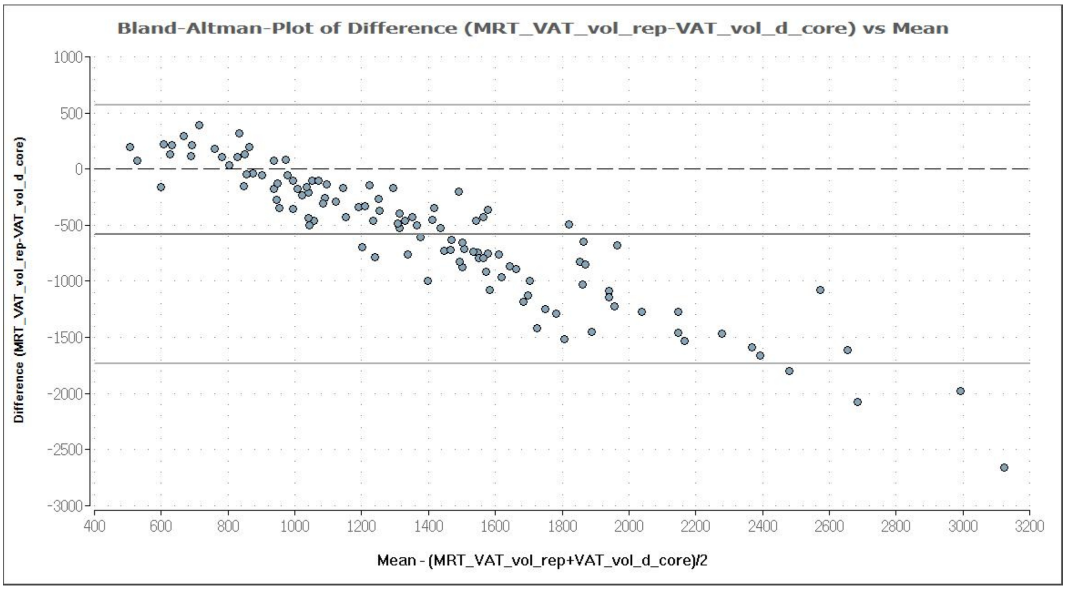

Figure 9. Bland–Altman plot of VAT volume (in cm³) measured by DXA in "thick" mode (VAT_vol_d_core) and MRI (MRT_VAT_vol_rep). The mean and the difference of both methods are demonstrated in a Bland–Altman plot. The analysis shows a negative association, which means an increasing deviation of DXA measurement results compared to MRI with increasing levels of VAT. DXA overestimates VAT systematically, compared with MRI, providing a mean difference of −579.1 cm³, which is represented by the fat (dark) solid line. The upper and lower solid (light grey) lines represent the limits of agreement (95%), and the broken line represents the line of zero differences.

Model Equation				
diffm1m2	=	1070.31	-	1.4892 MRT_VAT_vol_rep

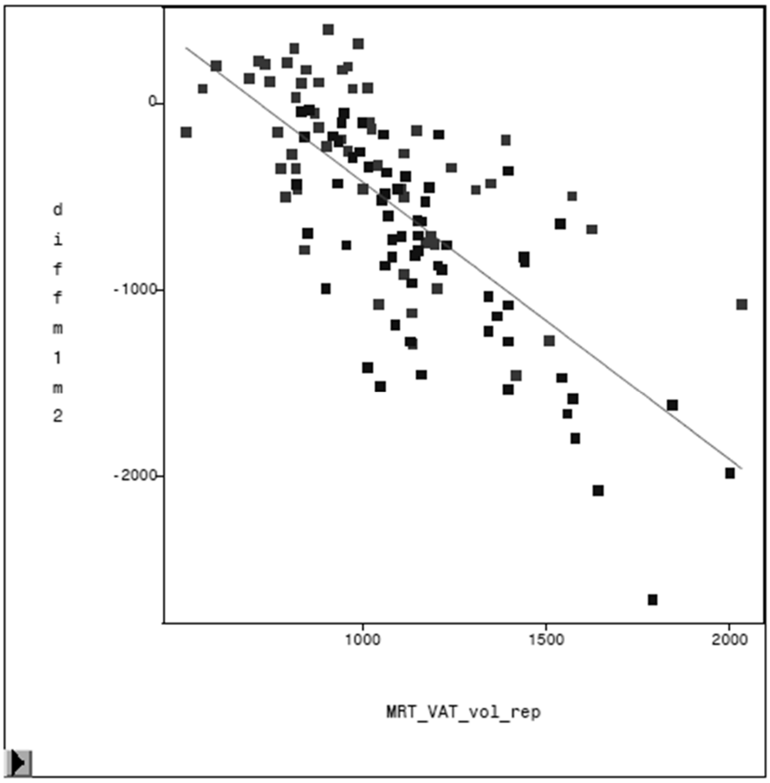

Summary of Fit			
Mean of Response	-579.1108	R-Square	0.5289
Root MSE	399.2467	Adj R-Sq	0.5248

Figure 10. Relationship between the difference of both methods (MRI and DXA-diffm1m2) and the VAT volume measured by MRI (MRT_VAT_vol_rep) in cm^3.

Table 4. Relationship between volume of VAT measured by MRI (MRT_VAT_vol_rep) and DXA "thick" mode and DXA "standard" mode.

	DXA VAT Volume "Thick" (cm^3)	DXA VAT Volume "Standard" (cm^3)
Model equation	−1070.31 + 2.4892 MRT_VAT_vol_rep	−537.384 + 2.4368 MRT_VAT_vol_rep
Root MSE	399.2	443.4
Adj. R-Sq	0.756	0.707
Pr > t	<0.0001	<0.0001

Root MSE = root mean square error; Adj. R-Sq = adjusted R-square; Pr > t = defines the significance level.

3.3. Relationship of VAT, Weight, and Age

The regression analysis between VAT volume of MRI and the weight of the animal shows an increasing VAT with increasing weights. One kilogram more weight leads to 18.3 cm^3 more visceral adipose tissue, as shown in Figure 11.

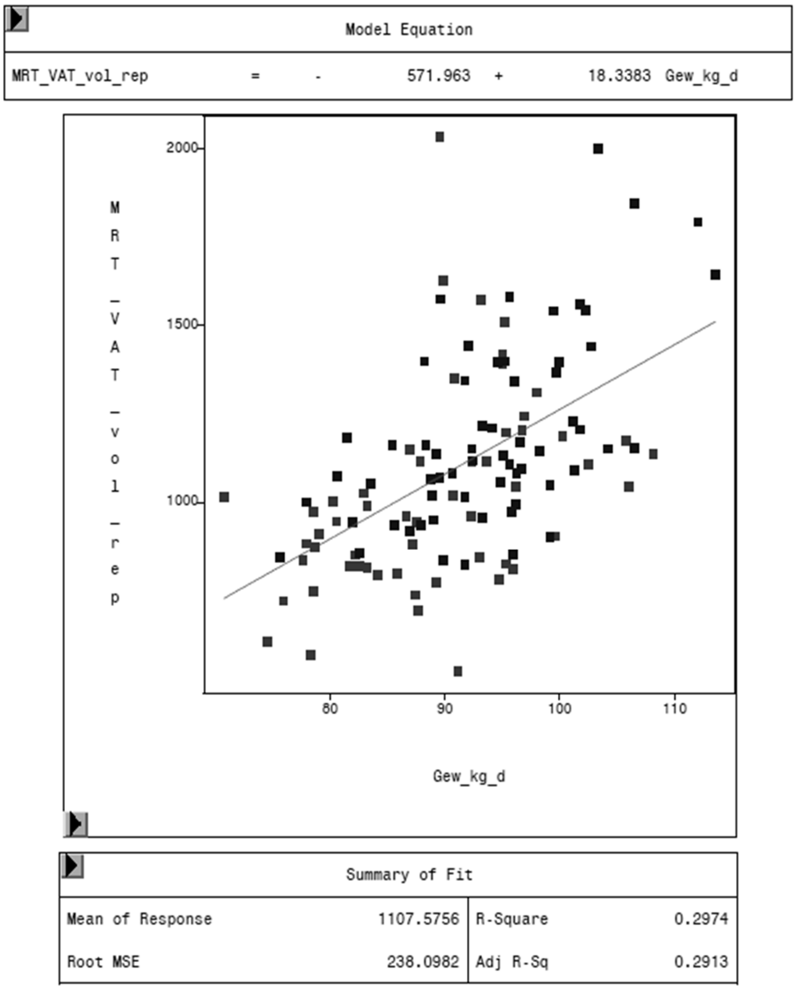

Figure 11. Relationship between VAT volume measured by MRI (MRT_VAT_vol_rep, in cm^3) and body weight (Gew_kg_d, in kg) of the animal.

Despite the small age range, differences were found in volumes of visceral adipose tissue. The regression analysis shows greater volumes in older pigs for MRI and DXA. Volumes of visceral adipose tissue increase by 34 cm^3 (MRI) and 109 cm^3 (DXA) per day of life, as shown in Table 5.

Table 5. Relationship between MRI VAT volume and DXA VAT volume in "thick" mode and the age of the pig.

	MRI VAT Volume (cm^3)	DXA VAT Volume "Thick" (cm^3)
Model equation	−3908.40 + 34.0868 age (days)	−14,353.7 + 109.005 age (days)
Root MSE	261.9	724.9
Adj. R-Sq	0.16	0.20
Pr > t	<0.0001	< 0.0001

Root MSE = root mean square error; Adj, R-Sq = adjusted R-square; Pr > t = defines the significance level.

3.4. Variation in Fat Mass and VAT Volume by Sex and Genetic Origin

The variance analysis of fat mass in the android region shows significant differences between sex groups (p = 0.0002) and both crossbred lines (p = 0.0243). MHF1 pigs have, on average, 319.6 g more fat in the android region than MHF2 individuals. We also observed a higher fat mass in castrated males compared to female pigs (+452.2 g). The mass and percentage of total body fat differs by sex and crossbred line in the same way as fat in the android region, with MHF1 animals and castrated pigs showing higher values than MHF2 individuals or females, respectively, although, the total body fat mass did not differ significantly (p = 0.0504 or p = 0.0787) between crossbred lines, as shown in Table 6.

Table 6. Least squares means (LSM), standard errors of estimation (SEE), and significance levels of examined parameters.

				Sex		Genetic Origin	
				Castrated Males	Females	MHF1	MHF2
DXA	Mode "Thick"	Gew_kg_d [kg]	LSM	93.59	89.69	93.19	90.09
			SEE	1.33	1.39	1.57	1.50
			Pr > t	0.0079		0.1268	
		F_g_d_ges [g]	LSM	15,092	12,554	14,532	13,114
			SEE	466	492	533	507
			Pr > t	<0.0001		0.0504	
		F_proz_d_ges [%]	LSM	16.35	14.14	15.86	14.63
			SEE	0.40	0.43	0.46	0.44
			Pr > t	<0.0001		0.0498	
		F_g_d_andro [g]	LSM	2409	1957	2343	2023
			SEE	91	96	104	99
			Pr > t	0.0002		0.0243	
		VAT_g_d_core [g]	LSM	1868	1290	1741	1416
			SEE	89	94	103	98
			Pr > t	<0.0001		0.0200	
		VAT_vol_d_core [cm^3]	LSM	1979.53	1367.33	1845.77	1501.88
			SEE	94.82	100.01	108.99	103.75
			Pr > t	<0.0001		0.0200	
	Mode "Standard"	F_g_s_ges [g]	LSM	16,164	13,677	15,537	14,304
			SEE	454	481	511	486
			Pr > t	<0.0001		0.0787	
		F_proz_s_ges [%]	LSM	17.56	15.46	17.01	16.02
			SEE	0.37	0.39	0.41	0.39
			Pr > t	<0.0001		0.0830	
		F_g_s_andro [g]	LSM	2604	2164	2531	2237
			SEE	86	91	96	91
			Pr > t	0.0003		0.0272	
		VAT_g_s_core [g]	LSM	2335	1744	2182	1897
			SEE	84	89	92	88
			Pr > t	<0.0001		0.0269	
		VAT_vol_s_core [cm^3]	LSM	2475.38	1848.46	2312.55	2011.30
			SEE	88.62	93.93	97.66	92.74
			Pr > t	<0.0001		0.0270	
MRI		MRT_VAT_vol_rep [cm^3]	LSM	1188.83	1016.65	1196.40	1009.08
			SEE	47.48	49.08	56.44	53.86
			Pr > t	0.0001		0.0074	

Gew_kg_d [kg]: Body weight; F_g_d_ges [g]: Total fat mass in mode "Thick"; F_proz_d_ges [%]: Percentage of total fat mass in mode "Thick"; F_g_d_andro [g]: Android fat mass in mode "Thick"; VAT_g_d_core [g]: VAT mass in mode "Thick"; VAT_vol_d_core [cm^3]: VAT volume in mode "Thick"; F_g_s_ges [g]: Body weight; F_proz_s_ges [%]: Total fat mass in mode "Standard"; F_g_s_andro [g]: Percentage of total fat mass in mode "Standard"; VAT_g_s_core [g]: Android fat mass in mode "Standard"; VAT_vol_s_core [cm^3]: VAT mass in mode "Standard"; MRT_VAT_vol_rep [cm^3]: MRI VAT volume.

The volume of VAT measured by DXA ("standard", "thick") and MRI differs significantly ($p < 0.05$) for sex and genetic origin. Castrated male pigs, and also the first generation of crossbreds (MHF1), have a larger VAT volume, as shown in Table 6.

3.5. Variation in Weight by Sex and Genetic Origin

Weight differed not significantly between both crossbred generations (p = 0.1268). As in the previous results, a sex-related difference was observed with castrated males, achieving higher values. On average, a castrated male pig weighed 3.9 kg more than a female individual, as shown in Table 6.

4. Discussion

MRI is considered as the gold standard of VAT determination in humans [22,23] and is, together with CT, the in vivo method of choice for directly quantifying the distribution of adipose tissue [22,24–26]. MRI is characterized by a high accuracy, no radiation exposure, and shows a good reproducibility with a coefficient of variation for repeated VAT measurements of approximately 9% to 18%, as Shen et al. summarized in their review. However, MRI has significant limitations: limited access; high cost; prolonged scan time [22,24]. MRI causes high investment costs (which increase with the field strength of the magnet), as well as high running costs for the system service, including temperature control and general maintenance. In addition, compared to DXA, an MRI system requires more building space and a Faraday cage surrounding the magnet. The MRI sequences in our study took 12.22 min and 10.27 min for examining the region of the abdomen and pelvis, respectively; with the repositioning of the animal between the sequences. In comparison, the more suitable DXA method ("thick" mode in our case) needs a whole body scan, which takes a maximum of 13.45 min ("standard" only 7.25 min). Besides the prolonged scan time, the evaluation of the MRI images is more time-consuming compared to the DXA evaluation. In our case, the number of slices needed to cover the whole region of the abdomen was about 30. The VAT had to be defined manually for each MRI slice, because an automatic or semi-automatic approach lacked sufficient anatomic accuracy. The DXA enCore software automatically suggests lines for specific body regions. These lines had to be only slightly adjusted in our study in order to cover the identical body region, as in the MRI evaluation. The DXA evaluation of VAT per animal usually took less than 5 min, while the MRI VAT evaluation took up to 5 h per animal. Furthermore, MRI specialists are needed both for the examination and for the image evaluation. In the DXA enCore software, no settings need to be especially defined, as is essential for MRI (due to different sequences). Since our study shows the ability of the DXA CoreScan feature to provide VAT estimates in pigs closely related to MRI, the CoreScan mode can be a fast, relatively simple, and a low-cost option to detect the volume of visceral adipose tissue, compared with MRI.

In Contrast to MRI or CT, however, DXA only measures two-dimensionally. Therefore, subcutaneous and visceral adipose tissue cannot be distinguished directly. The amount of VAT can only be estimated [27,28]. Consequently, VAT depends on the amount of SAT, and an inaccuracy of detecting SAT will lead to biased results of VAT. This might be one source of error explaining the overestimation of VAT measured by DXA that was found in our study. Further studies of quantifying the SAT in the android region may help to confirm or exclude this source of error. Fourman et al. found an overestimation of SAT combined with an underestimation of VAT compared to a single image CT in humans by using a Hologic Horizon A DXA scanner [29].

In pigs, MRI and DXA (including pure bone mineral analysis [30,31]) are also used for body composition analyses and achieve acceptable results compared to chemical analyses or dissection [32–36]. Our study shows that DXA overestimates VAT compared to MRI and the deviation rises with increasing VAT levels in accordance with other porcine and human studies, where DXA tends to overestimate the amount of fat [33,37–40]. Examinations in pigs related to VAT by MRI and DXA, however, have not been reported yet. Mohammad et al. compared VAT values from enCore software with MRI results, using identical anatomical regions for both techniques in Kuwaiti men and women, and found an overestimation of 79.7 cm^3 (95% limits of agreement, −767 cm^3 to 963 cm^3) in men and 46.8 cm^3 (95% limits of agreement, −482 cm^3 to 866 cm^3) in women and an increasing imprecision with increasing VAT levels [37]. In pigs, Mitchell et al. found that DXA (Lunar DPX-L) tends to overestimate the total body fat content in pigs that have more than 20% body fat and underestimates the fat content in leaner pigs, compared to chemical analysis [33].

The overestimation might be explained by the fact that scanning too quickly or with insufficient X-ray source current, depending on body thickness, a degradation of the image quality would result by "starving" each pixel of X-ray photons [41]. Therefore, especially in animals with a larger body thickness, the X-rays are attenuated to a greater extend and may result in an inaccuracy of the results. To compensate, the influence of body thickness, the enCore software offers different modes related to different body thicknesses ("standard": 15–25 cm; "thick": > 25 cm) combined with a prolonged scan time (more X-ray photons per scan area) in "thick" mode, leading to a higher absorbed dose (6 μGy in "thick" mode vs. 3 μGy in "standard" mode). With the "thick" mode, we measured VAT values closer to the MRI results than with the "standard" mode, which confirms the influence of X-ray photon intensity on the 2D image quality and underlying X-ray attenuation coefficients (R values).

Lukaski et al. examined the effect of body thickness on the difference in chemical and DXA analysis results using a Hologic 2000W scanner. The total errors in the determination of DXA body composition variables were similar with body thicknesses greater and less than 24 cm, and no effect was associated with the tissue thickness and estimation of fat [42]. This observation is in contrast to our study and to others, where tissue thicknesses of 20–25 cm were associated with an overestimation of fat in and ex vivo [43,44]. The results of our study show an increasing overestimation of VAT measured by DXA compared to MRI results with increasing levels of VAT. To compensate the overestimation of DXA, the VAT values need to be bias corrected, according to the regression equations shown in Table 4.

In general, the comparison of studies measuring VAT or total fat in the android region is difficult for several reasons. Firstly, it is essential to examine the same anatomical region with both applied methods. In CoreScan, the android region is defined as 20% of the distance between the top of the iliac crest and the base of the skull and, therefore, the region varies according to the length of the trunk [45]. Using a fixed region in MRI would lead to inaccuracies. For example, Neeland et al. used a single MRI slice at the L2–L3 intervertebral level and compared it with an estimation of VAT mass at the L4–L5 region in DXA [38]. To avoid this source of error, we defined an exact body region for the MR imaging, which starts at the origin of the last rib and reaches to the top of the iliac crest. The android region, by using the DXA enCore software, was adapted to cover this defined region. Secondly, other reasons for the difficulty of comparing studies are: different analytical methods, including multiple or single slice MRI, different equipment and software, such as GE Healthcare/CoreScan or Hologic/InnerCore instruments, and the measured parameters (area or volume). Summarizing our results, DXA "CoreScan" has the ability to estimate VAT in pigs with a close relationship to MRI, but it is biased, according to the Bland–Altman analysis, as shown in Tables 3 and 4 and Figures 8 and 9.

In humans, the well-known gender-related differences in fat distribution arise, among other things, due to sexual hormones, which have multiple effects on adipose tissue [46]. Various studies found that adipose tissue presents sexual steroid receptors for estrogens, androgens, and progesterone [47–49]. The expression of these receptors varies by depot and gender. In intra-abdominal preadipocytes, the number of androgen binding sites is higher than in subcutaneous fat depots in males and females [48]. In males, the density of estrogen receptors in visceral adipose tissue is lower than in subcutaneous depots, and the binding capacity in SAT is also higher compared to VAT [50,51]. Another fact, which underlines the effect of sexual hormones is that sexual maturity influences total body fat and subcutaneous and visceral adipose tissue [22].

For translational medicine, it is important to characterize the animal model by identifying the potentials and limitations. Especially in the field of obesity research (e.g., metabolic syndrome), gender-associated differences are an evolving issue in human medicine and should be addressed in the animal model. Therefore, it is essential to consider the discrepancies in sex hormone patterns between pigs and humans [52,53]. Several studies examined female and male (intact) minipigs and their ability to be a model for metabolic syndrome or in general for obesity research. Females had more total body fat, including more visceral fat. Metabolic abnormalities were more severe compared to intact male minipigs, which might be explained by the higher amount of fat. In conclusion, it was postulated that female minipigs might better display the obesity-related consequences in humans. Different hormone concentrations could be seen as a possible cause for the observed differences between male and female (mini-)pigs. Male (intact) minipigs have extremely high concentrations of testosterone, while their concentration of estradiol is even higher than in females before and after sexual maturity [52,53]. This phenomenon has also been reported for crossbreeds. Crossbred boars showed higher estradiol concentrations than crossbred females, already by the 98th day of life [54]. In general, the high concentration of testosterone and estradiol protects male minipigs from obesity and depositing fat (including VAT) at a high rate. Comparing the hormone concentrations to the situation in humans, the estradiol in female minipigs displays the concentration in post-menopausal women or men, while the concentration of estradiol in intact male minipigs is more similar to the concentration in pre-menopausal women, but is still even lower than in pre-menopausal women [52,53]. In our study, castrated male pigs and female pigs were examined shortly before sexual maturity. The observed amounts of VAT, which were higher in our castrated males, were similar to the human situation between intact men and women. However, they also showed a higher total fat content, which is in contrast to humans, where women have greater amounts of total body fat than intact men. Christoffersen et al. studied the influence of castration in Göttinger minipigs and found a complete disappearance of circulating testosterone and estradiol, resulting in an increased food intake, increased body weight, and also an increased body fat content. Already at 10 to 11 weeks after castration, the pigs were more insulin resistant, showed higher glucose intolerance and hyperglucagonemia. In general, low testosterone and estradiol concentrations are predictive for metabolic syndrome [55]. Therefore, castrated male pigs may be even more suitable to examine obesity-related consequences, because they achieved higher levels of VAT compared to females. In addition, castrated male pigs with a complete absence of sexual steroids might be used as a neutral basis for studies on the effects of hormones on obesity, VAT, and their related consequences after the application of steroids. The use of defined steroid concentrations offers the opportunity to readjust the situation in humans as accurately as possible with a simultaneous unchanged gene situation.

Similar findings are described in pigs, where the proportion of fat increases in the carcasses of older and heavier pigs [56,57]. In accordance with other studies, this study shows an increase in VAT of 18.3 cm^3 per kilogram weight in MRI, as shown in Figure 11. Mohrmann et al. found the highest accumulation of fat in animals with a weight range of 90-120 kg, whereas Giles et al. described a smaller range, 80–100 kg [58,59]. Consequently, the pigs in our study were in the weight range of highest fat accumulation and have the potential to be an appropriate model for VAT examination. A study of fat deposition in pigs by CT found an increasing proportion of abdominal fat in total fat with increasing live weight [60].

As described previously, the amount of fat in humans increases with age. In our study, pigs at a relatively young age of 5 months were examined. Already at this time, increasing fat contents were found. Deeper insights into the development of fat could be reached by studying the pigs at several time points and at later stages of age. However, the use of MRI and DXA is limited by the size and weight of the object under investigation. In addition, for research purposes, a preferably early examination of the animals is of interest to save costs and time. Koopmans et al. recorded in their study a weight of 70 kg with 1.2 kg VAT for obese minipigs and compared this pig model to humans. In humans, one kilogram of VAT is already considered as a health threat, usually present at body weights above 100 kg. Furthermore, it was postulated that it takes a time period of five to six months to develop the obese-metabolic-syndrome phenotype [61]. The pigs in our study are at this age and achieved VAT values of more than one kilogram (1.8 kg VAT in castrated males, 1.2 kg in females). Therefore, castrated male pigs are also a suitable model for obesity research.

In pigs, the influence of sex on body and/or carcass composition is widely investigated. The findings of this study, where castrated males have higher amounts of total body fat and also of VAT compared to females, are in agreement with other studies. Carcasses of boars are characterized by the highest lean meat content, combined with a low fat content, followed by gilts. Barrows (castrated male pigs) tend to have fatter carcasses with the lowest lean meat content [57,62]. The results of our study show that DXA has the ability to measure these sex-related differences of total body fat and VAT.

Besides sex, age, and weight, fat deposition is also influenced by genetic background. Body composition in pigs is polygenically controlled, and a large number of genes and markers associated with variations in fat and lean mass content have been identified [14,63,64]. Quantitative trait loci (QTL) should help to localize genes that—besides environmental effects—control specific phenotypes. The database PigQTLdb offers an extensive summary of published QTL information and, so far (as of 26.03.2020), 3138 QTL are associated with the trait "fatness" [65,66]. Rothammer et al. found, in a genome-wide QTL mapping study, 41 significant associations with the percentage of fat, measured by using a whole-body DXA scan on 13 chromosomes in pigs, and hypothesized, for example, the effect of the candidate gene *ZNF608* on fat mass [14]. In humans, the association of *ZNF608* and body mass index has likewise been reported [67,68]. In a recent study, Rothammer et al. examined the effect of regional body composition traits on QTL results. They compared the results of the QTL-mapping analysis using a whole-body DXA scan of 2014 with the findings of QTL in regional DXA analyses (e.g., in the region of the abdomen). Overall, it can be concluded that a whole-body DXA scan provides reliable and substantial results, but specific regional analyses will provide additional knowledge of locally active QTL. For example, seven QTL, that can be associated with possible candidate genes, have been found only in the region of the abdomen, and did not show up in the whole-body QTL analysis. Three of these seven QTL are associated with the phenotype of fat, and possible candidate genes are: polypeptide N-acetylgalactosaminyltransferase 17 (*GALNT17*, previous symbol: *WBSCR17,* chromosome 3); abhydrolase domain containing 6 (*ABHD6*, chromosome 13); pyruvate dehydrogenase E1 subunit beta (PDHB, chromosome 13) [69]. In mutant mice, *WBSCR17* is associated with a decrease in lean body mass. A selective knockdown of *ABHD6* protects mice from high-fat-induced obesity [70,71], while *PDHB* on chromosome 13 has been described in cattle and pigs and is a candidate gene for intramuscular fat deposition [72,73]. It can be hypothesized that the effects of QTL, which are found only by analyzing a specific body region, are predominantly local [69]. Therefore, the regional analyses of fat, and especially of VAT, conducted in our study might provide extra value for genomic analyses. In addition, the simultaneous occurrence of genetic and phenotypic differences is essential for marker-based mapping of QTL and, therefore, the use of different breeds in the initial generation will lead to a high variance in F2 generation [64]. For this reason, four conventional breeds are used in our study for phenotyping in the multiple F1 and F2 crossbreeding generations to create a basis for genomic analyses. Scholz et al. estimate the additive genetic variance components to account for 45–60% of the phenotypic variation of body composition traits [15,63]. A study by Kogelman et al. determines a higher heritability of DXA lean mass of 0.71 compared to 0.43 for DXA fat mass in a F2 population with Göttinger minipigs [74]. In addition to the heritability (proportion of additive genetic variance on phenotypic variance), heterosis effects in crossbred lines may be associated with a variation in body composition. The influence of heterosis is greatest in the F1 generation and declines in further generations. Therefore, especially F1 crossbreds are used for fattening and reproduction, due to their superiority [75,76]. Carcasses of F1 crossbreds are characterized by higher weights, more lean tissue mass, but also higher fat mass [77,78]. In a study by Müller et al., traits such as growth, carcass, and meat quality were examined in wild boars, Meishan and Pietran pigs, and their crossbreeds [78]. All crossbreds showed a higher amount of abdominal fat weight in the F1 compared to the F2 generation, which underlines the results of our study, where F1 pigs have higher amounts of total body fat, fat in the android region, and also more VAT, as shown in Table 6.

Our study dealt with the ability of the DXA CoreScan feature to provide VAT estimates in pigs as a model for human research. The results support the hypothesis that DXA and the CoreScan feature might be applicable to a wider range of species for fat measurements for translational research.

5. Conclusions

Our study shows the ability of the DXA CoreScan feature to provide VAT estimates in pigs, but needs a bias correction if MRI VAT is seen as the reference method. The low-cost measuring method described here is more easily accessible and has shorter examination times than MRI, and leads to less exposure to ionic radiation than CT. In addition, the variance analysis of the DXA results underlines the known genetic- and sex-related differences in body composition in pigs, where castrated males and the first crossbred generation tend to have higher amounts of total body fat and visceral fat depots. Further studies into distinct fat depots, especially SAT in the android region, will help to evaluate the CoreScan feature in more detail. A combination of describing the phenotypic variance by in vivo techniques (MRI, DXA) with genomic analyses will help to identify more genes related to body composition traits. These findings will have an impact on human health by contributing new prospects to the field of obesity research.

Author Contributions: Conceptualization, A.M.S.; data curation, A.C.W.; formal analysis, A.C.W. and A.M.S.; investigation, A.C.W., H.S., D.A.K. and A.M.S.; methodology, A.C.W. and A.M.S.; project administration, A.C.W. and A.M.S.; supervision, A.M.S.; validation, A.C.W. and A.M.S.; visualization, A.C.W.; writing—original draft, A.C.W.; writing—review and editing, A.C.W. and A.M.S.

Funding: This research received no external funding.

Conflicts of Interest: The authors declare no conflict of interest.

References

1. World Health Organization. Cardiovascular diseases (CVDs). https://www.who.int/news-room/fact-sheets/detail/cardiovascular-diseases-(cvds) (accessed on 27 March 2020).
2. Statistisches Bundesamt. Zahl der Todesfälle im Jahr 2017 um 2,3 % gestiegen. https://www.destatis.de/DE/Themen/Gesellschaft-Umwelt/Gesundheit/Todesursachen/todesfaelle.html;jsessionid=942A0C43C62E6604E5EB4BC9B457D203.internet721 (accessed on 27 March 2020).
3. Dornquast, C.; Kroll, L.E.; Neuhauser, H.K.; Willich, S.N.; Reinhold, T.; Busch, M.A. Regional Differences in the Prevalence of Cardiovascular Disease. Dtsch. Arztebl. Int. 2016, 113, 704–711, doi:10.3238/arztebl.2016.0704.
4. World Health Organization. The top 10 causes of death. https://www.who.int/news-room/fact-sheets/detail/the-top-10-causes-of-death (accessed on 27 March 2020).
5. Robert Koch-Institut. Gesundheit in Deutschland: Gesundheitsberichterstattung des Bundes. Gemeinsam getragen von RKI und Destatis 2015.
6. Bundesärztekammer (BÄK), Kassenärztliche Bundesvereinigung (KBV), Arbeitsgemeinschaft der Wissenschaftlichen Medizinischen Fachgesellschaften. Nationale VersorgungsLeitlinie Chronische Herzinsuffizienz - Langfassung, 3.Auflage, 2019.
7. Fox, C.S.; Massaro, J.M.; Hoffmann, U.; Pou, K.M.; Maurovich-Horvat, P.; Liu, C.-Y.; Vasan, R.S.; Murabito, J.M.; Meigs, J.B.; Cupples, L.A.; et al. Abdominal visceral and subcutaneous adipose tissue compartments: association with metabolic risk factors in the Framingham Heart Study. Circulation 2007, 116, 39–48, doi:10.1161/CIRCULATIONAHA.106.675355.
8. Liu, J.; Fox, C.S.; Hickson, D.A.; May, W.D.; Hairston, K.G.; Carr, J.J.; Taylor, H.A. Impact of

Abdominal Visceral and Subcutaneous Adipose Tissue on Cardiometabolic Risk Factors: The Jackson Heart Study. J. Clin. Endocrinol. Metab. 2010, 95, 5419–5426, doi:10.1210/jc.2010-1378.

9. Rodríguez, R.R.; González-Bulnes, A.; Garcia-Contreras, C.; Elena Rodriguez-Rodriguez, A.; Astiz, S.; Vazquez-Gomez, M.; Luis Pesantez, J.; Isabel, B.; Salido-Ruiz, E.; González, J.; et al. The Iberian pig fed with high-fat diet: a model of renal disease in obesity and metabolic syndrome. Int. J. Obes. (Lond) 2020, 44, 457–465, doi:10.1038/s41366-019-0434-9.

10. Lanzas, C.; Ayscue, P.; Ivanek, R.; Gröhn, Y.T. Model or meal? Farm animal populations as models for infectious diseases of humans. Nat. Rev. Microbiol. 2010, 8, 139–148, doi:10.1038/nrmicro2268.

11. Renner, S.; Blutke, A.; Clauss, S.; Deeg, C.A.; Kemter, E.; Merkus, D.; Wanke, R.; Wolf, E. Porcine models for studying complications and organ crosstalk in diabetes mellitus. Cell Tissue Res. 2020, 1–38, doi:10.1007/s00441-019-03158-9.

12. Rohrer, G.; Beever, J.E.; Rothschild, M.F.; Schook, L.; Gibbs, R.; Weinstock, G. Porcine genomic sequencing initiative. Porcine Sequencing White Paper 2002, 1–10.

13. Hishikawa, D.; Hong, Y.-H.; Roh, S.-g.; Miyahara, H.; Nishimura, Y.; Tomimatsu, A.; Tsuzuki, H.; Gotoh, C.; Kuno, M.; Choi, K.-C.; et al. Identification of genes expressed differentially in subcutaneous and visceral fat of cattle, pig, and mouse. Physiol. Genomics 2005, 21, 343–350, doi:10.1152/physiolgenomics.00184.2004.

14. Rothammer, S.; Kremer, P.V.; Bernau, M.; Fernandez-Figares, I.; Pfister-Schär, J.; Medugorac, I.; Scholz, A.M. Genome-wide QTL mapping of nine body composition and bone mineral density traits in pigs. Genet Sel Evol 2014, 46, 1–11, doi:10.1186/s12711-014-0068-2.

15. Scholz, A.M.; Bünger, L.; Kongsro, J.; Baulain, U.; Mitchell, A.D. Non-invasive methods for the determination of body and carcass composition in livestock: dual-energy X-ray absorptiometry, computed tomography, magnetic resonance imaging and ultrasound: invited review. Animal 2015, 9, 1250–1264, doi:10.1017/S1751731115000336.

16. Siemens AG. Technical Documents. MAGNETOM C! syngo MR, M4-030.815.01.03.02, 2004.

17. Pietrobelli, A.; Gallagher, D.; Baumgartner, R.; Ross, R.; Heymsfield, S.B. Lean R value for DXA two-component soft-tissue model: Influence of age and tissue or organ type. Applied Radiation and Isotopes 1998, 49, 743–744, doi:10.1016/S0969-8043(97)00100-0.

18. GE Healthcare. Lunar CoreScan Application from GE Healthcare. https://www.gehealthcare.com/-/jssmedia/1cd6ce71f5cd4ac1b782fa1815ddb23b.pdf (accessed on 21 May 2020).

19. GE Healthcare. Advancements in DXA Body Composition Analysis: Metabolic Phenotyping with CoreScan. https://www3.gehealthcare.com/~/media/downloads/us/product/product-categories/metabolic-health/gated-pdfs/Whitepaper-Metabolic-Phenotyping-with-CoreScan-JB47862XX.pdf (accessed on 27 March 2020).

20. GE Healthcare. Lunar. enCORE-based X-ray Bone Densitometer. User Manual, 5.th ed.; Madison, Wisconsin, USA, 2010.

21. Altman, D.G.; Bland, J.M. Measurement in Medicine: The Analysis of Method Comparison Studies. The Statistician 1983, 32, 307, doi:10.2307/2987937.

22. Staiano, A.E.; Katzmarzyk, P.T. Ethnic and sex differences in body fat and visceral and subcutaneous adiposity in children and adolescents. Int. J. Obes. (Lond) 2012, 36, 1261–1269, doi:10.1038/ijo.2012.95.

23. Maislin, G.; Ahmed, M.M.; Gooneratne, N.; Thorne-Fitzgerald, M.; Kim, C.; Teff, K.; Arnardottir, E.S.; Benediktsdottir, B.; Einarsdottir, H.; Juliusson, S.; et al. Single slice vs. volumetric MR assessment of visceral adipose tissue: reliability and validity among the overweight and obese. Obesity 2012, 20, 2124–2132, doi:10.1038/oby.2012.53.

24. Lee, S.Y.; Gallagher, D. Assessment methods in human body composition. Curr. Opin. Clin. Nutr. Metab. Care 2008, 11, 566–572, doi:10.1097/MCO.0b013e32830b5f23.

25. Shuster, A.; Patlas, M.; Pinthus, J.H.; Mourtzakis, M. The clinical importance of visceral adiposity: a critical review of methods for visceral adipose tissue analysis. Br. J. Radiol. 2012, 85,

1–10, doi:10.1259/bjr/38447238.

26. Thomas, E.L.; Bell, J.D. Influence of undersampling on magnetic resonance imaging measurements of intra-abdominal adipose tissue. Int. J. Obes. Relat. Metab. Disord. 2003, 27, 211–218, doi:10.1038/sj.ijo.802229.

27. Snijder, M.B.; Visser, M.; Dekker, J.M.; Seidell, J.C.; Fuerst, T.; Tylavsky, F.; Cauley, J.; Lang, T.; Nevitt, M.; Harris, T.B. The prediction of visceral fat by dual-energy X-ray absorptiometry in the elderly: a comparison with computed tomography and anthropometry. Int. J. Obes. Relat. Metab. Disord. 2002, 26, 984–993, doi:10.1038/sj.ijo.0801968.

28. Micklesfield, L.K.; Goedecke, J.H.; Punyanitya, M.; Wilson, K.E.; Kelly, T.L. Dual-energy X-ray performs as well as clinical computed tomography for the measurement of visceral fat. Obesity 2012, 20, 1109–1114, doi:10.1038/oby.2011.367.

29. Fourman, L.T.; Kileel, E.M.; Hubbard, J.; Holmes, T.; Anderson, E.J.; Looby, S.E.; Fitch, K.V.; Feldpausch, M.N.; Torriani, M.; Lo, J.; et al. Comparison of visceral fat measurement by dual-energy X-ray absorptiometry to computed tomography in HIV and non-HIV. Nutr. Diabetes 2019, 9, 1–10, doi:10.1038/s41387-019-0073-1.

30. Schlegel, P.; Gutzwiller, A. Dietary Calcium to Digestible Phosphorus Ratio for Optimal Growth Performance and Bone Mineralization in Growing and Finishing Pigs. Animals (Basel) 2020, 10, doi:10.3390/ani10020178.

31. Hartnett, P.; Boyle, L.; Younge, B.; O'Driscoll, K. The Effect of Group Composition and Mineral Supplementation during Rearing on Measures of Cartilage Condition and Bone Mineral Density in Replacement Gilts. Animals (Basel) 2019, 9, doi:10.3390/ani9090637.

32. Mitchell, A.D.; Scholz, A.M.; Wang, P.C.; Song, H. Body composition analysis of the pig by magnetic resonance imaging. J. Anim. Sci. 2001, 79, 1800–1813, doi:10.2527/2001.7971800x.

33. Mitchell, A.D.; Conway, J.M.; Potts, W.J. Body composition analysis of pigs by dual-energy x-ray absorptiometry. J. Anim. Sci. 1996, 74, 2663–2671, doi:10.2527/1996.74112663x.

34. Fowler, P.A.; Fuller, M.F.; Glasbey, C.A.; Cameron, G.G.; Foster, M.A. Validation of the in vivo measurement of adipose tissue by magnetic resonance imaging of lean and obese pigs. Am. J. Clin. Nutr. 1992, 56, 7–13, doi:10.1093/ajcn/56.1.7.

35. Scholz, A.M.; Förster, M. Genauigkeit der Dualenergie-Röntgenabsorptiometrie (DXA) zur Ermittlung der Körperzusammensetzung von Schweinen in vivo. Arch. Anim. Breed. 2006, 49, 462–476, doi:10.5194/aab-49-462-2006.

36. Baulain, U.; Friedrichs, M.; Höreth, R.; Henning, M.; Tholen, E. Use of MRI to assess carcass and primal cut composition in different pig breeds, 2010. www.kongressband.de/wcgalp2010/assets/pdf/0357.pdf.

37. Mohammad, A.; Lucia Rolfe, E. de; Sleigh, A.; Kivisild, T.; Behbehani, K.; Wareham, N.J.; Brage, S.; Mohammad, T. Validity of visceral adiposity estimates from DXA against MRI in Kuwaiti men and women. Nutr. Diabetes 2017, 7, e238, doi:10.1038/nutd.2016.38.

38. Neeland, I.J.; Grundy, S.M.; Li, X.; Adams-Huet, B.; Vega, G.L. Comparison of visceral fat mass measurement by dual-X-ray absorptiometry and magnetic resonance imaging in a multiethnic cohort: the Dallas Heart Study. Nutr. Diabetes 2016, 6, e221, doi:10.1038/nutd.2016.28.

39. Reinhardt, M.; Piaggi, P.; DeMers, B.; Trinidad, C.; Krakoff, J. Cross calibration of two dual-energy X-ray densitometers and comparison of visceral adipose tissue measurements by iDXA and MRI. Obesity (Silver Spring) 2017, 25, 332–337, doi:10.1002/oby.21722.

40. Taylor, A.E.; Kuper, H.; Varma, R.D.; Wells, J.C.; Bell, J.D.; V Radhakrishna, K.; Kulkarni, B.; Kinra, S.; Timpson, N.J.; Ebrahim, S.; et al. Validation of dual energy X-ray absorptiometry measures of abdominal fat by comparison with magnetic resonance imaging in an Indian population. PLOS ONE 2012, 7, e51042, doi:10.1371/journal.pone.0051042.

41. GE Healthcare. Lunar Technology Advantages. https://www3.gehealthcare.com/~/media/downloads/us/product/product-categories/metabolic-health/gated-pdfs/BMD-Global-Lunar-Technology-Advantages-JB45946XX.pdf (accessed on 28 April 2020).

42. Lukaski, H.C.; Marchello, M.J.; Hall, C.B.; Schafer, D.M.; Siders, W.A. Soft tissue composition of pigs measured with dual x-ray absorptiometry: comparison with chemical analyses and effects of carcass thicknesses. Nutrition 1999, 15, 697–703, doi:10.1016/S0899-9007(99)00154-9.

43. Laskey, M.A.; Lyttle, K.D.; Flaxman, M.E.; Barber, R.W. The influence of tissue depth and composition on the performance of the Lunar dual-energy X-ray absorptiometer whole-body scanning mode. Eur. J. Clin. Nutr. 1992, 46, 39–45.

44. Jebb, S.A.; Goldberg, G.R.; Jennings, G.; Elia, M. Dual-energy X-ray absorptiometry measurements of body composition: effects of depth and tissue thickness, including comparisons with direct analysis. Clin. Sci. 1995, 88, 319–324, doi:10.1042/cs0880319.

45. Kaul, S.; Rothney, M.P.; Peters, D.M.; Wacker, W.K.; Davis, C.E.; Shapiro, M.D.; Ergun, D.L. Dual-energy X-ray absorptiometry for quantification of visceral fat. Obesity (Silver Spring) 2012, 20, 1313–1318, doi:10.1038/oby.2011.393.

46. Björntorp, P. The regulation of adipose tissue distribution in humans. Int. J. Obes. Relat. Metab. Disord. 1996, 20, 291–302.

47. Pedersen, S.B.; Bruun, J.M.; Hube, F.; Kristensen, K.; Hauner, H.; Richelsen, B. Demonstration of estrogen receptor subtypes α and β in human adipose tissue: influences of adipose cell differentiation and fat depot localization. Molecular and Cellular Endocrinology 2001, 182, 27–37, doi:10.1016/S0303-7207(01)00557-3.

48. Dieudonne, M.N.; Pecquery, R.; Boumediene, A.; Leneveu, M.C.; Giudicelli, Y. Androgen receptors in human preadipocytes and adipocytes: regional specificities and regulation by sex steroids. Am. J. Physiol. 1998, 274, C1645-52, doi:10.1152/ajpcell.1998.274.6.C1645.

49. O'Brien, S.N.; Welter, B.H.; Mantzke, K.A.; Price, T.M. Identification of progesterone receptor in human subcutaneous adipose tissue. J. Clin. Endocrinol. Metab. 1998, 83, 509–513, doi:10.1210/jcem.83.2.4561.

50. Wells, J.C.K. Sexual dimorphism of body composition. Best Pract. Res. Clin. Endocrinol. Metab. 2007, 21, 415–430, doi:10.1016/j.beem.2007.04.007.

51. Pedersen, S.B.; Hansen, P.S.; Lund, S.; Andersen, P.H.; Odgaard, A.; Richelsen, B. Identification of oestrogen receptors and oestrogen receptor mRNA in human adipose tissue. Eur. J. Clin. Invest. 1996, 26, 262–269, doi:10.1046/j.1365-2362.1996.145278.x.

52. Christoffersen, B.; Golozoubova, V.; Pacini, G.; Svendsen, O.; Raun, K. The Young Göttingen Minipig as a Model of Childhood and Adolescent Obesity: Influence of Diet and Gender. Obesity 2012, 1, 11, doi:10.1038/oby.2012.176.

53. Christoffersen, B.O.; Grand, N.; Golozoubova, V.; Svendsen, O.; Raun, K. Gender-associated differences in metabolic syndrome-related parameters in Göttingen minipigs. Comp. Med. 2007, 57, 493–504.

54. Clapper, J.A.; Clark, T.M.; Rempel, L.A. Serum concentrations of IGF-I, estradiol-17beta, testosterone, and relative amounts of IGF binding proteins (IGFBP) in growing boars, barrows, and gilts. J. Anim. Sci. 2000, 78, 2581–2588, doi:10.2527/2000.78102581x.

55. Christoffersen, B.O.; Gade, L.P.; Golozoubova, V.; Svendsen, O.; Raun, K. Influence of castration-induced testosterone and estradiol deficiency on obesity and glucose metabolism in male Göttingen minipigs. Steroids 2010, 75, 676–684, doi:10.1016/j.steroids.2010.04.004.

56. Farnworth, E.R.; Kramer, J.K.G. Fat metabolism in growing swine: a review. Can. J. Anim. Sci. 1987, 67, 301–318, doi:10.4141/cjas87-029.

57. Irshad, A.; Kandeepan, G.; Kumar, S.; Ashish, K.A.; Vishnuraj; Shukla, V. Factors influencing carcass composition of livestock: A review. J. Anim. Prod. Adv 2013, 3, 177–186.

58. Mohrmann, M.; Roehe, R.; Susenbeth, A.; Baulain, U.; Knap, P.W.; Looft, H.; Plastow, G.S.; Kalm, E. Association between body composition of growing pigs determined by magnetic resonance imaging, deuterium dilution technique, and chemical analysis. Meat Sci. 2006, 72, 518–531, doi:10.1016/j.meatsci.2005.08.020.

59. Giles, L.R.; Eamens, G.J.; Arthur, P.F.; Barchia, I.M.; James, K.J.; Taylor, R.D. Differential growth and development of pigs as assessed by X-ray computed tomography. J. Anim. Sci. 2009, 87,

1648–1658, doi:10.2527/jas.2008-1437.

60. Kolstad, K. Fat deposition and distribution in three genetic lines of pigs from 10 to 105 kg liveweight. Quality of meat and fat in pigs as affected by genetics and nutrition. Proceedings of the joint session of the EAAP commissions on pig production, animal genetics and animal nutrition, Zurich, Switzerland, 25 August 1999. 2000, 199–202.

61. Koopmans, S.J.; Schuurman, T. Considerations on pig models for appetite, metabolic syndrome and obese type 2 diabetes: From food intake to metabolic disease. Eur. J. Pharmacol. 2015, 759, 231–239, doi:10.1016/j.ejphar.2015.03.044.

62. Bauer Aneka; Judas M. Schlachtkörperqualität von Mastebern in Vergleich zu Sauen und Börgen. Züchtungskunde 2014, 374–389.

63. Scholz, A.M. In-vivo-Methoden zur Analyse von Muskelstoffwechsel und Körperzusammensetzung beim Schwein unter besonderer Berücksichtigung genetischer Einflüsse. Habilitationsschrift; Tierärztliche Fakultät der Ludwig-Maximilians-Universität, München, 2002.

64. Ernst, C.W.; Steibel, J.P. Molecular advances in QTL discovery and application in pig breeding. Trends Genet. 2013, 29, 215–224, doi:10.1016/j.tig.2013.02.002.

65. Pig QTL Database. https://www.animalgenome.org/cgi-bin/QTLdb/SS/index (accessed on 27 March 2020).

66. Hu, Z.-l.; Dracheva, S.; Jang, W.; Maglott, D.; Bastiaansen, J.; Rothschild, M.F.; Reecy, J.M. A QTL resource and comparison tool for pigs: PigQTLDB. Mamm. Genome 2005, 16, 792–800, doi:10.1007/s00335-005-0060-9.

67. Ntalla, I.; Panoutsopoulou, K.; Vlachou, P.; Southam, L.; William Rayner, N.; Zeggini, E.; Dedoussis, G.V. Replication of established common genetic variants for adult BMI and childhood obesity in Greek adolescents: the TEENAGE study. Ann. Hum. Genet. 2013, 77, 268–274, doi:10.1111/ahg.12012.

68. Speliotes, E.K.; Willer, C.J.; Berndt, S.I.; et al. Association analyses of 249,796 individuals reveal 18 new loci associated with body mass index. Nat. Genet. 2010, 42, 937–948, doi:10.1038/ng.686.

69. Rothammer, S.; Bernau, M.; Kremer-Rücker, P.V.; Medugorac, I.; Scholz, A.M. Genome-wide QTL mapping results for regional DXA body composition and bone mineral density traits in pigs. Arch. Anim. Breed. 2017, 60, 51–59, doi:10.5194/aab-60-51-2017.

70. International Mouse Phenotyping Consortium. https://www.mousephenotype.org/(accessed on 21 April 2020).

71. Thomas, G.; Betters, J.L.; Lord, C.C.; Brown, A.L.; Marshall, S.; Ferguson, D.; Sawyer, J.; Davis, M.A.; Melchior, J.T.; Blume, L.C.; et al. The serine hydrolase ABHD6 Is a critical regulator of the metabolic syndrome. Cell Rep. 2013, 5, 508–520, doi:10.1016/j.celrep.2013.08.047.

72. Sasaki, Y.; Nagai, K.; Nagata, Y.; Doronbekov, K.; Nishimura, S.; Yoshioka, S.; Fujita, T.; Shiga, K.; Miyake, T.; Taniguchi, Y.; et al. Exploration of genes showing intramuscular fat deposition-associated expression changes in musculus longissimus muscle. Anim. Genet. 2006, 37, 40–46, doi:10.1111/j.1365-2052.2005.01380.x.

73. Serão, N.V.L.; Veroneze, R.; Ribeiro, A.M.F.; Verardo, L.L.; Braccini Neto, J.; Gasparino, E.; Campos, C.F.; Lopes, P.S.; Guimarães, S.E.F. Candidate gene expression and intramuscular fat content in pigs. Journal of Animal Breeding and Genetics 2011, 128, 28–34, doi:10.1111/j.1439-0388.2010.00887.x.

74. Kogelman, L.J.A.; Kadarmideen, H.N.; Mark, T.; Karlskov-Mortensen, P.; Bruun, C.S.; Cirera, S.; Jacobsen, M.J.; Jørgensen, C.B.; Fredholm, M. An f2 pig resource population as a model for genetic studies of obesity and obesity-related diseases in humans: design and genetic parameters. Front. Genet. 2013, 4, 29, doi:10.3389/fgene.2013.00029.

75. Wakchaure; R., Ganguly, S.; Praveen, K.P.; Sharma, S.; Kumar, A.; Mahajan, T.; Qadri, K. Importance of Heterosis in Animals: A Review. International Journal of Advanced Engineering Technology and Innovative Science 2015, 1, 1–5.

76. Christians, C.J.; Johnson, R.K. Crossbreeding programs for commercial pork production. EM-

Cooperative Extension Service, College of Agriculture, Washington State University (USA) 1978.

77. Bennnett, G.L.; Tess, M.W.; Dickerson, G.E.; Johnson, R.K. Simulation of Heterosis Effects on Costs of Pork Production. J. Anim. Sci. 1983, 56, 792–800, doi:10.2527/jas1983.564792x.

78. Müller, E.; Moser, G.; Bartenschilager, H.; Geldermann, H. Trait values of growth, carcass and meat quality in Wild Boar, Meishan and Pietrain pigs as well as their crossbred generations. Journal of Animal Breeding and Genetics 2000, 117, 189–202, doi:10.1046/j.1439-0388.2000.00239.x.

IV. DISCUSSION AND OUTLOOK

MRI and DXA offer suitable methods to analyze various phenotypic traits in pigs *in vivo*. In terms of body composition analyses, DXA has the ability to predict the fat and lean composition as well as the bone mineral content including the bone mineral density of pigs exactly. The results show that – based on the MRI reference – DXA is also a suitable method for determining the Visceral Adipose Tissue (VAT) in pigs by using the CoreScan software of GE Healthcare.

Determining the exact phenotype builds the basis for genomic analyses and enables a more precise description of the effect of genes, QTL (quantitative trait loci), or expression of specific proteins based on variations found in the phenotype. Furthermore, regional analyses of specific traits will provide additional knowledge of QTL that have predominantly local effects. Therefore, phenotyping the VAT and not only the fat in the android region is appropriate. In addition, VAT may play an increasing role in the breeding work and in experimental animals for human obesity-related studies.

1. Medical imaging results

1.1. MRI results serve as reference

MRI is the method of choice for quantifying adipose tissue in humans and for localizing its distribution, and is, besides CT, considered as gold standard for VAT determination (Chapter II.4.1.4 Use of MRI for VAT examination in humans). In pigs, MRI has been shown to be able being used as a reference method for body composition analyses *in vivo* and in carcasses (Chapter II.4.1.3 MRI in pigs). In the own study, the MR images were analyzed manually and only by one person to prevent an inter-operator error. Multiple slices were analyzed to directly asses the volume of VAT. Due to artifacts (Chapter II.4.1.2 Artifacts in the MR image), which can occur in MR images especially in the abdominal cavity, an imprecision for VAT volume may have resulted. However, the MRI results show significantly the same sex and genotype related differences of VAT volume as for the DXA results. In addition, the MRI and DXA results showed a close relationship confirming the accuracy of the DXA method. The own results show a significantly larger VAT volume in castrated males (1,188.83 cm^3) than in females (1,016.65 cm^3), while pigs of the first crossbreeding generation (MHF1) reached larger volumes of VAT than the F2 (MHF2) with 1,196.40 cm^3 compared to 1,009.08 cm^3, respectively. There are, so far, no other studies known examining the VAT volume of pigs by using DXA and MRI. Therefore, the results presented here cannot be discussed in comparison to other related “pig studies” – but only in relation to human studies.

1.2. Evaluation of the DXA results

Only one person evaluated all DXA images to minimize that source of error. Furthermore, only images of pigs without motion or other artifacts entered the analysis. In general, due to the fact, that VAT estimates are based on the content of SAT and total adipose tissue in the android region, measurement inaccuracies of SAT will affect VAT estimations as shown by Mohammad et al. (2017) and Fourman et al. (2019) (Mohammad et al., 2017; Fourman et al., 2019). An overestimation of SAT would lead to an underestimation of VAT and vice versa. In addition, the CoreScan mode of the *i*DXA system determines the VAT mass by assuming a density of 0.9435 g/cm^3 for adipose tissue. A review of the literature provides a range of densities for adipose tissue. Adipose tissue consists – besides of fat – of water, proteins and minerals, resulting in a density, which is different to this of fat (lipids only). Snijder et al. (2002) and Hill et al. (2007) used a density of 0.923 g/cm^3 for adipose tissue, whereas McCauley et al. (2020) and Kaul et al. (2012) calculate with 0.94 g/cm^3. Martin et al. (1994) examined in their study the density of adipose tissue in six male cadavers and found a range of 0.925 to 0.970 g/ml (Martin et al., 1994). By using a constant correction factor (such as the density) to calculate the volume based on the VAT mass, the hydration state is assumed to be the same for all subjects and may lead to inaccuracies of the results (Thomas and Bell, 2003).

In addition, all pigs were scanned in the two different DXA modes “thick” and “standard”. The own results show higher values in mode “standard” for total body fat mass, percentage of total body fat, fat in the android region, as well as for the volume and mass of VAT compared to “thick” mode. The enCore software related to the body thickness suggests the different scan modes. The mode “standard” uses an absorbed dose of 3 µGy and is supposed to be suitable for a body thickness of 15 to 25 cm, whereas the mode “thick” with a higher absorbed dose (6 µGy) is set for a body thickness greater than 25 cm. The present results underline the importance to use the mode “thick” in individuals with a body thickness > 25 cm to achieve reasonable results. All examined pigs had a body thickness of more than 25 cm. Correspondingly, the DXA results of mode “thick” showed a closer relationship to the MRI results than did the “standard” mode ($R^2 = 0.76$, RMSE = 399.25 cm^3 vs. $R^2 = 0.71$, RMSE = 443.42 cm^3).

The results of VAT volume and mass cannot be put into the context of other studies, as VAT in pigs has not yet been studied.

Comparing the absolute values of DXA results for total fat mass, percentage fat, and lean mass content with results of other studies, it turns out, that the own records for percentage fat are mainly lower, but combined with a variable fat content, and a clearly higher lean tissue mass. In general, the genetic origin and the body weights must be considered. Scholz and Förster (2006) examined Piétrain purebreds and their crossbreds in a weight range of 70 to 90 kg using DXA and recorded a lean tissue content of 6,1684 g, a fat mass of 1,5681 g which leads to 19.37% of fat (Scholz and Förster, 2006). The present results for heavier pigs (mean: 91.6 kg) are expectedly higher for the lean tissue mass (75,891 g), but lower for the fat mass (13,866 g) and for the percentage of fat with 15.28%. This is in contrast to other findings in pigs, where the proportion of fat increases in older and heavier pigs (Farnworth and Kramer, 1987; Irshad et al., 2013).

Kremer et al. (2012) analyzed different breeds by using DXA. For the comparison to the present research, only the crossbreds of Piétrain, Duroc, German Landrace and Large White were considered. These crossbreeding lines show a clearly lower weight (68.2 kg) at a similar age of 152.8 days. The percentage of fat, however, was practically identical to the own results with 15.74%, while the lean and fat mass (58.54 kg and 12.15 kg) were expectedly lower due to lower weights (Kremer et al., 2012).

Pappenberger (2014) studied the body composition of conventional and “alternative” crossbreds. For the three-breed-cross of Piétrain, German Landrace, and Large White, she obtained a lean tissue content of 73,885 g and a fat content of 14,169 g, resulting in a fat percentage of 15.2%. The animals were about 150 days old and had at this time a body weight of 90.4 kg. These results are very close to the own findings, which might be explained by similar genetics and an almost identical time of investigation (Pappenberger, 2014).

Dölle (2019) examined the body composition of hybrids (Piétrain and German

Landrace) by DXA at three time points. During the third scan, the pigs of the outdoor-climate barn weighed on average 101.0 kg and obtained a lean tissue content of 81,988 g, a fat mass of 16,857 g, and a percentage fat of 16.75%. The greater fat percentage can be explained by the fact that the pigs in the study of Dölle (2019) were older and heavier, and by the faster accumulation of fat compared to muscle growth in the later development of individuals (Switonski et al., 2010; Dölle, 2019).

1.3. Comparison of MRI and DXA results

The results of this study show a high relationship between the VAT measurement by DXA and MRI with a regression coefficient of $R^2 = 0.76$ (RMSE = 399.25 cm^3) for mode "thick". However, the average volume of VAT measured by DXA is about 1.5 to 2 times greater than the VAT volume by MRI. The Bland-Altman analysis provides a mean difference of -579.1 cm^3, while the bias increases with higher levels of VAT. As described in the publication, this finding is in accordance with other studies, where higher values of VAT lead to a lower agreement between both methods – most likely due to an increase of inaccuracy by DXA.

Several studies showed the imprecision of DXA in individuals with higher body mass indices (Chapter II.4.2.2 The CoreScan feature and the use for detecting VAT in humans). The higher body thickness and the influence of the hydration state in combination with the used density (for fat tissue) influence the precision (Chapter IV.1.2 Evaluation of the DXA results). In addition, it must be considered that MRI is able to directly measure the volume of VAT, while DXA only calculate VAT by measuring the fat/lipids content in SAT within the android region. Moreover, a deviation of the examined regions could be responsible for the differences between MRI and DXA. Even by using specific anatomic landmarks in order to exactly define the regions to be examined, it could not be excluded that there might be an error source by not capturing the identical region in both methods. Furthermore, the difficulty to determine VAT on MRI images in the abdominal cavity among other tissues/organs may influence the results. In conclusion, the CoreScan feature has the ability to provide VAT estimates in pigs, but the values need to be corrected if MRI is used as the gold standard.

2. Differences of body composition

2.1. Sex related differences

The present study evaluated the body composition of 63 castrated male and 57 female pigs. All traits, including regional fat and body weight, differed significantly between sexes. Barrows were characterized by a higher content (15,092 g vs. 12,554 g) and percentage (16.35% vs. 14.14%) of total body fat, as well as for fat in the android region (2,409 g vs. 1,957 g), and for the mass (1,868 g vs. 1,290 g) and volume (1,979.53 cm^3 vs. 1,367.33 cm^3) of VAT compared to gilts (Chapter III Publication, Table 6). The lean tissue content showed no significant difference (Chapter VIII Supplementary Material: Table 4). Castrated males, however, reached on average 76,819 g lean tissue and gilts only 74,862 g at an age of 147 days. The own findings for fat and weight are in accordance to several studies examining sex related differences in pigs, where barrows tend to have fatter carcasses than gilts (Chapter II.2.2.3 Sex related differences of adipose tissue in pigs). Pappenberger (2014) also found significant sex differences for the body composition by DXA. Castrated male pigs obtained in general higher values for all traits, excluding the percentage of lean tissue compared to females. The results are similar to the present ones, although a slightly higher percentage of fat in barrows was found (18% vs. 16%) even so the pigs were lighter and younger than here (Pappenberger, 2014). Dölle (2019) compared the DXA body composition results for barrows and gilts as well. The castrated males were heavier (104.7 kg vs. 95.5 kg), reached higher contents of fat (19,277 g vs. 14,152 g) and lean tissue (83,270 g vs. 79,373 g), and also the percentage of fat (18.56% vs. 14.95%) was higher compared to females (Dölle, 2019).

The results of the own study show, that the mass and volume of VAT were also significantly different between castrated males and females, while the percentage of VAT of the total body fat was also higher for the barrows than for gilts (12.4% vs. 10.3%).

In conclusion, the sex related differences obtained in this study, where barrows are heavier and fatter than gilts, are in accordance to other studies. To evaluate the sex related differences in more detail, it would be important to consider the feed intake or possible phases of illness of the pigs during growth. One possibility to evaluate the influence of feed intake could be to examine the feed conversion in different growth periods based on live weight gain and lean tissue gain (Schwanitz et al., 2017).

2.2. Genotype related differences

As described in Chapter II.3 Genetic origin, the examined multiple F1 (MHF1) and F2 (MHF2) crossbreds vary due to different characteristics of the body composition traits of the four breeds used in the crossbreeding scheme (Chapter VIII Supplementary Material: Figure 6). Concerning external characteristics, clear differences can be observed between the two examined crossbred generations F1 and F2. Animals of the first (multiple) crossbred generation (MHF1) are expectedly very uniform with a similar size and white coloring, while the second (multiple) crossbred generation (MHF2) shows a high variance, what can already be seen by the variation in skin coloring (Chapter VIII Supplementary Material: Figure 7).

Body composition is polygenic controlled, and a large number of genes and markers has been identified (Chapter III Publication, 4 Discussion). The proportion of additive genetic variance on phenotypic variance, is called heritability and builds an essential basis for the genetic evaluation (Baumung, 2005; Irshad et al., 2013). A high heritability (in closer sense) indicates that the additive genetic effect is large and a selection towards a specific trait is effective (Stewart et al., 1999). The publication compared heritability estimates for body composition traits of several studies. Besides the additive genetic effects, non-additive genetic effects like dominance and epistasis might influence the body composition traits, explaining the observed heterosis.

The own study found expectedly higher values for all traits in the first crossbreeding generation (MHF1) compared to the F2 (MHF2). The MHF1 achieved about 3.1 kg higher body weights (93.2 kg vs. 90.1 kg), more total body fat (14,532 g vs. 13,114 g), more fat in the android region (2,343 g vs. 2,023 g), and also a higher VAT mass (1,741 g vs. 1,416 g), which resulted in an approximately 23% higher VAT volume (1,845.77 cm^3 vs. 1,501.08 cm^3) compared to the F2 (MHF2) (Chapter III Publication, Table 6). In terms of absolute numbers, the lean tissue mass was slightly higher for the F1 than for the F2 pigs (75,899 g vs. 75,793 g), but the difference was not significant (Chapter VIII Supplementary Material: Table 4).

Since the additive genetic effects are presumably similar between the crossbred generations, the expected heterosis effect in the first crossbred generation and the expected 50% decline in the F2 mainly explain the "superiority" of the first generation. This assumption is further supported by the similar and partly identical environmental conditions, as some of the animals from both generations were born, raised and studied at the same time. Anyway, a year and season effect cannot be excluded completely when comparing the two crossbreeding generations, although the scan date entered the variance analysis as random effect (Chapter III Publication, 2 Materials and Methods).

Besides the significant differences of VAT mass and volume between the two crossbreeding generations, a further difference comparing the percentage VAT of total body fat occurred. The first crossbreeding generation yielded 12.9% VAT of total body fat, whereas in the F2 generation the percentage was lower with only 9.8%.

Consequently, the superiority of the F1 generation compared to the F2 is debatable. The animals of the first generation showed a significantly higher fat content for the whole body and for the different examined regions, while the lean tissue mass was not significantly higher. Since the content of fat negatively affects the payment rate to a great extent (Chapter II.2.2.1 Adipose tissue in meat production), the first generation might not be superior compared to the second generation from the perspective of the producers. Additionally, the first generation utilized more excess energy for fat accumulation, which is a possible reason for the higher fat content compared to the second generation.

In summary, the results of this study for lean and fat tissue comparing both crossbreeding generations are in accordance with other studies, in which the first crossbred generation reaches higher values for body composition traits, such as more total body fat, more fat in the android region, a higher VAT mass. The higher lean tissue mass of the first crossbred generation was not significant in this study (Chapter III Publication, 4 Discussion).

3. Phenotyping of crosses between four different breeds

The basis for genomic analyses, including marker-based mapping of QTL, is a simultaneous occurrence of genetic and phenotypic differences. A high phenotypic variance occurs expectedly in a F2 crossbreeding generation after crossing the "uniform" F1 animals, which origin from a reciprocal four-way cross including four "significantly" different breeds (Landrace, Large White, Piétrain, and Duroc) as conducted in the own study (Chapter III Publication, 2 Materials and Methods; Chapter VIII Supplementary Material: Figure 6).

In order to be able to draw conclusions for the practical breeding work, this study used the most common conventional pig breeds in Germany for the creation of the multiple F1 and F2 crossbred generations. The creation and continuation of such a population enables further research approaches by describing the phenotype of specific traits in the F2 crossbred generation and allows the association of these phenotypic results with genomic analyses.

4. Further investigations

Within the scope of the own study, the entire abdominal cavity and the area of the ham were examined by MRI, and additionally a whole body scan by DXA was conducted. Furthermore, blood samples of all scanned pigs were collected, and from all parental animals which were not scanned within the study period, a small ear notch was taken. By performing genomic analyses, specific genes or QTL might be detected. Furthermore, the influence of these genes/QTL can be evaluated by comparison with the determined phenotypes. Since the study described VAT in detail, a genomic analysis may allow the identification of specific QTL or candidate genes, which are associated with an increased or decreased VAT content. It has already been shown in the literature that candidate genes found by porcine QTL analysis have a similar association with phenotypic traits like in humans (Rothammer et al., 2014). Therefore, these findings might have an impact on human health in the field of obesity research, as VAT, especially in humans, plays a major role in the development of cardiovascular diseases.

For an even more precise evaluation of the CoreScan feature, it would be useful determining the SAT content based on the MR images and comparing this content with the difference of total body fat in the android region and VAT measured by DXA, which represents SAT. Evaluating SAT could help to figure out if an overestimation or underestimation of VAT is accompanied by an over- or underestimation of SAT. In addition, the SAT-VAT ratio can be determined. This ratio might lead to an estimation equation for VAT based on SAT or a combination of SAT and the weight in pigs.

In general, the evaluation of the CoreScan feature in detail could have a huge impact on performance testing in pigs for VAT, or obesity research as model for human studies. The DXA technology in combination with CoreScan has the ability to investigate the VAT content in pigs *in vivo* in comparison to currently used dissection analyses. Therefore, the animals can be examined several times to carry out growth studies or may find further use in related experiments in order to answer e.g. nutritional or physiological research questions. Due to the repeated use of the same animals, a reduction of the animals needed for a specific research question might be the positive consequence.

V. SUMMARY

The visceral adipose tissue (VAT) plays an important role in the field of obesity-associated diseases in humans. The most common causes of death worldwide are cardiovascular diseases, which are accompanied by risk factors such as hypertension, dyslipidemia, or metabolic syndrome. Several studies show a causal relationship of VAT with these factors. Due to its high similarity of anatomic or physiologic characteristics with humans, the pig is an appropriate animal model for obesity research. Compared to the genome of mice, the porcine genome is even more similar to humans. In addition, new insights into the fat depot metabolism will bring advantages for the breeding work and could help to produce high quality meat at reasonable costs.

The aim of this thesis was to phenotype the visceral adipose tissue in pigs in combination with the evaluation of the CoreScan feature within the enCore software of GE Healthcare for *i*DXA scanners. CoreScan offers the possibility to determine the VAT mass and volume indirectly by using the DXA technology in combination with a specific geometric software algorithm. MRI as a direct method to measure VAT served as reference for evaluating the DXA feature.

This thesis examined a number of 120 crossbred pigs of the first and second filial generation with the parental breeds German Landrace, Large White, Piétrain and Duroc by MRI and by two DXA whole body scan modes ("thick" and "standard"). At time of investigation, the pigs were averagely 147 days old and had an average weight of 91.6 kg. The VAT values of MRI and DXA showed a close linear relationship with a regression coefficient of 0.76 for mode “thick” (RMSE = 399.25 cm^3) and of 0.71 for mode “standard” (RMSE = 443.42 cm^3). The Bland-Altman analysis showed an overestimation of DXA VAT compared to MRI values. The deviation between the two methods, however, increased with increasing levels of VAT.

In addition, this study confirms the well-known sex related differences of body composition. Castrated males tend to have higher body weights, more total body fat, and also more VAT. Compared to the female animals, the male castrated pigs were characterized by averagely 578 g more VAT and averagely 3.9 kg heavier weights. The lack of androgens and estrogens in barrows, which have an anabolic effect, can explain the difference.

Total fat and visceral fat content of the first and second multiple crossbred generations (MHF1 vs. MHF2) differed significantly. The animals of the MHF1 had on average 325 g more VAT. The expected full heterosis effect in the first crossbreeding generation (MHF1) and the expected 50% decline in the F2 crossbreeding generation by crossing the breeding animals of F1 (MHF1) mainly explain the "superiority" of the first generation.

In conclusion, CoreScan has the ability to provide VAT estimates in pigs but needs a bias correction if MRI is seen as "gold reference standard". Consequently, GE Healthcare offers a fast, simple and low-cost alternative compared with MRI or CT. The phenotyping of VAT could form the basis for further genomic studies. In general, these findings could have an impact on human health by contributing new prospects to the field of obesity research.

VI. ZUSAMMENFASSUNG

Phänotypisierung des viszeralen Fettes beim Schwein mittels MRT und DXA

Das viszerale Fett (VAT) spielt eine große Rolle im Bereich der Adipositas-assoziierten Krankheiten beim Menschen. Die Haupttodesursache weltweit sind kardiovaskuläre Krankheiten, die durch bestimmte Risikofaktoren wie Bluthochdruck, Fettstoffwechselstörung oder dem metabolischen Syndrom begünstigt werden. In mehreren Studien konnte eine Beziehung zwischen dem viszeralen Fett und diesen Risikofaktoren gezeigt werden. Aufgrund der großen Ähnlichkeit der Anatomie und Physiologie ist das Schwein ein häufig eingesetztes Tiermodell in der Adipositasforschung. Im Vergleich zu dem Genom von Mäusen, ist das porzine Genom dem des Menschen ähnlicher. Neue Erkenntnisse über den Fettmetabolismus bringen Vorteile für die Zuchtarbeit und helfen bei der Produktion von Schweinefleisch mit hoher Qualität bei vergleichsweise akzeptablen Kosten.

Das Ziel dieser Doktorarbeit war es, das viszerale Fett des Schweines zu phänotypisieren und zeitgleich die CoreScan Funktion der enCore Software für *i*DXA von GE Healthcare zu evaluieren. CoreScan ist eine indirekte Methode zur Bestimmung des Volumens und der Masse des viszeralen Fettes. Im Gegensatz dazu kann das Volumen des viszeralen Fettes durch eine MRT-Untersuchung direkt erfasst werden und diente zur Bewertung der DXA-Methode als Referenz.

Es wurden insgesamt 120 Vierrassen-Kreuzungstiere aus Deutscher Landrasse, Deutschem Edelschwein, Piétrain und Duroc in der ersten und zweiten Filialgeneration mittels MRT und mittels zweier DXA-Ganzkörper-Scanmodi ("Dick" und "Standard") untersucht. Die Tiere waren zum Zeitpunkt der DXA- und MRT-Untersuchung im Durchschnitt 147 Tage alt mit einem durchschnittlichen Gewicht von 91,6 kg.

Mit einem Regressionskoeffizienten für Modus "Dick" von 0,76 (RMSE = 399,25 cm^3) und von 0,71 für Modus "Standard" (RMSE = 443,42 cm^3) konnte eine enge lineare Beziehung zwischen den DXA VAT-Werten und den MRT-Ergebnissen ermittelt werden. Durch eine Bland-Altman-Analyse konnte eine Überschätzung des VAT-Gehaltes durch DXA verglichen mit den MRT-

Werten aufgezeigt werden. Diese Tendenz nimmt mit steigenden VAT-Volumina zu. Darüber hinaus konnte der bereits bekannte Geschlechterunterschied der Körperzusammensetzung dargestellt werden, bei welchem männlich kastrierte Schweine durch höhere Gewichte, höheren Gesamtfettgehalt als auch höheren viszeralen Fettgehalt im Vergleich zu weiblichen Tieren charakterisiert sind. Im Vergleich zu den weiblichen Tieren hatten die männlich kastrierten Schweine durchschnittlich 578 g mehr VAT und waren im Durchschnitt 3,9 kg schwerer. Der Unterschied kann auf die fehlende Produktion von Androgenen und Östrogenen in Kastraten, welche eine anabole Wirkung besitzen, zurückgeführt werden.

Zwischen der ersten und zweiten multiplen Kreuzungsgeneration (MHF1 vs. MHF2) konnten signifikante Unterschiede für das Gewicht, den Gesamtfettgehalt und für den viszeralen Fettgehalt festgestellt werden. Die MHF1-Tiere zeigten durchschnittlich 325 g höhere VAT-Gehalte. Diese Überlegenheit kann durch den Heterosiseffekt erklärt werden, der in der ersten Kreuzungs-Filialgeneration erwartungsgemäß mit 100% am höchsten ist und in der folgenden Kreuzungs-Generation theoretisch nur noch 50% beträgt.

Zusammenfassend bietet CoreScan die Möglichkeit viszerales Fett in Schweinen zu quantifizieren. Wird MRT als Referenz angesehen, müssen die ermittelten, von der MRT-Messung abweichenden DXA-Werte entsprechend der Bland-Altman-Analyse angepasst werden. GE Healthcare liefert mit dem CoreScan *i*DXA-System eine einfachere, preiswertere und besser zugängliche Alternative zu den klassischen Methoden wie MRT oder CT. Die Ergebnisse der Phänotypisierung können die Basis für Genomanalysen bilden und somit einen Beitrag zur Adipositasforschung beim Menschen durch die Verwendung des Schweines als Tiermodell leisten.

VII. References

Abate, N., Burns, D., Peshock, R.M., Garg, A., Grundy, S.M., 1994. Estimation of adipose tissue mass by magnetic resonance imaging: validation against dissection in human cadavers. Journal of lipid research 35, 1490–1496.

Ahima, R.S., Flier, J.S., 2000. Leptin. Annual review of physiology 62, 413–437.

Aiello, R.J., Nevin, D.N., Ebert, D.L., Uelmen, P.J., Kaiser, M.E., MacCluer, J.W., Blangero, J., Dyer, T.D., Attie, A.D., 1994. Apolipoprotein B and a second major gene locus contribute to phenotypic variation of spontaneous hypercholesterolemia in pigs. Arteriosclerosis and thrombosis : a journal of vascular biology 14, 409–419.

Annison, E.F., Australia, Standing Committee on Agriculture - Pig Subcommittee, 1987. Feeding standards for Australian livestock. Pigs. CSIRO, East Melbourne, Australia.

Bauer Aneka, Judas M., 2014. Schlachtkörperqualität von Mastebern in Vergleich zu Sauen und Börgen. Züchtungskunde, 374–389.

Baulain, U., Friedrichs, M., Höreth, R., Henning, M., Tholen, E., 2010. Use of MRI to assess carcass and primal cut composition in different pig breeds. www.kongressband.de/wcgalp2010/assets/pdf/0357.pdf.

Baumung, R., 2005. Kreuzungszucht und Heterosis: Seminar des Ausschusses für Genetik der ZAR, 3–10.

Bayerische Landesanstalt für Landwirtschaft (LfL), 2011. Fütterungsfibel 2011.

Bayerische Landesanstalt für Landwirtschaft (LfL), 2020. Jahresbericht 2019 über Leistungsprüfungen und Zuchtwertschätzung beim Schwein in Bayern. https://www.lfl.bayern.de/mam/cms07/publikationen/daten/informationen/jahresbericht-2019-leistungspruefungen-zuchtwertschaetzung-schwein-lfl-information.pdf. Accessed 16 August 2020.

Bayerisches Staatsministerium für Ernährung, Landwirtschaft und Forsten, 2018. Schweinezucht und -haltung in Bayern: Daten und Fakten.

Bazzocchi, A., Ponti, F., Albisinni, U., Battista, G., Guglielmi, G., 2016. DXA: Technical aspects and application. European journal of radiology 85, 1481–1492.

Beckhove, A., 2019. Deutschland ist der fünftgrößte Schweinehalter der Welt. https://www.topagrar.com/markt/news/deutschland-ist-der-fuenftgroesste-schweinehalter-der-welt-11544997.html. Accessed 16 August 2020.

Bellof, G., Granz, S. (Eds.), 2018. Tierproduktion: Nutztiere züchten, halten und ernähren, 15th ed. Georg Thieme Verlag, Stuttgart, 639 pp.

Bernau, M., 2011. Untersuchungen zu einer möglichen Vorverlegung der Schlachtleistungsprüfung beim Schwein mit Hilfe der Magnetresonanztomographie (MRT) und Dualenergie-Röntgenabsorptiometrie (DXA) in vivo.

Bernau, M., Kremer, P.V., Lauterbach, E., Tholen, E., Petersen, B., Pappenberger, E., Scholz, A.M., 2015a. Evaluation of carcass composition of intact boars using linear measurements from performance testing, dissection, dual energy X-ray absorptiometry (DXA) and magnetic resonance imaging (MRI). Meat science 104, 58–66.

Bernau, M., Kremer, P.V., Pappenberger, E., Kreuzer, L.S., Cussler, K., Hoffmann, A., Scholz, A.M., 2015b. Safety testing of veterinary vaccines using magnetic resonance imaging in pigs. ALTEX 32, 51–58.

Bernau, M., Liesner, B.G., Schwanitz, S., Kraus, A.-S., Falkenau, A., Leipig-Rudolph, M., Hermanns, W., Scholz, A.M., 2018a. Vaccine safety testing using magnetic resonance imaging in suckling pigs. Vaccine 36, 1789–1795.

Bernau, M., Schwanitz, S., Kremer-Rücker, P.V., Kreuzer, L.S., Scholz, A.M., 2018b. Size matters: Boar taint in relationship with body composition and testis volume measured by magnetic resonance imaging. Livestock Science 213, 7–13.

Bhanu Prakash, K.N., Gopalan, V., Lee, S.S., Velan, S.S., 2014. Quantification of abdominal fat depots in rats and mice during obesity and weight loss interventions. PloS one 9.

Biedermann, G., Jatsch, C., Peschke, W., Lindner, J.-P., Wittmann, W., 2000. Mast- und Schlachtleistung sowie Fleisch- und Fettqualität von Pietrain-Schweinen unterschiedlichen MHS-Genotyps und Geschlechts: 2. Mitteilung: Fettsäurenmuster der Depotfette Rückenspeck, Flomen und intermuskuläres Fett sowie der Gesamt- und Phospholipide des M. long, dorsi. Arch. Anim. Breed. 43, 165–178.

Borkan, G.A., Hults, D.E., Gerzof, S.G., Robbins, A.H., Silbert, C.K., 1983. Age changes in body composition revealed by computed tomography. Journal of gerontology 38, 673–677.

Bracher-Jakob, A., 2000. Jungebermast in Forschung und Praxis: Literaturstudie und Standortbestimmung. Arbeit im Auftrag der Eidgenössischen

Forschungsanstalt für Nutztiere.

Breeds of Livestock - Department of Animal Science, 2020. Breeds of Livestock - Duroc Swine. http://afs.okstate.edu/breeds/swine/duroc/index.html. Accessed 16 August 2020.

Bundesministerium für Ernährung und Landwirtschaft, 2019. Schweine. https://www.bmel.de/DE/Tier/Nutztierhaltung/Schweine/schweine_node.html. Accessed 16 August 2020.

Bundesverband Rind und Schwein e.V., 2019. Rinder- und Schweineproduktion in Deutschland 2018.

Cameron, N.D., Enser, M.B., 1991. Fatty acid composition of lipid in Longissimus dorsi muscle of Duroc and British Landrace pigs and its relationship with eating quality. Meat science 29, 295–307.

Carver, T.E., Court, O., Christou, N.V., Reid, R.E.R., Andersen, R.E., 2014. Precision of the iDXA for visceral adipose tissue measurement in severely obese patients. Medicine and science in sports and exercise 46, 1462–1465.

Chandra, A., Neeland, I.J., Berry, J.D., Ayers, C.R., Rohatgi, A., Das, S.R., Khera, A., McGuire, D.K., Lemos, J.A. de, Turer, A.T., 2014. The relationship of body mass and fat distribution with incident hypertension: observations from the Dallas Heart Study. Journal of the American College of Cardiology 64, 997–1002.

Christian, L.L., Strock, K.L., Carlson, J.P., 1980. Effects of Protein, Breed Cross, Sex and Slaughter Weight on Swine Performance and Carcass Traits. Journal of animal science 51, 51–58.

Claus, R., Weiler, U., 1994. Endocrine regulation of growth and metabolism in the pig: a review. Livestock Production Science 37, 245–260.

Close, W.H., Mount, L.E., 1978. The effects of plane of nutrition and environmental temperature on the energy metabolism of the growing pig. 1. Heat loss and critical temperature. The British journal of nutrition 40, 413–421.

Coffey, M., 2010. British Cattle Breeders Club: Newsletter. https://www.cattlebreeders.org.uk/newsletters/2010/spring/. Accessed 16 August 2020.

Correa, J.A., Gariépy, C., Marcoux, M., Faucitano, L., 2008. Effects of growth rate, sex and slaughter weight on fat characteristics of pork bellies. Meat science 80, 550–554.

Davies, A.S., Pryor, W.J., 1977. Growth changes in the distribution of dissectable and intramuscular fat in pigs. J. Agric. Sci. 89, 257–266.

Demerath, E.W., Shen, W., Lee, M., Choh, A.C., Czerwinski, S.A., Siervogel, R.M., Towne, B., 2007. Approximation of total visceral adipose tissue with a single magnetic resonance image. The American journal of clinical nutrition 85, 362–368.

Dieudonne, M.N., Pecquery, R., Boumediene, A., Leneveu, M.C., Giudicelli, Y., 1998. Androgen receptors in human preadipocytes and adipocytes: regional specificities and regulation by sex steroids. The American journal of physiology 274, C1645-52.

Dölle, T., 2019. Untersuchungen zu Klauengesundheit, Knorpelvolumina und Körperzusammensetzung beim Mastschwein in verschiedenen Haltungssystemen unter Verwendung von Magnetresonanz-Tomographie und Dualenergie-Röntgenabsorptiometrie, München.

Dunshea, F.R., D'souza, D.N., 2003. Review: fat deposition and metabolism in the pig. Manipulating pig production, 127–150.

Duziński, K., Knecht, D., Lisiak, D., Janiszewski, P., 2015. Factors affecting the tissues composition of pork belly. Animal : an international journal of animal bioscience 9, 1897–1903.

Ergun, D.L., Rothney, M.P., Oates, M.K., Xia, Y., Wacker, W.K., Binkley, N.C., 2013. Visceral adipose tissue quantification using Lunar Prodigy. Journal of clinical densitometry : the official journal of the International Society for Clinical Densitometry 16, 75–78.

Erzeugergemeinschaft und Züchtervereinigung für Zucht- und Hybridzuchtschweine in Bayern w.V. (EGZH), 2015. Bayern beschließt neue Zuchtziele für Vater- und Mutterrassen. https://www.egzh.de/index.php?id=152. Accessed 16 August 2020.

Falkenberg, H., Hammer, H., 2007. Zur Geschichte und Kultur der Schweinezucht und -haltung. 3. Mitt.: Schweinezucht und -haltung in Deutschland von 1650 bis 1900. Züchtungskunde, 92–110.

Faraj, M., Havel, P.J., Phélis, S., Blank, D., Sniderman, A.D., Cianflone, K., 2003. Plasma acylation-stimulating protein, adiponectin, leptin, and ghrelin before and after weight loss induced by gastric bypass surgery in morbidly obese subjects. The Journal of clinical endocrinology and metabolism 88, 1594–1602.

Farnworth, E.R., Kramer, J.K.G., 1987. Fat metabolism in growing swine: a review. Can. J. Anim. Sci. 67, 301–318.

Fischer, K., Lindner, J.P., Judas, M., Höreth, R., 2006. Schlachtkörperzusammensetzung und Gewebebeschaffenheit von schweren Schweinen: I. Mitteilung: Material und Methoden, Mastleistung, Schlachtkörperzusammensetzung und Teilstückanteile. Arch. Anim. Breed. 49, 269–278.

Fourman, L.T., Kileel, E.M., Hubbard, J., Holmes, T., Anderson, E.J., Looby, S.E., Fitch, K.V., Feldpausch, M.N., Torriani, M., Lo, J., Stanley, T.L., Grinspoon, S.K., 2019. Comparison of visceral fat measurement by dual-energy X-ray absorptiometry to computed tomography in HIV and non-HIV. Nutrition & diabetes 9, 1–10.

Fowler, P.A., Fuller, M.F., Glasbey, C.A., Cameron, G.G., Foster, M.A., 1992. Validation of the in vivo measurement of adipose tissue by magnetic resonance imaging of lean and obese pigs. The American journal of clinical nutrition 56, 7–13.

Fox, C.S., Massaro, J.M., Hoffmann, U., Pou, K.M., Maurovich-Horvat, P., Liu, C.-Y., Vasan, R.S., Murabito, J.M., Meigs, J.B., Cupples, L.A., D'Agostino, R.B., O'Donnell, C.J., 2007. Abdominal visceral and subcutaneous adipose tissue compartments: association with metabolic risk factors in the Framingham Heart Study. Circulation 116, 39–48.

Freyer, G., Mayer, M., 2012. Züchterische Analyse ausgewählter Fruchtbarkeitsmerkmale bei Landrasse und Edelschwein sowie deren Kreuzungen auf der Basis von Daten aus dem Hybridschweinezuchtverband Nord/Ost eV. Züchtungskunde, 500–510.

Galic, S., Oakhill, J.S., Steinberg, G.R., 2010. Adipose tissue as an endocrine organ. Molecular and Cellular Endocrinology 316, 129–139.

GE Healthcare, 2011. Core health. It's vital.: CoreScan application: Dedicated to quantifying visceral fat. http://www3.gehealthcare.pl/~/media/documents/us-global/products/bone-health/brochures/applications/gehealthcare_corescan_brochure.pdf. Accessed 16 August 2020.

GE Healthcare, 2017a. Advancements in DXA Body Composition Analysis: Metabolic Phenotyping with CoreScan. https://www3.gehealthcare.com/~/media/downloads/us/product/product-categories/metabolic-health/gated-pdfs/Whitepaper-Metabolic-Phenotyping-with-CoreScan-JB47862XX.pdf. Accessed 16 August 2020.

GE Healthcare, 2017b. Lunar CoreScan Application from GE Healthcare. https://www.gehealthcare.com/-/jssmedia/1cd6ce71f5cd4ac1b782fa1815ddb23b.pdf. Accessed 16 August 2020.

GE Healthcare, 2017c. Lunar Technology Advantages. https://www3.gehealthcare.com/~/media/downloads/us/product/product-categories/metabolic-health/gated-pdfs/BMD-Global-Lunar-Technology-Advantages-JB45946XX.pdf. Accessed 16 August 2020.

German Genetic, 2020. GG*Landrasse - German Genetic - Mit Sicherheit besser. https://www.german-genetic.de/zuchtarbeit/zuchtprogramme/landrasse. Accessed 16 August 2020.

Gesellschaft zur Erhaltung alter und gefährdeter Haustierrassen e. V., 2020a. Deutsche Landrasse. http://www.g-e-h.de/index.php/rassebeschreibungen/50-schweine/303-deutsche-landrasse. Accessed 16 August 2020.

Gesellschaft zur Erhaltung alter und gefährdeter Haustierrassen e. V., 2020b. Deutsches Edelschwein. http://www.g-e-h.de/index.php/rassebeschreibungen/50-schweine/445-deutschesedelschwein. Accessed 16 August 2020.

Gilbert, H., Bidanel, J.-P., Gruand, J., Caritez, J.-C., Billon, Y., Guillouet, P., Lagant, H., Noblet, J., Sellier, P., 2007. Genetic parameters for residual feed intake in growing pigs, with emphasis on genetic relationships with carcass and meat quality traits. Journal of animal science 85, 3182–3188.

Giles, L.R., Eamens, G.J., Arthur, P.F., Barchia, I.M., James, K.J., Taylor, R.D., 2009. Differential growth and development of pigs as assessed by X-ray computed tomography. Journal of animal science 87, 1648–1658.

Giusti, M. de, Barbato, D., Lia, L., Colamesta, V., Lombardi, A.M., Cacchio, D., Villari, P., La Torre, G., 2019. Collaboration between human and veterinary medicine as a tool to solve public health problems. The Lancet Planetary Health 3, e64-e65.

Glodek, P., Kratz, R., Schulz, E., Flachowsky, G., 2004. Der Einfluss unterschiedlicher Vaterrassen in praxisüblichen Schweinekreuzungen auf deren Ansatzleistung, Schlachtkörperzusammensetzung sowie Fleisch- und Fettbeschaffenheit. Archives Animal Breeding, 59–74.

Goldstein, J.L., 1995. The metabolic basis of inherited disease. Familial hypercholesterolemia, 1981–2030.

Hansson, I., Lundstroem, K., Malmfors, B., 1975. Effect of sex and weight on growth, feed efficiency and carcass characteristics of pigs, 2: Carcass characteristics of boars, barrows and gilts, slaughtered at four different weights. Swedish Journal of Agricultural Research.

Hasler-Rapacz, J., Ellegren, H., Fridolfsson, A.-K., Kirkpatrick, B., Kirk, S., Andersson, L., Rapacz, J., 1998. Identification of a mutation in the low density lipoprotein receptor gene associated with recessive familial hypercholesterolemia in swine. Am. J. Med. Genet. 76, 379–386.

Hishikawa, D., Hong, Y.-H., Roh, S.-g., Miyahara, H., Nishimura, Y., Tomimatsu, A., Tsuzuki, H., Gotoh, C., Kuno, M., Choi, K.-C., Lee, H.-g., Cho, K.-k., Hidari, H., Sasaki, S., 2005. Identification of genes expressed differentially in subcutaneous and visceral fat of cattle, pig, and mouse. Physiological genomics 21, 343–350.

Hoffman, D.J., Wang, Z., Gallagher, D., Heymsfield, S.B., 2005. Comparison of visceral adipose tissue mass in adult African Americans and whites. Obesity research 13, 66–74.

Hotta, K., Funahashi, T., Arita, Y., Takahashi, M., Matsuda, M., Okamoto, Y., Iwahashi, H., Kuriyama, H., Ouchi, N., Maeda, K., Nishida, M., Kihara, S., Sakai, N., Nakajima, T., Hasegawa, K., Muraguchi, M., Ohmoto, Y., Nakamura, T., Yamashita, S., Hanafusa, T., Matsuzawa, Y., 2000. Plasma concentrations of a novel, adipose-specific protein, adiponectin, in type 2 diabetic patients. Arteriosclerosis, thrombosis, and vascular biology 20, 1595–1599.

Hybridschweinezuchtverband Nord/Ost e.V., 2013. Zuchtreport 2012. https://www.lallf.de/fileadmin/media/PDF/tierzuch/Schweine/Zuchtreport_2012_-_HSZV.pdf. Accessed 16 August 2020.

Hybridschweinezuchtverband Nord/Ost e.V., 2020. Hybridschweinezuchtverband Nord/Ost e.V. - Schweinezucht Zuchtschweine Erhaltungszucht Mecklenburg-Vorpommern Schweine. http://www.hszv.de/index.php?page=Zuchtprogramm. Accessed 16 August 2020.

Ibrahim, M.M., 2010. Subcutaneous and visceral adipose tissue: structural and functional differences. Obesity Reviews 11, 11–18.

Innerarity, T.L., Mahley, R.W., Weisgraber, K.H., Bersot, T.P., Krauss, R.M., Vega, G.L., Grundy, S.M., Friedl, W., Davignon, J., McCarthy, B.J., 1990. Familial defective apolipoprotein B-100: a mutation of apolipoprotein B that causes hypercholesterolemia. Journal of lipid research 31, 1337–1349.

Irshad, A., Kandeepan, G., Kumar, S., Ashish, K.A., Vishnuraj, Shukla, V., 2013. Factors influencing carcass composition of livestock: A review. J. Anim. Prod. Adv 3, 177–186.

Jackson, A.S., Stanforth, P.R., Gagnon, J., Rankinen, T., Leon, A.S., Rao, D.C., Skinner, J.S., Bouchard, C., Wilmore, J.H., 2002. The effect of sex, age and race on estimating percentage body fat from body mass index: The Heritage Family Study. International journal of obesity and related metabolic disorders : journal of the International Association for the Study of Obesity 26, 789–796.

Jaturasitha, S., Kamopas, S., Suppadit, T., Khiaosa-ard, R., Kreuzer, M., 2006. The Effect of Gender of Finishing Pigs Slaughtered at 110 Kilograms on Performance, and Carcass and Meat Quality. ScienceAsia 32, 297.

Karastergiou, K., Smith, S.R., Greenberg, A.S., Fried, S.K., 2012. Sex differences in human adipose tissues - the biology of pear shape. Biology of sex differences 3, 1–13.

Kaul, S., Rothney, M.P., Peters, D.M., Wacker, W.K., Davis, C.E., Shapiro, M.D., Ergun, D.L., 2012. Dual-energy X-ray absorptiometry for quantification of visceral fat. Obesity (Silver Spring, Md.) 20, 1313–1318.

Kirchgeßner, M., 2004. Tierernährung: Leitfaden für das Studium, Beratung und Praxis. 11. überarb. Aufl., Frankfurt am Main, DLG-Verlag. 37690059.

Knapp, K.M., Welsman, J.R., Hopkins, S.J., Shallcross, A., Fogelman, I., Blake, G.M., 2015. Obesity increases precision errors in total body dual-energy x-ray absorptiometry measurements. Journal of clinical densitometry : the official journal of the International Society for Clinical Densitometry 18, 209–216.

Knecht, D., Duziński, K., 2016. The effect of sex, carcass mass, back fat thickness and lean meat content on pork ham and loin characteristics. Arch. Anim. Breed. 59, 51–57.

Kolstad, K., 2000. Fat deposition and distribution in three genetic lines of pigs from 10 to 105 kilograms liveweight. Quality of meat and fat in pigs as affected by genetics and nutrition. Proceedings of the joint session of the EAAP commissions on pig production, animal genetics and animal nutrition, Zurich, Switzerland, 199–202.

Kouba, M., Hermier, D., Le Dividich, J., 2001. Influence of a high ambient temperature on lipid metabolism in the growing pig. Journal of animal science 79, 81–87.

Kräusslich, H., Brem, G. (Eds.), 1997. Tierzucht und allgemeine

Landwirtschaftslehre für Tiermediziner. Enke, Stuttgart, 596 pp.

Kremer, P.V., Fernández-Fígares, I., Förster, M., Scholz, A.M., 2012. In vivo body composition in autochthonous and conventional pig breeding groups by dual-energy X-ray absorptiometry and magnetic resonance imaging under special consideration of Cerdo Ibérico. Animal : an international journal of animal bioscience 6, 2041–2047.

Krotkiewski, M., Björntorp, P., Sjöström, L., Smith, U., 1983. Impact of obesity on metabolism in men and women. Importance of regional adipose tissue distribution. The Journal of clinical investigation 72, 1150–1162.

Kuk, J.L., Katzmarzyk, P.T., Nichaman, M.Z., Church, T.S., Blair, S.N., Ross, R., 2006. Visceral fat is an independent predictor of all-cause mortality in men. Obesity (Silver Spring, Md.) 14, 336–341.

Kullberg, J., Ahlström, H., Johansson, L., Frimmel, H., 2007. Automated and reproducible segmentation of visceral and subcutaneous adipose tissue from abdominal MRI. International journal of obesity (2005) 31, 1806–1817.

Kurt, E., Klont, R., 2010. WHC of pork from Pietrain-sired pigs measured under different commercial slaughterhouse conditions in Germany. Effect of gender and 50 per cent Duroc genetics within the female line. Fleischwirtschaft 90, 184–187.

Laskey, M.A., 1996. Dual-energy X-ray absorptiometry and body composition. Nutrition 12, 45–51.

Lawrence, T.L.J., Fowler, V.R., 2002. Growth of farm animals, 2nd ed. CABI Pub, Oxon, UK, New York, 347 pp.

Lear, S.A., Humphries, K.H., Kohli, S., Chockalingam, A., Frohlich, J.J., Birmingham, C.L., 2007. Visceral adipose tissue accumulation differs according to ethnic background: results of the Multicultural Community Health Assessment Trial (M-CHAT). The American journal of clinical nutrition 86, 353–359.

Lee, S.Y., Gallagher, D., 2008. Assessment methods in human body composition. Current opinion in clinical nutrition and metabolic care 11, 566–572.

Leenhouwers, J.I., Merks, J.W.M., 2013. Suitability of traditional and conventional pig breeds in organic and low-input production systems in Europe: Survey results and a review of literature. Anim. Genet. Resour. 53, 169–184.

Leskanich, C.O., Noble, R.C., Morgan, C.A., 1993. Effect of long-chain dietary polyunsaturated fatty acid content on pig meat. Proc. Br. Soc. Anim. Prod

(1972) 1993, 11.

Littmann, E., Götz, K.U., Dodenhoff, J., 2006. Schweinezucht und Schweineproduktion. Schriftenreihe der Bayerischen Landesanstalt für Landwirtschaft 7.

Liu, J., Fox, C.S., Hickson, D.A., May, W.D., Hairston, K.G., Carr, J.J., Taylor, H.A., 2010. Impact of Abdominal Visceral and Subcutaneous Adipose Tissue on Cardiometabolic Risk Factors: The Jackson Heart Study. The Journal of clinical endocrinology and metabolism 95, 5419–5426.

Marcadenti, A., de Abreu-Silva, E.O., 2015. Different adipose tissue depots: Metabolic implications and effects of surgical removal. Endocrinologia y nutricion : organo de la Sociedad Espanola de Endocrinologia y Nutricion 62, 458–464.

Marcoux, M., Faucitano, L., Pomar, C., 2005. The accuracy of predicting carcass composition of three different pig genetic lines by dual-energy X-ray absorptiometry. Meat science 70, 655–663.

Martin, A.D., Daniel, M.Z., Drinkwater, D.T., Clarys, J.P., 1994. Adipose tissue density, estimated adipose lipid fraction and whole body adiposity in male cadavers. International journal of obesity and related metabolic disorders : journal of the International Association for the Study of Obesity 18, 79–83.

McCauley, L.S., Ghatas, M.P., Sumrell, R.M., Cirnigliaro, C.M., Kirshblum, S.C., Bauman, W.A., Gorgey, A.S., 2020. Measurement of Visceral Adipose Tissue in Persons With Spinal Cord Injury by Magnetic Resonance Imaging and Dual X-Ray Absorptiometry: Generation and Application of a Predictive Equation. Journal of clinical densitometry : the official journal of the International Society for Clinical Densitometry 23, 63–72.

Meier, U., Gressner, A.M., 2004. Endocrine regulation of energy metabolism: review of pathobiochemical and clinical chemical aspects of leptin, ghrelin, adiponectin, and resistin. Clinical chemistry 50, 1511–1525.

Mellis, M.G., Oldroyd, B., Hind, K., 2014. In vivo precision of the GE Lunar iDXA for the measurement of visceral adipose tissue in adults: the influence of body mass index. European journal of clinical nutrition 68, 1365–1367.

Meredith-Jones, K., Haszard, J., Stanger, N., Taylor, R., 2018. Precision of DXA-Derived Visceral Fat Measurements in a Large Sample of Adults of Varying Body Size. Obesity (Silver Spring, Md.) 26, 505–512.

Mihaljevic, M., Gomercic, H., Kramer, M., 2009. CT- und MRT-Atlas:

Transversalanatomie des Hundes. Parey, Stuttgart, 222 pp.

Mitchell, A., Scholz, A., Pursel, V., 2002. Prediction of the in vivo Body Composition of Pigs Based on Cross-Sectional Region Analysis of Dual Energy X-Ray Absorptiometry (DXA) Scans. Archives of Animal Breeding 45, 5–545.

Mitchell, A.D., Conway, J.M., Potts, W.J., 1996. Body composition analysis of pigs by dual-energy x-ray absorptiometry. Journal of animal science 74, 2663–2671.

Mitchell, A.D., am Scholz, Pursel, V.G., Evock-Clover, C.M., 1998a. Composition analysis of pork carcasses by dual-energy X-ray absorptiometry. Journal of animal science 76, 2104–2114.

Mitchell, A.D., Scholz, A.M., Conway, J.M., 1998b. Body composition analysis of small pigs by dual-energy x-ray absorptiometry. Journal of animal science 76, 2392–2398.

Mitchell, A.D., Scholz, A.M., Wang, P.C., Song, H., 2001. Body composition analysis of the pig by magnetic resonance imaging. Journal of animal science 79, 1800–1813.

Mohammad, A., Lucia Rolfe, E. de, Sleigh, A., Kivisild, T., Behbehani, K., Wareham, N.J., Brage, S., Mohammad, T., 2017. Validity of visceral adiposity estimates from DXA against MRI in Kuwaiti men and women. Nutrition & diabetes 7, e238.

Mohrmann, M., Roehe, R., Susenbeth, A., Baulain, U., Knap, P.W., Looft, H., Plastow, G.S., Kalm, E., 2006. Association between body composition of growing pigs determined by magnetic resonance imaging, deuterium dilution technique, and chemical analysis. Meat science 72, 518–531.

Montague, C.T., O'Rahilly, S., 2000. The perils of portliness: causes and consequences of visceral adiposity. Diabetes 49, 883–888.

Monziols, M., Collewet, G., Bonneau, M., Mariette, F., Davenel, A., Kouba, M., 2006. Quantification of muscle, subcutaneous fat and intermuscular fat in pig carcasses and cuts by magnetic resonance imaging. Meat science 72, 146–154.

Müller, S., Otto, M., Reimann, G., 2010. Eber auf Herz und Nieren geprüft. dlz primus schwein, 40–45.

Myers, M.G., Leibel, R.L., Seeley, R.J., Schwartz, M.W., 2010. Obesity and leptin resistance: distinguishing cause from effect. Trends in endocrinology and metabolism: TEM 21, 643–651.

Neeland, I.J., Turer, A.T., Ayers, C.R., Powell-Wiley, T.M., Vega, G.L., Farzaneh-Far, R., Grundy, S.M., Khera, A., McGuire, D.K., Lemos, J.A. de, 2012.

Dysfunctional adiposity and the risk of prediabetes and type 2 diabetes in obese adults. JAMA 308, 1150–1159.

Newell, J.A., Bowland, J.P., 1972. Performance, carcass composition, and fat composition of boars, gilts, and barrows fed two levels of protein. Can. J. Anim. Sci. 52, 543–551.

Nicklas, B.J., Penninx, B.W.J.H., Cesari, M., Kritchevsky, S.B., Newman, A.B., Kanaya, A.M., Pahor, M., Jingzhong, D., Harris, T.B., 2004. Association of visceral adipose tissue with incident myocardial infarction in older men and women: the Health, Aging and Body Composition Study. American journal of epidemiology 160, 741–749.

Ntalla, I., Panoutsopoulou, K., Vlachou, P., Southam, L., William Rayner, N., Zeggini, E., Dedoussis, G.V., 2013. Replication of established common genetic variants for adult BMI and childhood obesity in Greek adolescents: the TEENAGE study. Annals of human genetics 77, 268–274.

O'Brien, S.N., Welter, B.H., Mantzke, K.A., Price, T.M., 1998. Identification of progesterone receptor in human subcutaneous adipose tissue. The Journal of clinical endocrinology and metabolism 83, 509–513.

OECD/FAO, 2019. Agricultural Outlook 2019-2028. OECD Publishing, Paris, 148 pp.

Pandey, M.P., Schöggl, K., Viszelj, J., Widhalm, K., 2011. Body Composition: Dual-Röntgen-Absorptiometrie (DEXA). Journal für Ernährungsmedizin 13, 32–34.

Pappenberger, E., 2014. Vergleich der Körperzusammensetzung konventioneller und alternativer Masthybriden mittels Dualenergieröntgenabsorptiometrie und Magnetresonanztomographie.

Pedersen, M.L.M., Velander, I.H., Nielsen, M.B.F., Lundeheim, N., Nielsen, B., 2019. Duroc boars have lower progeny mortality and lower fertility than Pietrain boars. Translational animal science 3, 885–892.

Pedersen, S.B., Bruun, J.M., Hube, F., Kristensen, K., Hauner, H., Richelsen, B., 2001. Demonstration of estrogen receptor subtypes α and β in human adipose tissue: influences of adipose cell differentiation and fat depot localization. Molecular and Cellular Endocrinology 182, 27–37.

Pedersen, S.B., Hansen, P.S., Lund, S., Andersen, P.H., Odgaard, A., Richelsen, B., 1996. Identification of oestrogen receptors and oestrogen receptor mRNA in human adipose tissue. European journal of clinical investigation 26, 262–269.

Peinado, J., Medel, P., Fuentetaja, A., Mateos, G.G., 2008. Influence of sex and castration of females on growth performance and carcass and meat quality of heavy pigs destined for the dry-cured industry. Journal of animal science 86, 1410–1417.

Pfalzgraf, A., Frigg, M., Steinhart, H., Kirchgeßner, M., Roth, F.X., 1995. Influence of Dietary Fat and Vitamin E on the Lipids in Pork Meat. Fett/Lipid 97, 13–20.

Pietrobelli, A., Formica, C., Wang, Z., Heymsfield, S.B., 1996. Dual-energy X-ray absorptiometry body composition model: review of physical concepts. The American journal of physiology 271, E941-51.

Prevrhal, S., 2006. Absorptiometrie. Der Radiologe 46, 847–860.

Reinhardt, M., Piaggi, P., DeMers, B., Trinidad, C., Krakoff, J., 2017. Cross calibration of two dual-energy X-ray densitometers and comparison of visceral adipose tissue measurements by iDXA and MRI. Obesity (Silver Spring, Md.) 25, 332–337.

Renner, S., Dobenecker, B., Blutke, A., Zöls, S., Wanke, R., Ritzmann, M., Wolf, E., 2016. Comparative aspects of rodent and nonrodent animal models for mechanistic and translational diabetes research. Theriogenology 86, 406–421.

Rettenberger, G., Klett, C., Zechner, U., Kunz, J., Vogel, W., Hameister, H., 1995. Visualization of the conservation of synteny between humans and pigs by heterologous chromosomal painting. Genomics 26, 372–378.

Ribani, A., Utzeri, V.J., Geraci, C., Tinarelli, S., Djan, M., Veličković, N., Doneva, R., Dall'Olio, S., Nanni Costa, L., Schiavo, G., Bovo, S., Usai, G., Gallo, M., Radović, Č., Savić, R., Karolyi, D., Salajpal, K., Gvozdanović, K., Djurkin-Kušec, I., Škrlep, M., Čandek-Potokar, M., Ovilo, C., Fontanesi, L., 2019. Signatures of de-domestication in autochthonous pig breeds and of domestication in wild boar populations from MC1R and NR6A1 allele distribution. Animal genetics 50, 166–171.

Robert Koch-Institut (RKI), 2012. Übergewicht und Adipositas in Deutschland: Werden wir immer dicker? DEGS-Symposium.

Rohrer, G., Beever, J.E., Rothschild, M.F., Schook, L., Gibbs, R., Weinstock, G., 2002. Porcine genomic sequencing initiative. Porcine Sequencing White Paper, 1–10.

Rosická, M., Krsek, M., Matoulek, M., Jarkovská, Z., Marek, J., Justová, V., Lacinová, Z., 2003. Serum ghrelin levels in obese patients: the relationship to serum leptin levels and soluble leptin receptors levels. Physiological research

52, 61–66.

Rothammer, S., Kremer, P.V., Bernau, M., Fernandez-Figares, I., Pfister-Schär, J., Medugorac, I., Scholz, A.M., 2014. Genome-wide QTL mapping of nine body composition and bone mineral density traits in pigs. Genet Sel Evol 46, 1–11.

Rothney, M.P., Xia, Y., Wacker, W.K., Martin, F.-P., Beaumont, M., Rezzi, S., Giusti, V., Ergun, D.L., 2013. Precision of a new tool to measure visceral adipose tissue (VAT) using dual-energy X-Ray absorptiometry (DXA). Obesity 21, E134-E136.

Rothschild, M.F., Hu, Z.-l., Jiang, Z., 2007. Advances in QTL mapping in pigs. International journal of biological sciences 3, 192–197.

Sambraus, H.H., 1987. Atlas der Nutztierrassen: 220 Rassen in Wort u. Bild, 2nd ed. Ulmer, Stuttgart.

Sandhofer, A., Laimer, M., Ebenbichler, C.F., Kaser, S., Paulweber, B., Patsch, J.R., 2003. Soluble leptin receptor and soluble receptor-bound fraction of leptin in the metabolic syndrome. Obesity research 11, 760–768.

Schaeffer, L.R., 2018. Selection: Traditional Methods, Encyclopedia of Animal Science-(Two-Volume Set). CRC Press, pp. 961–963.

Schild, H.H., 1997. Made easy MRI, 2nd ed. Schering, S.l., 105 pp.

Scholz, A.M., 2002. In-vivo-Methoden zur Analyse von Muskelstoffwechsel und Körperzusammensetzung beim Schwein unter besonderer Berücksichtigung genetischer Einflüsse. Habilitationsschrift, München.

Scholz, A.M., Bünger, L., Kongsro, J., Baulain, U., Mitchell, A.D., 2015. Non-invasive methods for the determination of body and carcass composition in livestock: dual-energy X-ray absorptiometry, computed tomography, magnetic resonance imaging and ultrasound: invited review. Animal : an international journal of animal bioscience 9, 1250–1264.

Scholz, A.M., Förster, M., 2006. Genauigkeit der Dualenergie-Röntgenabsorptiometrie (DXA) zur Ermittlung der Körperzusammensetzung von Schweinen in vivo. Arch. Anim. Breed. 49, 462–476.

Schwanitz, Bernau, M., Kreuzer, L.S., Kremer-Rücker, P.V., Scholz, A.M., 2017. Körperzusammensetzung und Ebergeruch bei intakten Ebern, immunologisch und chirurgisch kastrierten Schweinen. Züchtungskunde 89, 413–433.

Schweineschlachtkörper-Handelsklassenverordnung (SchwHKlV), 2020. Verordnung über gesetzliche Handelsklassen für Schweineschlachtkörper. http://www.gesetze-im-internet.de/hdlklschwv_1986/index.html. Accessed 16

August 2020.

Shadid, S., Koutsari, C., Jensen, M.D., 2007. Direct free fatty acid uptake into human adipocytes in vivo: relation to body fat distribution. Diabetes 56, 1369–1375.

Shen, W., Punyanitya, M., Silva, A.M., Chen, J., Gallagher, D., Sardinha, L.B., Allison, D.B., Heymsfield, S.B., 2009. Sexual dimorphism of adipose tissue distribution across the lifespan: a cross-sectional whole-body magnetic resonance imaging study. Nutr Metab (Lond) 6, 1–9.

Shen, W., Wang, Z., Punyanita, M., Lei, J., Sinav, A., Kral, J.G., Imielinska, C., Ross, R., Heymsfield, S.B., 2003. Adipose tissue quantification by imaging methods: a proposed classification. Obesity research 11, 5–16.

Shepherd, J., Ng, B., Sommer, M., Heymsfield, S.B., 2017. Body Composition by DXA. Bone 104, 101–105.

Shuster, A., Patlas, M., Pinthus, J.H., Mourtzakis, M., 2012. The clinical importance of visceral adiposity: a critical review of methods for visceral adipose tissue analysis. The British journal of radiology 85, 1–10.

Soladoye, O.P., López Campos, Ó., Aalhus, J.L., Gariépy, C., Shand, P., Juárez, M., 2016. Accuracy of dual energy X-ray absorptiometry (DXA) in assessing carcass composition from different pig populations. Meat science 121, 310–316.

Speliotes, E.K., Willer, C.J., Berndt, S.I., et al., 2010. Association analyses of 249,796 individuals reveal 18 new loci associated with body mass index. Nature genetics 42, 937–948.

Staiano, A.E., Katzmarzyk, P.T., 2012. Ethnic and sex differences in body fat and visceral and subcutaneous adiposity in children and adolescents. International journal of obesity (2005) 36, 1261–1269.

Statista, 2020. Bestand von Schweinen nach Ländern in Europa bis 2019. https://de.statista.com/statistik/daten/studie/935015/umfrage/schweinebestand-nach-laendern-in-europa/. Accessed 16 August 2020.

Statistisches Bundesamt, 2019. Land und Forstwirtschaft, Fischerei: Viehbestände. https://www.destatis.de/DE/Themen/Branchen-Unternehmen/Landwirtschaft-Forstwirtschaft-Fischerei/Tiere-Tierische-Erzeugung/Publikationen/Downloads-Tiere-und-tierische-Erzeugung/viehbestand-2030410195314.pdf?__blob=publicationFile. Accessed 16 August 2020.

Statistisches Bundesamt, 2020. Zahl der Todesfälle im Jahr 2017 um 2,3 %

gestiegen. https://www.destatis.de/DE/Themen/Gesellschaft-Umwelt/Gesundheit/Todesursachen/todesfaelle.html;jsessionid=942A0C43C62E6604E5EB4BC9B457D203.internet721. Accessed 16 August 2020.

Stewart, T.S., Neal, S.M., Irvin, K.M., 1999. Multiple trait selection for pork improvement. NSIF-FS10.

Swindle, M.M., Makin, A., Herron, A.J., Clubb, F.J., Frazier, K.S., 2012. Swine as models in biomedical research and toxicology testing. Veterinary pathology 49, 344–356.

Switonski, M., Stachowiak, M., Cieslak, J., Bartz, M., Grzes, M., 2010. Genetics of fat tissue accumulation in pigs: a comparative approach. Journal of applied genetics 51, 153–168.

Thomas, E.L., Bell, J.D., 2003. Influence of undersampling on magnetic resonance imaging measurements of intra-abdominal adipose tissue. International journal of obesity and related metabolic disorders : journal of the International Association for the Study of Obesity 27, 211–218.

TOPIGS-SNW GmbH, 2019. Delta Kanada bringt verbesserte Zuchtstruktur mit zusätzlichem Mehrwert. https://topigsnorsvin.de/news-de1/ct-scan-de/delta-kanada-bringt-verbesserte-zuchtstruktur-mit-zusaetzlichem-mehrwert/. Accessed 16 August 2020.

Trezona, M., Nogueira, E.T., McCullough, S.M., D’Souza, D. N., Williams, I. H., Mullan, B.P. (Eds.), 2002. The effects of hot environments on the growth performance and carcass characteristics of growing pigs, 123 pp.

Vališ, L., Pulkrábek, J., Pavlík, J., Vítek, M., Wolf, J., 2011. Conformation and meatiness of pork belly. Czech J. Anim. Sci. 50, 116–121.

Vogt, M., 2016. Broschüre Gefährdete Schweinerassen und Alternative Schweinezüchtung - Deutsche Landrasse Universal - DL(U). http://www.g-e-h.de/geh-schweine/18-deutsche.htm. Accessed 16 August 2020.

Weishaupt, D., Köchli, V.D., Marincek, B., Fröhlich, J.M., 2014. Wie funktioniert MRI?: Eine Einführung in Physik und Funktionsweise der Magnetresonanzbildgebung ; mit 9 Tabellen, 7th ed. Springer, Berlin, 180 pp.

Weiß, J., 2011. Tierproduktion. Enke Verl., Stuttgart.

Weißmann, F., Lapp, J., Baulain, U., Brade, W., Fischer, K., Brandt, H., 2010. Zum Einfluss unterschiedlich hoher Duroc-Genanteile auf Mastleistung sowie Schlachtkörper- und Fleischqualität unter ökologischen Produktionsbedingungen. Praxis trifft Forschung Neues aus der Ökologischen

Tierhaltung, 27–32.

Wells, J.C.K., 2007. Sexual dimorphism of body composition. Best practice & research. Clinical endocrinology & metabolism 21, 415–430.

Willam, A., Simianer, H., 2017. Tierzucht, 2nd ed. UTB Verlag Eugen Ulmer, Stuttgart.

Winkler, K., 2017. Erfassung der Knorpelvolumina am Kniegelenk von Zucht- und Mastschweinen unterschiedlicher Genotypen mittels Magnetresonanztomographie und Knochenmineraldichtemessung mittels Dualenergie-Röntgenabsorptiometrie.

World Health Organization, 2017. Cardiovascular diseases (CVDs). https://www.who.int/news-room/fact-sheets/detail/cardiovascular-diseases-(cvds). Accessed 16 August 2020.

World Health Organization, 2020. Obesity and overweight. https://www.who.int/news-room/fact-sheets/detail/obesity-and-overweight. Accessed 16 August 2020.

Xue, J., Dial, G.D., Pettigrew, J.E., 1997. Performance, carcass, and meat quality advantages of boars over barrows: A literature review. Journal of Swine Health and Production 5, 21–28.

Zhu, S., Wang, Z., Heshka, S., Heo, M., Faith, M.S., Heymsfield, S.B., 2002. Waist circumference and obesity-associated risk factors among whites in the third National Health and Nutrition Examination Survey: clinical action thresholds. The American journal of clinical nutrition 76, 743–749.

VIII. Supplementary Material

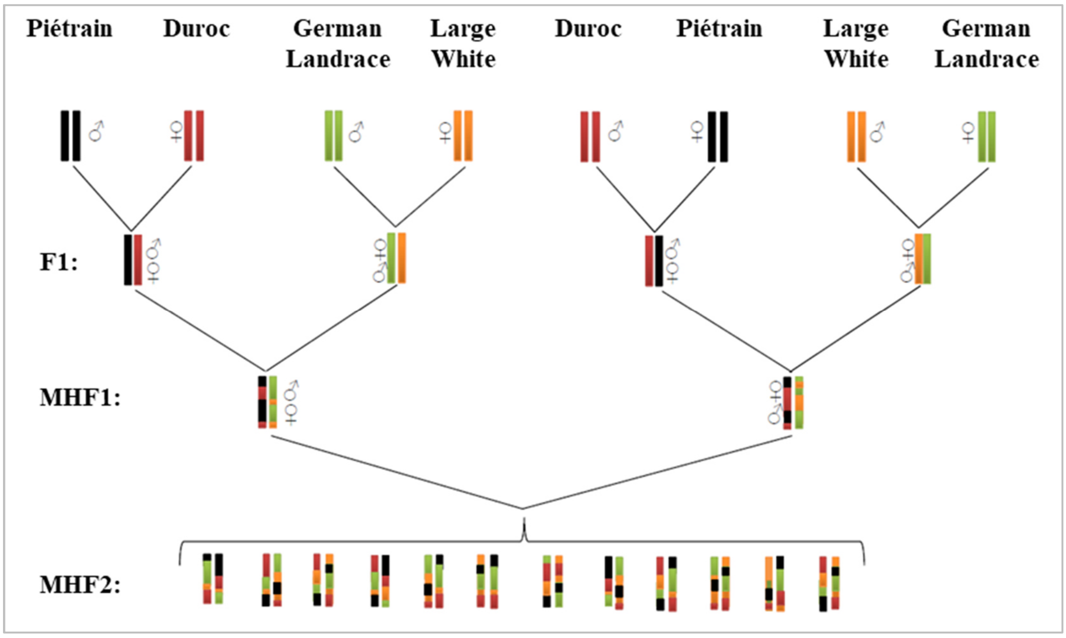

Figure 6. Crossbreeding scheme of four different parental breeds

Figure 7. Pigs of the first (A) and second (B) crossbreeding generation.

Table 4. Least squares means (LSM), standard errors of estimation (SEE), and significance level (Pr>t) of soft lean tissue mass

Soft lean tissue mass (g)			
	LSM	SEE	Pr>t
Castrated males	76,731	760.76	0.1072
Females	74,962	805.87	
MHF1	75,899	823.7	0.9263
MHF2	75,793	779.68	

IX. DANKSAGUNG

Bei all denjenigen, die mich während der Anfertigung dieser Dissertation unterstützt und motiviert haben, bedanke ich mich an dieser Stelle.

Mein hauptsächlicher Dank gilt meinem Doktorvater Herrn Prof. Armin M. Scholz für das interessante Thema und die freundliche Betreuung und Unterstützung dieser Arbeit. Im Besonderen danke ich ihm für das geschenkte Vertrauen in meine Fähigkeiten und den nötigen Zuspruch mich den speziellen Herausforderungen zu stellen.

Allen Mitarbeitern des Lehr- und Versuchsguts Oberschleißheim, insbesondere Dr. Stefan Nüske, Richard Bätz, Christa Gurgui und dem gesamten Team des Rinderbereiches danke ich für die schöne Zeit am LVG. Herzlichen Dank an Deise Knob, Helen Schweizer, dem gesamten Team des Schweinebereiches und jedem weiteren Helfer, für das Durchhaltevermögen an den langen und anstrengenden Scan-Tagen. Durch euch sind diese zu effektiven, angenehmen und manchmal auch sehr lustigen Arbeitstagen geworden.

Ein großer Dank gilt meiner Schwester und ihrem Partner Tom für ihre konstruktive Kritik und ihre außerordentliche Diskussionsbereitschaft bei fachlichen Fragestellungen.

Darüber hinaus möchte ich mich bei meinen Eltern und meinen Freunden Franziska, Julia, Lisa und Miodrag ganz besonders bedanken. Danke für eure mentale Unterstützung bei der Anfertigung dieser Arbeit und eure stets offenen Ohren für jegliches meiner Probleme.